Modelling the Evolution of Structured Populations involving Multiplayer Games under Coordinated Movement Systems

Hasan Haq

Doctor of Philosophy

CITY UNIVERSITY
LONDON

City, University of London

Department of Mathematics

April 2025

Contents

Contents iii

List of Figures vii

List of Tables xiii

Acknowledgements xv

Declaration xvii

Abstract xix

1 Introduction 1

1.1 Classical Game Theory 2

1.2 Evolutionary Game Theory 3

1.2.1 Evolutionarily Stable Strategies (ESS) 4

1.2.2 The Replicator equation 5

1.3 Evolutionary processes in a finite population 7

1.3.1 Evolutionary games in finite populations 10

1.4 Evolutionary Graph Theory 11

1.4.1 Modelling evolutionary games on graphs 13

1.5 Multiplayer Games 14

1.6 The Broom-Rychtář Framework 16

1.6.1 Structure 17

1.6.2 Fitness 19

1.6.3 Evolutionary updating rules 20

1.7 The development of the Territorial Raider model 22

1.7.1 Population structure 22

1.7.2 Evolutionary updating process 22
1.7.3 The fixation probability 24
1.7.4 Multiplayer games 25
1.8 History-dependence: Markov Movement Model 26
1.9 Row-dependent movement 29
1.9.1 Deterministic movement: follow the majority 31
1.9.2 Probabilistic movement: the Polya-urn 32
1.9.3 The wheel and base model 33
1.10 Outline 33

2 Extending the Territorial Raider Model to incorporate Row-dependent Movement 37

2.1 Introduction 37
2.2 The Model 38
2.2.1 The population structure and distribution 38
2.2.2 Evolutionary dynamics 38
2.2.3 Fixation probability 39
2.3 Theoretical results 39
2.3.1 A generalised movement modelling approach 39
2.3.2 Fitness calculations 41
2.3.3 General fixation probability formulae 42
2.3.4 Weak selection 44
2.4 Numerical results 48
2.5 Discussion 57

3 Predictors of Fixation Probability under Coordinated Movement Systems 61

3.1 Introduction 61
3.2 The Model 62
3.3 Results 62
3.3.1 Evolutionary measures impacting the fixation probability . . 62
3.3.2 Numerical results 66
3.3.3 Differences between processes 75
3.4 Discussion 78

4 Extending the Movement Methodology to Incomplete Networks 81

4.1 Introduction . . . 81

4.2 The Model . . . 82

4.3 Results . . . 82

4.3.1 Upper and lower bounds on T_{max} . . . 83

4.3.2 Example of an unfaithful process . . . 84

4.3.3 Extending the wheel to incomplete graph structures . . . 87

4.3.4 The wheel alignment process . . . 87

4.4 Simulations . . . 98

4.5 Discussion . . . 103

5 Hybrid models 107

5.1 Introduction . . . 107

5.2 Hybrid type 1 . . . 107

5.3 Hybrid type 2 . . . 108

5.4 Simulations . . . 109

5.5 Discussion . . . 113

6 Conclusion 115

Bibliography 137

List of Figures

1.1 The Moran process (Moran 1958, 1962) describes the stochastic evolution of a finite population. At each time step, an individual is selected to reproduce with probability proportional to its fitness. The offspring then randomly replaces another individual (excluding its parent) ensuring the population size remains constant. 8

1.2 These two figures represent a population composed of type A and B individuals. Figure (a) shows an unstructured population where all individuals can interact with one another whereas figure (b) represents a structured population. The population is represented by a graph where the vertices represent individuals such that individuals can only interact with each other if they are connected. 11

1.3 The fully independent model from (Broom and Rychtar 2012). There are N individuals who are distributed over M places such that I_n visits place P_m with probability p_{nm}. Individuals interact with one another when they meet, for example, I_1 and I_2 can interact with one another when they meet in P_1 20

1.4 The population structures and apriori distributions for small graphs with three, four and five nodes. An individual remains on their home vertex with probability $\frac{h}{h+m}$ and moves to a neighbouring vertex with probability $\frac{1}{h+m}$, where m is the number of neighbours. (a) the line with three nodes. (b) the complete triangle graph. (c) the square with both diagonals connected i.e. the complete graph with four vertices. (d) the circle graph with four nodes. (e) the star graph with 5 nodes. 23

1.5 Payoffs for the pairwise and multiplayer versions of the Public Goods, Hawk–Dove, and Stag–Hunt games. In the Public Goods game, strategy A corresponds to cooperation and B to defection, with a denoting the number of cooperators and b the number of defectors in the group. In the Hawk–Dove game, A represents hawks and B represents doves, where a is the number of hawks and b the number of doves within the group. In the Stag–Hunt game, A corresponds to the cooperative strategy and B represents the defectors' strategy, with a denoting the number of cooperators and b the number of defectors in the group. . 27

1.6 (a) $M = 3$ places with $a_1 = \frac{1}{3}, a_2 = \frac{1}{6}, a_3 = \frac{1}{2}$. (b) represents the $N = 3$ individuals as spikes. The angle between individuals I_i and I_j is given by $2\pi\theta_{ij}$. In this case, $\theta_{12} = \frac{1}{4} = -\theta_{21}$. (c) shows the simultaneous placement of all individuals after the upper disc is spun on top of the base. In this case, individuals I_1, I_2, I_3 move to places P_3, P_1, P_3 respectively. 33

2.1 The fixation probability of a mutant cooperator in a population of defectors on complete decagon and pentadecagon graphs under BDB and BDD dynamics for varying h under distinct polya-urn movement processes, For (a), (c), (e) and (g), we set $B = 0$ (follow the majority), $B = 2$, $B = 6$ and $B = 10{,}000$ (a sufficiently large value to mirror independent movement). For (b), (d), (f) and (h) we set $h = 0.5$, $h = 1$, and $h = 10$ and vary B. 50

2.2 The fixation probability of a mutant dove in a population of hawks on complete decagon and pentadecagon graphs under BDB and BDD dynamics for varying h under distinct polya-urn movement processes, For (a), (c), (e) and (g), we set $B = 0$ (follow the majority), $B = 2$, $B = 6$ and $B = 10{,}000$ (a sufficiently large value to mirror independent movement). For (b), (d), (f) and (h) we set $h = 0.5$, $h = 1$ and $h = 10$ and vary B. 51

2.3 The fixation probability of a mutant cooperator in a population of defectors on complete decagon and pentadecagon graphs under BDB and BDD dynamics for varying h under distinct wheel movement processes, For (a), (c), (e) and (g), we set $\theta = 0$ (follow the majority), $\theta = \frac{2\pi}{N}$ (represents a near complete dispersal process), $\theta = \frac{\pi}{N}$. For (b), (d), (f) and (h) we set $h = 0.5$, $h = 1$ and $h = 10$ and vary θ. . . 52

2.4 The fixation probability of a mutant dove in a population of hawks on complete decagon and pentadecagon graphs under BDB and BDD dynamics for varying h under distinct wheel movement processes, For (a), (c), (e) and (g), we set $\theta = 0$ (follow the majority), $\theta = \frac{2\pi}{N}$ (represents a near complete dispersal process), $\theta = \frac{\pi}{N}$. For (b), (d), (f) and (h) we set $h = 0.5$, $h = 1$, and $h = 10$ and vary θ. 53

3.1 The fixation probabilities of the cooperator and defector in the Stag-Hunt game on the complete decagon under the Polya-urn and wheel processes. (the payoffs are set as $R = 10, C = 1, V = 12$ and $L = 2$). (a), (b), (c) and (d) show the fixation probability of a mutant cooperator in a population of defectors and vice-versa for (e), (f), (g) and (h). Figures (a), (b), (c) and (d) represent the cooperator's fixation probability and figures (e), (f), (g) and (h) represent the defector's. For the Polya-urn, in (a) and (e) we set $B = 0$ (follow the majority), $B = 2$, $B = 6$ and $B = 10{,}000$ (a sufficiently large value to mirror independent movement). For the wheel, in (c) and (g) we set $\theta = 0$ (follow the majority), $\theta = \frac{2\pi}{N}$ (represents a near complete dispersal process), $\theta = \frac{\pi}{N}$. For (b) and (f), we plot the fixation probability against B (for the Polya-urn) and set $h = 1$, $h = 20$ and $h = 500$. For (d) and (h), we plot the fixation probability against θ (for the wheel) and set $h = 1$, $h = 20$ and $h = 500$. 67

3.2 The mean group size and temperature of individuals within the a well-mixed population on the complete decagon for varying h under distinct Polya-urn processes and wheel processes. (a) and (b) show the mean group size and (c) and (d) show the temperature. We set $B = 0$ (follow the majority), $B = 2$, $B = 6$ and $B = 10{,}000$ (a sufficiently large value of B representing independent movement). We also set $\theta = 0$ (follow the majority), $\theta = \frac{2\pi}{N}$ (represents a near complete dispersal process) and $\theta = \frac{\pi}{N}$. 68

3.3 The fixation probability plotted against the mean group size for a well-mixed population in the Public Goods, Hawk-Dove and Stag-Hunt games on the complete decagon graph. As we vary h, we plot the corresponding fixation probability and mean group size values against each other. Figures (a), (c) and (e) illustrate Polya-urn processes where we set $B = 0$ (follow the majority), $B = 2$, $B = 6$ and $B = 10{,}000$ (a sufficiently large value of B representing independent movement). (b), (d) and (f) show wheel processes where we set $\theta = 0$ (follow the majority), $\theta = \frac{2\pi}{N}$ (represents a near complete dispersal process) and $\theta = \frac{\pi}{N}$. 69

3.4 The fixation probability plotted against the temperature for a well-mixed population in the Public Goods, Hawk-Dove and Stag-Hunt games on the complete decagon graph. As we vary h, we plot the corresponding fixation probability and temperature values against each other. Figures (a), (c) and (e) illustrate Polya-urn processes where we set $B = 0$ (follow the majority), $B = 2$, $B = 6$ and $B = 10{,}000$ (a sufficiently large value of B representing independent movement). (b), (d) and (f) show wheel processes where we set $\theta = 0$ (follow the majority), $\theta = \frac{2\pi}{N}$ (represents a near complete dispersal process) and $\theta = \frac{\pi}{N}$. 70

3.5 The fixation probability plotted against the temperature in the Public Goods games on the complete decagon graph under BDD dynamics for distinct Polya-urn processes. We set $B = 0$ (follow the majority), $B = 2$, $B = 6$ and $B = 10,000$ (a sufficiently large value of B representing independent movement). 76

4.1 The line graph for three individuals. I_1 resides on place X, I_2 resides on place Y, I_3 resides on place Z. 85

4.2 The wheel process for incomplete graphs. (a) The wheels for different individuals, where each wheel represents the accessible locations for each individual. Individual I_1 can move to places A, B and C, I_2 can move to U, V and W and I_3 can move to X, Y and Z. (b) represents the wheel stacking procedure. Each individual's spike is positioned above their respective wheel, ensuring that movements are correctly carried out on incomplete graph structures. 87

4.3 The alignments for each individual on the line graph with three nodes 91

4.4 A graphical representation of a network considered in the alignment process. 92

4.5 The alignments for four individuals on the circle graph. (a) shows the circle graph with four individuals $I_1, I_2.I_3$ and I_4 with vertices labelled as $1, 2, 3$ and 4. (b) shows the wheel alignments for each individual. 99

4.6 The fixation probability of a mutant cooperator and defector plotted against the home fidelity parameter, h in the Public Goods game under the wheel alignment process on the line and circle graphs with nine nodes. (a), (c), (e) and (g) show the cooperator's fixation probability and (b), (d), (f) and (h) show the defector's fixation probability. For the wheel process, we set $\theta = 0, \frac{\pi}{12}$ and $\frac{2\pi}{9}$ (to represent a near dispersal process). 100

4.7 The fixation probability of a mutant dove and hawk plotted against the home fidelity parameter, h in the Public Goods game under the wheel alignment process on the line and circle graphs with nine nodes. (a), (c), (e) and (g) show the hawk's fixation probability and (b), (d), (f) and (h) show the dove's fixation probability. For the wheel process, we set $\theta = 0, \frac{\pi}{12}$ and $\frac{2\pi}{9}$ (to represent a near dispersal process). . . . 101

5.1 The fixation probability of a mutant cooperator and defector plotted against the home fidelity parameter, h in the Public Goods game under the hybrid models on the complete decagon and pentadecagon graphs. (a), (c), (e) and (g) show the cooperator's fixation probability. (b), (d), (f) and (h) show the defector's fixation probability. The hybridised movement processes are the wheel process ($\theta = 2\pi/10$) and the follow the majority process ($B = 0$). 111

5.2 The fixation probability of a mutant hawk and dove plotted against the home fidelity parameter, h in the Public Goods game under the hybrid models on the complete decagon graph. (a), (c), (e) and (g) show the hawk's fixation probability. (b), (d), (f) and (h) show the dove's fixation probability. The hybridised movement processes are the wheel process ($\theta = 2\pi/10$) and the follow the majority process ($B = 0$). 112

List of Tables

1.1 Notation used in the Broom-Rychtar framework. 16

1.2 Dynamics defined using the evolutionary graph $\mathbf{W}_t$ and fitnesses $F_{n,t}$. 21

1.3 Notation used in subsequent chapters of the thesis. 35

2.1 Fixation probabilities (FP) of cooperators and doves under different movement processes: follow the majority ($B = 0$), polya-urn (increasing B), random movement ($B \to \infty$), and the wheel (separation angle). 57

3.1 Summary of the relative effectiveness of mean group size and temperature in predicting fixation probability across the Public-Goods, Hawk–Dove and Stag–Hunt games under BDB dynamics. 75

3.2 Summary of the three effects across different dynamics. A tick (✓) represents the presence of the effect, whereas a cross (x) indicates its absence. 77

4.1 Alignment rule for individuals on a line or circle graph of size N, where each individual's wheel is divided into three equal segments. The table shows how individuals indexed I_{3k}, I_{3k+1}, and I_{3k+2} align to locations A, B, and C based on their relative positions in the network. 98

Acknowledgements

I express my utmost and sincerest thanks to

my supervisor, Professor Mark Broom, to whom I am truly indebted for giving me the opportunity to pursue a doctorate under his guidance. Nearing the end of my bachelors at City in 2021, I reached out to Mark to inquire about potential research projects. He was incredibly encouraging and supportive, and I was fortunate to secure funding from City to support my doctorate, for which I am very grateful. Upon beginning my PhD, I quickly realised that Mark is not only one of the world's leading experts in this field, but also an exceptionally kind and approachable person. It has truly been an honour to be his PhD student.

My collaborator, Professor Pedro H.T. Schimit, based in São Paulo at Universidade Nove de Julho, has played an invaluable role throughout my doctorate. His computational expertise was instrumental to the simulations presented in this thesis. His presence as my collaborator made my research very enjoyable. Although the aftermath of the COVID period prevented us from collaborating in person, it has nonetheless been a pleasure to work with him. I sincerely hope we are able to meet in person next year as planned.

One of my dearest friends, Dr Olalla Castro Alvaredo, was my tutor during my undergraduate studies at City. Throughout that time, her office door was always open to my many questions whether about work, research, pursuing further study or just general life advice. Olalla encouraged me to get in touch with Mark for PhD opportunities. I honestly don't think I would have pursued this path without her guidance and belief in me. Even during my doctorate, she has continued to provide invaluable advice and support, such as taking me out for lunch several times when I needed a break, lending me many books over the years and always reminding me of the importance of maintaining a healthy work-life balance. I will always be deeply grateful for the kindness, encouragement and friendship she has shown me.

My co-supervisor, Dr Robert Noble who encouraged me to think more deeply about the directions I was exploring and their real-life implications. During the early period of the PhD, Rob often included me in his research group's social events, whether it was going out for drinks or taking us out for lunch. I'm very grateful for that as it eased my transition from undergraduate study to the world of doctoral research.

Dr Alessandro de Martino, Dr Maud de Visscher and Professor Joseph Chuang who were among my favourite lecturers during my undergraduate studies, and were friendly and supportive presences in the department.

My mother, Sadia, for the unconditional love she has given me throughout my life and for instilling in me the importance of prioritising my education and encouraging me to pursue mathematics. I don't think I would have had the opportunity to pursue this doctorate without it and I will always be grateful for that.

My sister, Anum for her support. She has been fundamental to maintaining my work-life balance throughout my doctorate. I will always cherish her support and remain deeply thankful for the many ways she has supported me.

My brother, Mahad. I've appreciated his perspective throughout different stages of my life. Having also completed his doctorate, he has always set a strong example of academic achievement that I have always respected.

My brother-in-law Zain, for encouraging me to switch off when I needed it most. Those moments helped me maintain balance, especially during the more demanding periods of my research.

My dear friend Manjyot, who uplifted the final period of my doctorate. Manjyot joined the department as one of Mark's new PhD students during my third year and his presence brought a real sense of warmth to my research experience. Having someone to share ideas and meaningful conversations with during the day made a huge difference, especially after the more solitary earlier years. It's a shame he joined the department when my doctorate was already nearing its end, as his presence would have made the earlier stages far more enjoyable too.

The PhD office crew, Dmitrii, Aman and Beth, who would often check in on my research progress and invite me to take breaks over coffee, chess or general catch-ups. Those moments made the process much more manageable, especially during the final stretch of the doctorate, and I thank them all for that.

Declaration

I hereby confirm that the research presented in this thesis, titled *"Modelling the Evolution of Structured Populations involving Multiplayer Games under Coordinated Movement Systems",* submitted for the degree of Doctor of Philosophy in Mathematics to the Department of Mathematics at City St George's, University of London, has been entirely composed by myself during the period October 2021 to April 2025, under the supervision of Professor Mark Broom. I confirm that this thesis has not been previously submitted for the award of a degree at any university.

Abstract

This thesis investigates the evolution of structured populations involving multiplayer evolutionary games, with a particular focus on realistic, coordinated movement behaviours. Building on recent advancements in evolutionary graph theory, most notably the Broom-Rychtář framework, which extends the classical evolutionary models to incorporate more realistic features such as multiplayer interactions, this thesis addresses a gap in the existing mathematical literature concerning the modelling of coordinated movement within evolutionary settings. Existing models have primarily focused on independent movement, and more recently, history-dependent movement. Although the theory underlying the framework has been explored in various directions, several movement mechanisms have been developed that characterise coordinated movement, for example, herding and dispersal. By extending existing parameters within the framework, this thesis develops a general methodology for embedding a wide range of considered movement processes into evolutionary settings on arbitrary network structures. We demonstrate that certain levels of aggregation and dispersal can benefit specific types of individuals depending on the considered game, for example, public goods. Throughout this thesis, we consider key evolutionary measures, including fixation probabilities, predictors such as mean group size and temperature and aggregation metrics, and show that their influence is determined by the nature of both the movement process and game.

Chapter 1

Introduction

Despite being a well-established theory, the field of evolution has remained at the forefront of scientific research due to the very nature of its description. Evolution describes the origin of the diversity of life through the mechanism of *natural selection*. In 1859, Charles Darwin published the book *On the Origin of Species*, which provided the first accurate exposition on the subject. Natural selection is the process by which individuals exhibiting advantageous characteristics are more likely to survive and, therefore, reproduce, passing their favourable genetics to their offspring. This is because an individual with a survival advantage is more likely to reproduce than one without such traits. Similarly, an individual who exhibits a disadvantageous trait is less likely to survive and reproduce; consequently, its genetic code is likely to disappear over time. In simple terms, natural selection is the non-random differential survival of genes within gene pools. Genetic *mutation* also plays a significant role in the evolutionary process. Through mutation, the genetic code passed to offspring may change. When mutated genes provide an advantage or disadvantage to the host, then they are subject to the forces of natural selection. However, if the mutated genes are neither beneficial nor detrimental to the host, they are considered *neutral*. These neutral genes may become incorporated into the population through *neutral drift*. Evolution is a multifaceted theory and can be studied through various approaches, particularly through evolutionary game theory.

Evolutionary game theory, as it is broadly recognised today, was formalised by John Maynard Smith, particularly through his influential book *Evolution and the Theory of Games* (1982). Evolutionary game theory is a versatile mathematical modelling tool that has become increasingly popular for studying the evolution of

populations. It has cross-disciplinary influences in Economics and Biology, appealing to practitioners in both fields. This is because evolutionary game theory not only serves as a theoretical foundation for modelling population evolution but also offers a diverse framework with the potential to explore and explain a vast range of natural phenomena (Broom & Rychtar 2013).

The purpose of this section is to first explain the foundation on which evolutionary game theory is built: classical game theory. We then highlight key developments in this area and demonstrate the connection between game theory and evolution, which led to the emergence of evolutionary game theory. Subsequently, we discuss significant, established work in the field, such as the Moran Process, Evolutionary graph theory and the Broom-Rychtář framework before outlining the contributions presented in this thesis.

1.1 Classical Game Theory

Game theory is a mathematical framework used to analyse interactions between individuals involving strategic decisions. Its inception can be traced to the publication of John von Neumann and Oskar Morgenstern's book *Game Theory and Economic Behaviour*, (von Neumann & Morgenstern 1944), and it has since been widely applied across various fields. This section begins by defining a game, highlighting important developments before applying them to population evolution.

A *game* is primarily considered as a mathematical model that describes a situation where a finite number of entities, or players, interact with each other, with each player acting in their own self-interest. At each stage of the game, every player must perform an action. The actions that players choose to take against one other are defined by their strategies. A *strategy* catalogues all of the actions a player can take in every scenario of the game. While a *pure strategy* specifies a single action for all possible scenarios, a *mixed strategy* is a combination of pure strategies, where each pure strategy is played with a certain probability. The motivation for a player to adopt a particular strategy is represented by the *payoff* they receive from playing that strategy. In *symmetric games*, players have the same set of strategies, and for a two player symmetric game, with N strategies, $S_1, ..., S_N$, the game can be

represented by a *payoff matrix* given by

	S_1	S_2	$\cdots$	S_N
S_1	$E(1,1)$	$E(1,2)$	$\cdots$	$E(1,N)$
S_2	$E(2,1)$	$E(2,2)$	$\cdots$	$E(2,N)$
$\vdots$	$\vdots$	$\vdots$	$\ddots$	$\vdots$
S_N	$E(N,1)$	$E(N,2)$	$\cdots$	$E(N,N)$

(1.1)

where each entry $E(i,j)$ is the payoff to a player using strategy S_i against their opponent using strategy S_j. For simplicity, consider a symmetric two-player game with the payoff matrix given by

	A	B
A	a	b
B	c	d

(1.2)

The matrix entries a, b, c, d represent the payoffs for the individuals. For example, both players receive the payoff a if they both use strategy A. Games are analysed in terms of the best responses. A *best response* is a strategy that provides the highest payoff compared to all other available strategies. If both players adopt their best response strategies, the game reaches a *Nash equilibrium*, (Nash 1951) a situation where neither individual can improve their payoff by switching to another strategy. This concept represents a significant development in game theory, providing a robust method for determining optimal strategies within this framework.

1.2 Evolutionary Game Theory

One of the first indirect uses of game theory in an evolutionary setting was by Fisher (1930) who mathematically developed Darwin's argument regarding why natural selection should act to equalise the sex ratio (1874). This was later explicitly explained by Hamilton (1967), who published one of the first works on the subject. While classical game theory attempts to describe the Nash equilibria in isolated social interactions, typically between two individuals, evolutionary game theory explains changes in macro-behavioural regularities within a given population by determining the evolutionary stability points, where the composition of the population remains constant over time.

The strategy that an individual adopts reflects their phenotype, which is genetically determined. The payoff an individual receives from interacting with others contributes to their *fitness*. Fitness measures the likelihood of an individual reproducing and propagating their genetic code to their offspring and, thus, to future generations. During reproduction, the forces of natural selection come into play, as individuals with a higher fitness will reproduce more frequently, leading to an increased proportion of such individuals within the population. Conversely, the frequency of individuals with lower fitness decreases.

However, mutations within the population may occur, which can be interpreted as an offspring adopting a different strategy from their parent. Evolutionary processes have generally been studied in unstructured, infinite populations, where each individual is equally likely to encounter others. Traditionally, this research has consisted of two approaches: static and dynamic analyses.

1.2.1 Evolutionarily Stable Strategies (ESS)

The term Evolutionarily Stable Strategy (ESS) was coined by John Maynard Smith and George Price (1973) and is arguably one of the most central concepts in Evolutionary game theory. ESSs are commonly used to analyse evolutionary games, where a strategy qualifies as an ESS if it is adopted by all members of the population and can resist invasion by any alternative strategy. The mathematical definition of an ESS considers the population at a certain point in time when a mutant strategy is introduced and adopted by a small subset of individuals. The ESS provides a condition under which the mutant strategy is not favoured by natural selection, meaning the fitness of the mutant is lower than that of the resident strategy. Consequently, over time, the mutants die out.

Assuming an infinite population where individuals are equally likely to interact with each other, then the condition for an ESS is given as follows. If $1 - \epsilon$ of the population plays the resident strategy i, and a small ϵ proportion of the population adopts a mutant strategy j (where $j \neq i$), then strategy i is an ESS for the population if

$$(1 - \epsilon)E(i, i) + \epsilon E(i, j) > (1 - \epsilon)E(j, i) + \epsilon E(j, j) \tag{1.3}$$

where the fitness of a resident using strategy i is given by $(1 - \epsilon)E(i, i) + \epsilon E(i, j)$ and the fitness of a mutant using strategy j is given by $(1 - \epsilon)E(j, i) + \epsilon E(j, j)$.

Alternatively, one can derive a pair of conditions from the equation above by letting $\epsilon \to 0$. A strategy i can be classified as an ESS if and only if for all $j \neq i$. we have:

$$E(i,i) > E(i,j) \text{ or } E(i,i) = E(j,i), \text{ and } E(i,j) > E(j,j). \tag{1.4}$$

The first condition states that a mutant must not perform better within the population compared to a resident. This is called the *equilibrium condition*. The second condition states that if a mutant performs as well as a resident when playing against another resident, then the mutant must perform worse than a resident when playing against a mutant. This is known as the *stability condition*.

1.2.2 The Replicator equation

Whereas the static approach analyses a population playing a given strategy against mutants to assess stability, the dynamic approach examines how the composition of the population changes over time. This involves defining a reproduction stage within the evolutionary structure, which can be described by an equation, specifically the *replicator equation* (Taylor & Jonker 1978, Hofbauer et al. 1979, Hofbauer & Sigmund 1998).

$$\frac{d}{dt}p_i = p_i(F_i - \gamma). \tag{1.5}$$

Here, p_i represents the frequency of individuals playing strategy i, F_i denotes the fitness of an individual who plays strategy i and γ is the average fitness of the population. Evidently, if the fitness of an individual using strategy i is greater than the average fitness of the population, the frequency of such individuals will increase. Conversely, if their fitness is lower than the average fitness of the population, their frequency will decrease. Hence, the replicator equation describes a deterministic dynamic process in which advantageous strategies gradually spread throughout the population. It is important to note, however, that the replicator dynamics do not consider mutation, therefore, any strategy not originally present in the population will never appear throughout the evolutionary process.

We can determine the evolutionary equilibria for the two strategy game from (1.2) by solving the equation (1.5). Assume that the frequency of individuals playing strategy A is z. The fitness of each type of individual is given by

$$F_A = za + (1-z)b \text{ and } F_B = zc + (1-z)d.$$

We have that the average fitness of the population is

$$\gamma = zF_A + (1-z)F_B$$

By substituting these fitnesses into equation (1.5), the change in the frequency of type A individuals is given by

$$\begin{aligned}\frac{d}{dt}p_A &= p_A(F_A - \gamma) \\ &= z(F_A - zF_A - (1-z)F_B) \\ &= z(1-z)(F_A - F_B) \\ &= z(1-z)(z(a-b-c+d)+b-d).\end{aligned}$$

In order to determine the equilibrium values z^*, we must solve $\frac{d}{dt}p_A = 0$. Evidently, this gives the equilibrium values

$$z^* = 0, z^* = 1 \text{ and } z^* = \frac{d-b}{a-b-c+d}.$$

The stability of the equilibrium points depends upon the values of the payoffs. We have the following cases:

- $z^* = 1$ stable: This corresponds to $a > c$ and $b > d$. i.e. strategy A is a strict Nash Equilibrium. Therefore, regardless of the starting frequency z of type A individuals, the population eventually reaches an equilibrium state where there are only type A individuals.

- $z^* = 0$ stable: in this case we have that $c > a$ and $d > b$, which is the exact opposite of the previous case i.e. strategy B is a strict Nash Equilibrium.

- $z^* = 0$ and $z^* = 1$ are both stable: in this case, $a > c$ and $d > b$. This means that both A and B are the best responses to themselves. The equilibrium point the population converges to depends upon the starting frequency z. If $z > \frac{d-b}{a-b-c+d}$, the population converges to $z^* = 1$, and $z^* = 0$ otherwise.

- $z^* = \frac{d-b}{a-b-c+d}$ is stable: in this case $a < c$ and $d < b$, showing that strategy A is the best response to strategy B and vice versa. As a result, both strategies

can coexist and eventually stabilise at the equilibrium state.

1.3 Evolutionary processes in a finite population

The ESS and the replicator equation are determinstic models, providing valuable insights into how effective particular strategies are at resisting invasion and determining the stability points of a given population. However, these concepts assume that the population in question is infinite, which is unrealistic since biological populations are finite. Capturing natural phenomena such as genetic drift and neutral drift is important and requires a different set of evolutionary dynamics, incorporating a stochastic process.

One of the earliest stochastic models in population genetics, which examines the changes in allele frequencies within a population's gene pool, is the Wright-Fisher model (Fisher 1930, Wright 1930). This classical process originally modelled neutral populations, but has since been extended in several directions such as the implementation of multiple alleles and selection (Edwards 2000, Waxman 2011) and acts as an important framework for inferring selection on genetic data (Paris et al. 2019). For large finite populations, the Wright-Fisher model can be approximated by a diffusion process, which was first done by Kimura (1964) and Zheng et al. (2011) extensively consider diffusion approximation in the context of evolutionary games.

Another stochastic model, the Moran process (Moran 1958, 1962), was developed to investigate evolution in finite, homogeneous populations, consisting of two types of individuals where each individual is equally likely to interact with every other individual. This framework was later extended to consider evolutionary games (Nowak et al. 2004, Taylor et al. 2004).

Consider an N-sized population with k type A individuals and $N-k$ type B individuals. Type A individuals have fitness r, while type B individuals have fitness 1. Unlike the previously considered evolutionary setting governed by the replicator equation, the fitness of individuals within the Moran process is frequency-independent, i.e. it does not depend on the population composition. The stochastic dynamics incorporated into the Moran process ensure that the population always remains at size N. At each time step, an individual is selected to reproduce a copy of itself with probability proportional to its fitness. Its offspring then replaces a

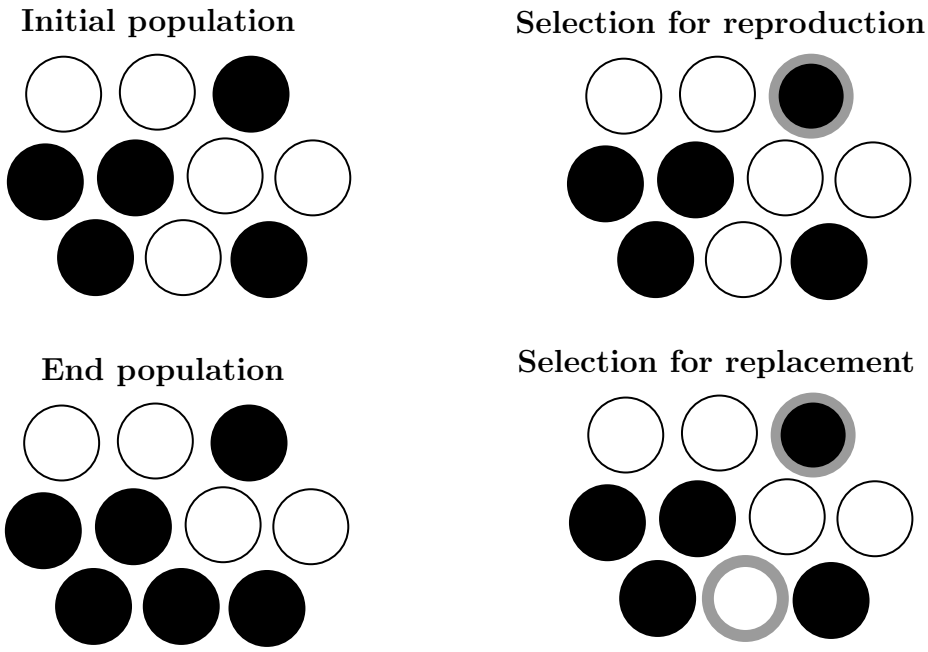

Figure 1.1: The Moran process (Moran 1958, 1962) describes the stochastic evolution of a finite population. At each time step, an individual is selected to reproduce with probability proportional to its fitness. The offspring then randomly replaces another individual (excluding its parent) ensuring the population size remains constant.

random member of the population other than its parent. The probability that a type A or B individual is selected for reproduction is given by

$$b_A = \frac{r}{kr + (N-k)},\ b_B = \frac{1}{kr + (N-k)},$$

The offspring then replaces another random member of the population (excluding its parent) with probability $\frac{1}{N-1}$ (as seen in Fig.1.1).

It should be noted that the order of the birth and death events matters, as the parent of the offspring is excluded from being replaced. The Moran process follows birth-death dynamic with selection occurring at birth (BD-B). Similar to the replicator equation, we assume that there are no mutations during the evolutionary process. However, this does not mean that mutation is entirely disregarded. The evolutionary system is set up by assuming a population of native type B individuals, into which a single type A individual is introduced via mutation. As the population is of finite size, one of the types will eventually fixate and replace the other. Naturally, one may ask "What is the probability of the type A mutant fixating the population?". More precisely, this is referred to as the *fixation probability* of a type A individual, denoted ρ_A.

To calculate ρ_A, we must consider the *transition probabilities*, which are used to

determine the fixation probability. The transition probabilities $P_{k,m}$ describe the population transitioning from a state where there are k type A individuals to a state where there are m type A individuals. Since there is only one birth and one replacement in each time step, m can only be equal to $k+1$, $k-1$ or k.

$$P_{k,m} = \begin{cases} \frac{kr}{kr+N-k}\frac{N-k}{N}, & m = k+1 \\ \frac{N-k}{kr+N-k}\frac{k}{N}, & m = k-1 \\ 1 - \frac{kr}{kr+N-k}\frac{N-k}{N} - \frac{N-k}{kr+N-k}\frac{k}{N}, & m = k \end{cases} \tag{1.6}$$

The standard expression of the fixation probability is provided in (Karlin & Taylor 1975).

$$\rho_A = \frac{1}{1 + \sum_{j=1}^{N-1} \prod_{k=1}^{j} \frac{P_{k,k-1}}{P_{k,k+1}}} \tag{1.7}$$

Substituting the transition probabilities gives

$$\rho_A = \begin{cases} \frac{1-(\frac{1}{r})}{1-(\frac{1}{r})^N}, & r \neq 1 \\ \frac{1}{N}, & r = 1 \end{cases} \tag{1.8}$$

This solution is known as the *Moran probability* and serves as the standard benchmark for comparing fixation probabilities in other complex evolutionary models. The phenomenon of *neutral drift* is captured by this solution. Consider $r = 1$, which represents a neutral mutation that provides neither a benefit nor a disadvantage to the type A individual compared to the type B residents. In this case, $\rho_A = \frac{1}{N}$. Evidently, selection favours neither type of individual, as a type A mutant has an equal chance of fixating within the population as a type B individual. When $r < 1$, selection favours the type B residents, as the fixation probability is less than that of a neutral individual (i.e., $\rho_A < \frac{1}{N}$). Conversely, when $r > 1$, selection favours the type A mutant, as $\rho_A > \frac{1}{N}$. It is important to note that even when $r \neq 1$, the fixation or extinction of a mutant is not guaranteed. This is because even the fittest or weakest member of the population may not be necessarily be selected for reproduction or replacement.

1.3.1 Evolutionary games in finite populations

The Moran process was later extended by Taylor et al.(2004) to incorporate frequency-dependent fitness, where individuals play a game whose payoff matrix is shown in (1.2). In this extension, the fitness of individuals (previously constant in the Moran process) becomes variable due to the inclusion of evolutionary games. With these fitnesses, the transition probabilities (1.6) must be recalculated in this new context and substituted into (1.7). This yields a new rule that indicates when a type A individual is favoured by selection. Assume there are k type A individuals, the fitnesses are given by

$$F_A(n) = 1 - w + w\left(\frac{a(k-1) + (N-k)b}{N-1}\right). \tag{1.9}$$

$$F_B(n) = 1 - w + w\left(\frac{ck + (N-k-1)d}{N-1}\right). \tag{1.10}$$

The terms inside the brackets represent the average payoff to the individual, as all members of the population are equally likely to interact with each other. For example, for a type A individual, the probability they meet another type A individual is $\frac{k-1}{N-1}$, which gives a payoff of a. The probability they meet a type B individual is $\frac{N-k}{N-1}$, which gives a payoff of b. The background payoff gained from activities unrelated to the games is 1, and the intensity of selection is governed by $0 \leq w \leq 1$. A small w presents *weak selection*, meaning that the game has a minimal effect on fitness compared to the background payoff. At $w = 1$, the fitness is equal to the payoff in the game. Therefore, selection with respect to the game is strong, as it fully determines the fitness of the individuals. With the fitnesses calculated, we can determine the transition probabilities (1.6) and substitute them into (1.7). For small $w \approx 0$,

$$\frac{p_{i,i-1}}{p_{i,i+1}} \approx 1 + w\left(\frac{ak + (N-k)b}{N-1} - \frac{ck + (N-k-1)d}{N-1}\right) \tag{1.11}$$

Selection favours type A individuals if $\rho_A > \frac{1}{N}$. By substituting (1.11) into (1.7) and applying approximation methods, we have

$$a(N-2) + b(2N-1) > c(N+1) + d(2N-4)$$

Assuming a large population, we need only consider the terms multiplied by N, which gives

$$b < d \quad \text{and} \quad a + 2b < c + 2d$$

where the second equation can be simplified to $\frac{d-b}{a-c+d-b} < \frac{1}{3}$, which Taylor et al. (2004) referred to as the *rule of 1/3*. This states that selection favours a type A mutant fixating if the internal equilibrium point is less than $\frac{1}{3}$. Note that it was previously shown in section 1.2.2 that $\frac{d-b}{a-c+d-b}$ is an internal equilibrium using the replicator equation.

1.4 Evolutionary Graph Theory

Traditionally, developments in evolutionary game theory have often relied on the unrealistic assumption that populations are homogeneous, that is, all members of the population are equally likely to interact with one another. However, in reality, populations often exhibit heterogeneous structures, influencing the relationships among members of the population, as individuals are more likely to interact with neighbours in their local vicinity than with those who are distant. Recently, the process of modelling the evolution of structured populations using a graph, where individuals exclusively interact with their neighbours, was formalised as *Evolutionary graph theory* (Lieberman et al. 2005).

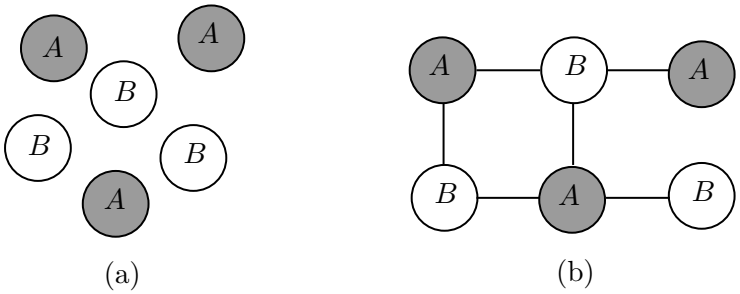

Figure 1.2: These two figures represent a population composed of type A and B individuals. Figure (a) shows an unstructured population where all individuals can interact with one another whereas figure (b) represents a structured population. The population is represented by a graph where the vertices represent individuals such that individuals can only interact with each other if they are connected.

The population structure is defined as follows. The matrix $W = [w_{ij}]$ determines the structure of the graph. Individuals are labelled $i = 1, 2, ..., N$ and are situated on the vertices of the graph. The probability that the offspring of individual i replaces individual j is given by $w_{ij} > 0$. If $w_{ij} = 0$ and $w_{ji} = 0$, then the vertices i and j are not connected; therefore, the individuals i and j cannot interact with each other. The BD-B dynamics used in the Moran process were adapted to be used in this evolutionary framework such that at each time step, an individual i is selected

to reproduce with probability proportional to its fitness (as in the Moran process) but its offspring replaces individual j and occupies its vertex with probability w_{ij}. The *temperature* measures how likely individuals are to be replaced and is given by

$$T_{ij} = \sum_{i=1}^{N} w_{ij} \tag{1.12}$$

Similar to the Moran process, it is possible to determine the fixation probability of a type A mutant within a structured population of type B residents. In some cases, an explicit solution can be derived such as in Broom & Rychtar (2008).

Lieberman et al. (2005) were able to generalise the Moran process to certain graph structures with specific properties by establishing the *isothermal theorem*, which states the fixation probability of a type A mutant, ρ_A, equals the Moran probability (1.8) if and only if the underlying graph is *isothermal*. A graph is said to be isothermal if every individual has the same temperature. This significant result allows us to classify structures that hold no influence on the evolutionary process. This result was further generalised in Lieberman et al. (2005) to all graph structures whose evolutionary behaviour matches that of the Moran process by the *circulation theorem*. The circulation theorem states that if a graph is a *circulation*, that is, the sum of the incoming weights is equal to the sum of the outgoing weights at each vertex, then ρ_A is equal to the Moran probability (1.8).

Lieberman et al. (2005) also provided examples of graphs that can act as either amplifiers or suppressors of selection. For example, consider the burst graph, where a central node has edges directed outward to other nodes. Regardless of the mutant's fitness, the fixation probability is always equal to $\frac{1}{N}$, as the individual occupying the central node will always fixate the population. In contrast, the super-star graph has the property that for any advantageous mutant ($r > 1$), the fixation probability of the mutant tends to one as $\mathrm{N} \to \infty$.

The significant advantage of evolutionary graph theory lies in its ability to consider a wide range of population structures (Antal & Scheuring 2006, Broom & Rychtar 2008, Shakarian et al. 2013, Maciejewski 2014, Hindersin & Traulsen 2014, Cuesta et al. 2017). Both population structure and evolutionary dynamics play influential roles in population evolution (Santos & Pacheco 2006, Broom & Rychtar 2008, Voorhees 2013, Tkadlec et al. 2020, Shakarian et al. 2012). In fact, heterogeneous structures are pivotal in facilitating the formation of clusters of cooperators

(Li et al. 2013).

Beyond evolutionary graph theory, structured population modelling has been widely applied in metapopulation and epidemic modelling. In metapopulations, communities naturally form due to migration and habitat segmentation (Hanski 1998). Typically, these models distinguish between within-community reproduction and between-community migration, which are referred as metapopulation dynamics. Yagoobi et al. (2023) recently provided a systematic classification of these dynamics. Further extensions have incorporated group-level events such as group splitting (Traulsen et al. 2008) and group reproduction (Akdeniz & van Veelen 2020), which entail the replacement of entire groups by other groups or by a single individual.

Epidemic modelling also makes extensive use of graphs to investigate the effects of network topology on the spread of infection and disease. The original models were developed by Kermack & McKendrick (1927, 1932, 1933), which act as a foundation for modern epidemiology. Subsequent work has extended this area to consider network structure Keeling & Eames (2005). More recent work on epidemic modelling has been explored on heterogeneous graphs (Ball & House 2017).

1.4.1 Modelling evolutionary games on graphs

The development of evolutionary graph theory enables the consideration of frequency-dependent fitness on heterogeneous structures (Santos & Pacheco 2006, Hadjichrysanthou et al. 2011, Ohtsuki et al. 2006). For example, Broom et al. (2010) applied the classical Hawk-Dove game on the three non-directed graphs: the star, the circle and the complete graph. They generated theoretical formuale for the exact solutions of fixation probabilities and also for the speed of the evolutionary processes, namely the *fixation time*, which was also studied in Frean et al. (2013).

Also, Ohtsuki et al. (2006) considered a two-player Public Goods game where players are required to cooperate to reach the optimal outcome. The payoff matrix is defined as

	A	B
A	$b-c$	$-c$
B	b	0

(1.13)

where the type A individuals are cooperators because they are willing to endure a cost c to provide a public good to the individual they are interacting with. Type B individuals are defectors because they never pay a cost and, therefore, do not

provide a public good to the individual they interact with. However, defectors will receive a public good if the individual they interact with is a cooperator. Consider a regular graph with k-degree, the payoff to a cooperator who is connected to i other cooperators is $bi - ck$. The payoff to a defector connected to j cooperators is bj. Therefore, the fitnesses of cooperators and defectors is given by

$$F_A = 1 - w + w(bi - ck), \quad F_B = 1 - w + wbj \tag{1.14}$$

Under weak selection i.e. small w, Ohtsuki et al. (2006) demonstrated that for a large population, the fixation probability of a mutant cooperator is greater than $1/N$ and of a mutant defector is less than $1/N$ if

$$\frac{b}{c} > k, \tag{1.15}$$

where k is the degree of the graph. This tells us that the more limited the connections on the graph, the easier it is for cooperation to spread, therefore, the complete graph is the most difficult regular graph for the spread of cooperation.

1.5 Multiplayer Games

The previous models we considered primarily focused on pairwise games, as many real-life conflicts often involve two participants, and valuable insights can be gained from analysing them. However, interactions in real life often involve several individuals, and this emphasis on pairwise games has created a notable gap in the study of multiplayer games within biological populations. The significant challenge lies in the mathematical framework and analysis required for multiplayer games, which are significantly more complex, making it difficult to derive generalisable results. For example, in species such as killer whales, cooperative behaviours such as collective hunting require coordination among all members of the group. However, not all whales may cooperate, and some may act selfishly, and hunt alone, which can affect the group's success. These types of interactions, where multiple individuals are involved, need to be captured by the mathematical theory to more accurately model real-life dynamics.

One of the earliest contributions to evolutionary multiplayer games was made by Palm (1984). However, the theoretical foundations of evolutionary multiplayer

games were substantially developed by Broom et al. (1997) who considered multiplayer matrix games specifically, *symmetric games*, meaning that there was no significance to the ordering of the players within the group interaction. Thus an individual's payoff depends only upon its strategy and the strategies of the other individuals. However, in *assymetric* games, the order of the players and their strategies affects the payoff. Gokhale & Traulsen (2010) demonstrated that if groups are wholly randomly selected from the population, then there is no real difference between symmetric and non-symmetric games and this was the assumption made in Broom et al. (1997), who considered an infinite population, where groups of m players were randomly selected to play a game (see also Bukowski & Miekisz (2004) and Gokhale & Traulsen (2014)). Under these assumptions, the ESS for an m-player game can be stated as follows: a strategy $\mathbf{p}$ in an m-player game is called an evolutionarily stable strategy against a strategy $\mathbf{q}$ if there is an $\epsilon_{\mathbf{q}} \in (0, 1]$ such that for all $\epsilon \in (0, \epsilon_{\mathbf{q}}]$

$$\mathcal{E}[\mathbf{p}; (1-\epsilon)\delta_{\mathbf{p}} + \epsilon\delta_{\mathbf{q}}] > \mathcal{E}[\mathbf{q}; (1-\epsilon)\delta_{\mathbf{p}} + \epsilon\delta_{\mathbf{q}}] \tag{1.16}$$

where

$$\mathcal{E}[\mathbf{x}; (1-\epsilon)\delta_{\mathbf{y}} + \epsilon\delta_{\mathbf{z}}] = \sum_{l=0}^{m-1} \binom{m-1}{l} (1-\epsilon)^l \epsilon^{m-1-l} E[\mathbf{x}; \mathbf{y}^l, \mathbf{z}^{m-1-l}]. \tag{1.17}$$

We say that $\mathbf{p}$ is an ESS for the game if for every $\mathbf{q} \neq \mathbf{p}$, there is $\epsilon_{\mathbf{q}} > 0$ such that (1.16) is satisfied for all $\epsilon \in (0, \epsilon_{\mathbf{q}}]$. (1.17) is derived under the assumption that groups within the infinite population are formed randomly, therefore the probability of a group with two strategies forming can be described by a binomial distribution. Gokhale & Traulsen (2010) extended this analysis to finite populations under the Moran process, where individuals participated in two-strategy, m-player matrix games. They were able to derive rules within finite populations on how the internal dynamics proceed. Also, Lessard (2011) considered the extension of the law of 1/3 from two-player to m-player games.

Similarly, as in (1.4), we have that for an m-player matrix game,the mixed strategy $\mathbf{p}$ is evolutionarily stable against $\mathbf{q}$ if and only if there is a $j \in \{0, 1, \ldots, m-1\}$ such that

$$E[\mathbf{p}; \mathbf{p}^{m-1-j}, \mathbf{q}^j] > E[\mathbf{q}; \mathbf{p}^{m-1-j}, \mathbf{q}^j], \tag{1.18}$$

$$E[\mathbf{p}; \mathbf{p}^{m-1-j}, \mathbf{q}^i] = E[\mathbf{q}; \mathbf{p}^{m-1-i}, \mathbf{q}^i] \text{ for all } i < j, \tag{1.19}$$

A strategy $\mathbf{p}$ is called an ESS at level J if, for every $\mathbf{q} \neq \mathbf{p}$, the conditions (1.18) and (1.19) are satisfied for some $j \leq J$ and there is at least one $\mathbf{q} \neq \mathbf{p}$ for which the conditions are met for $j = J$ precisely.

In recent years, m-player multiplayer games have been extensively explored in the mathematical literature. For instance, the evolution of cooperation in such games was examined by Platkowski & Bujnowski (2009) and Bach et al. (2006). Additionally, Souza et al. (2009) investigated m-player snowdrift games and extended the classical Hawk-Dove game to an m-player setting. From a dynamical perspective, multiplayer games have also been widely studied (Bukowski & Miekisz 2004, Platkowski 2004, Miekisz 2008).

Notation	*Description*
N	Size of the population
$I_1, \ldots, I_N$	List of individuals within population
M	Number of available places
$P_1, \ldots, P_M$	List of places
$\mathbf{X}(t)$	Matrix representing population distribution at time t
$X_{n,m}(t)$	Represents I_n's presence at place P_m at time t
$\mathbf{x}$	The current distribution of $\mathbf{X}(t)$
$x_{n,m}$	Represents I_n's presence at place P_m under the current distribution
$\mathbf{x}_{<t}$	The entire history of the evolutionary system
$p_{n,m,t}(\mathbf{x}_{<t})$	The probability of I_n being at place P_m at time t given $\mathbf{x}_{<t}$
$\mathcal{P}_n$	I_n's home range or territory
$R(n, \mathbf{x}, t, \mathbf{x}_{<t})$	Reward function
R_n	Mean reward

Table 1.1: Notation used in the Broom-Rychtar framework.

1.6 The Broom-Rychtář Framework

A significant limitation of evolutionary graph theory is its pairwise modelling of interactions, which fails to account for more realistic arbitrary multilayer game scenarios, thus lacking adaptability and realism. To address this limitation, recent research has developed a comprehensive modelling approach that enables the study of structured population evolution involving multiplayer contests, which we denote as the Broom-Rychtář framework (Broom & Rychtar 2012, Broom et al. 2015, Broom, Pattni & Rychtar 2019, Broom et al. 2021). The motivation behind the development of the Broom-Rychtář framework was to model arbitrary-sized group interactions in

overlapping territories observed in real life scenarios, such as in African wild dogs (Ginsberg & Macdonald 1990), roadrunners (Kelley et al. 2011), cheetahs (Marker et al. 2008), lynx (Schmidt et al. 1997) and chimpanzees (Herbinger et al. 2001). The framework assumes that there are N individuals distributed across M places, and group interactions occur whenever two or more individuals are present in the same place at the same time. The original paper by Broom & Rychtar (2012) focused primarily on defining the basic setup of the framework and developed examples of models, while the evolutionary dynamics were not implemented until Broom et al. Broom et al.. This robust framework serves as the foundation for the work presented in this thesis, and we first outline the framework in its full generality.

1.6.1 Structure

The population consists of N individuals, $I_1, ..., I_N$ who move stochastically and interact across M distinct places, $P_1, ..., P_M$. The distribution of individuals across the places is mathematically represented by the N x M binary matrix $\mathbf{X}(t) = (X_{n,m}(t))$ which gives the exact position of every individual within the population.

$$X_{n.m}(t) = \begin{cases} 1, & \text{if the individual } I_n \text{ is in place } P_m \text{ at time } t, \\ 0, & \text{otherwise.} \end{cases} \tag{1.20}$$

The n^{th} row of $\mathbf{X}$ represents individual I_n, and the m^{th} column represents place P_m. The probability of $\mathbf{X}(t)$ taking a particular value $\mathbf{x}$ can depend on the entire history of the evolutionary system, $\mathbf{x}_{<t} = (\mathbf{x}_1, ..., \mathbf{x}_{t-1})$ which is expressed as a conditional distribution

$$P(\mathbf{X}(t) = \mathbf{x})(\mathbf{x}_{<t}) = P(\mathbf{X}(t) = \mathbf{x})|\mathbf{X}(1) = \mathbf{x}_1, ..., \mathbf{X}(t-1) = \mathbf{x}_{t-1}). \tag{1.21}$$

Given that, at any time t, an individual must be at exactly one place (as the places are distinct), every evolutionary system constructed under this framework must satisfy the following property

$$\sum_{\mathbf{x}} P(\mathbf{X}(t) = \mathbf{x})(\mathbf{x}_{<t}) = 1 \quad \forall t, \mathbf{x}_{<t}. \tag{1.22}$$

In addition to describing the population as a whole, the framework also captures the movements and position of any individual. The probability of I_n being at place

P_m at time t, conditional on the history of the system $\mathbf{x}_{<t}$ is given by

$$P(X_{m,n}(t) = 1)(\mathbf{x}_{<t}) = p_{n,m,t}(\mathbf{x}_{<t}) \tag{1.23}$$

Since any individual can only be present at one location at any time, every system must satisfy the property

$$\sum_m p_{n,m,t}(\mathbf{x}_{<t}) = 1 \quad \forall n, t, \mathbf{x}_{<t}. \tag{1.24}$$

Some individuals may not be able to move to certain places, therefore, each individual I_n has a subset of places they can move to, referred to as their *home range* or *territory*.

$$\mathcal{P}_n = \{P_m : p_{n,m,t}(\mathbf{x}_{<t}) > 0, \text{ for some } t \text{ and some history } \mathbf{x}_{<t}\}. \tag{1.25}$$

This represents the set of places that individual I_n has a non-zero probability of visiting at some point in time.

History-dependence

The complexity of the framework can vary based on the specific assumptions made about the movement of individuals. For example, the movement of individuals can be defined such that it depends on the history of the system. This allows for a vast range of evolutionary models therefore Broom & Rychtar (2012) also considered varying levels of dependency on movement distributions which include the following:

- *History independent*: This represents the simplest level of dependency, where the current distribution of the population is entirely independent of all previous distributions in the evolutionary process. The population distribution is expressed as

$$P(\mathbf{X}(t) = \mathbf{x})(\mathbf{x}_{<t}) = P(\mathbf{X}(t) = \mathbf{x}) \tag{1.26}$$

- *Markov*: The current population distribution at time t depends only on the previous distribution at time $t-1$, which is expressed as

$$P(\mathbf{X}(t) = \mathbf{x})(\mathbf{x}_{<t}) = P(\mathbf{X}(t) = \mathbf{x}|\mathbf{X}(t-1) = \mathbf{x}_{t-1}) \tag{1.27}$$

- *Entire history-dependence*: The current population distribution depends on all previous distributions since the beginning of the evolutionary process. This is the case discussed earlier (1.21).

Row-dependence

The notion of *row independence* was defined as individuals moving independently of one another at time t. If two individuals, I_{n_1} and I_{n_2} move to places P_{m_1} and P_{m_2}, respectively, then we have

$$P(X_{n_1,m_1}(t) = 1 \text{ and } X_{n_2,m_2}(t) = 1)(\mathbf{x}_{<t}) = p_{n_1,m_1,t}(\mathbf{x}_{<t})p_{n_2,m_2,t}(\mathbf{x}_{<t}). \quad (1.28)$$

Complete independence

The simplest case developed from the framework is the fully independent model (see Fig.1.3), which assumes that the movement of individuals is independent of the previous population distributions and that individuals move independently of one another. Consider a population of N individuals $I_1, ..., I_N$ who can move between M places $P_1, ..., P_M$. The probability of individual I_n being at place P_m is denoted by p_{nm}; see Fig.1.3 for a visual representation using a bi-partite graph. Individuals move along the graph according to their own movement distributions and form groups on the vertices of the graph. Let G denote a group of individuals, then $\chi(m, G)$, the probability of group G forming at place P_m is given by

$$\chi(m, G) = \prod_{i \in G} p_{im} \prod_{j \notin G} (1 - p_{jm}). \quad (1.29)$$

In Broom & Rychtar (2012), the mean group size from the individual's perspective was found to be

$$\bar{G} = \sum_m \sum_G \frac{\chi(m, G)|G|^2}{\sum_m \sum_G \chi(m, G)|G|}. \quad (1.30)$$

1.6.2 Fitness

To model the evolution of a population, we must evaluate the fitnesses of the individuals. In general, the *reward* individual I_n receives from playing a game at time t, given the current distribution of individuals $\mathbf{X}(t) = \mathbf{x}$ and the previous distributions

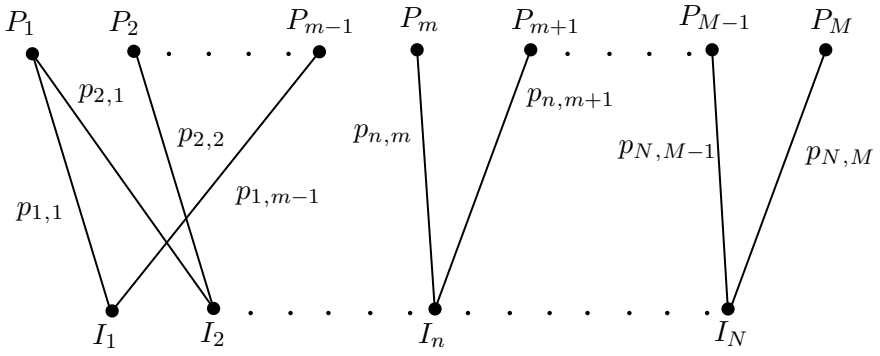

Figure 1.3: The fully independent model from (Broom and Rychtar 2012). There are N individuals who are distributed over M places such that I_n visits place P_m with probability p_{nm}. Individuals interact with one another when they meet, for example, I_1 and I_2 can interact with one another when they meet in P_1

$\mathbf{x}_{<t}$ was denoted as

$$R(n, \mathbf{x}, t, \mathbf{x}_{<t},) \tag{1.31}$$

The *mean reward* is the average reward over all possible population distributions at time t conditional on the previous distributions of the population.

$$R_n = \sum_{\mathbf{x}} \mathbb{P}(\mathbf{X}(t) = \mathbf{x}) R(n, \mathbf{x}, t, \mathbf{x}_{<t}). \tag{1.32}$$

Under the fully-independent model, individual I_n's average fitness is calculated by considering all payoffs they can receive averaged over all possible groups and places,

$$F_n = \sum_{m} \sum_{\substack{G \\ n \in G}} \chi(m, G) R_{n,m,G}. \tag{1.33}$$

1.6.3 Evolutionary updating rules

The evolutionary dynamics of structured populations are based on the Moran process, ensuring that the population size remains constant. In Broom et al. (2015), the development of the Broom-Rychtar framework was completed through the introduction of evolutionary dynamics into the *territorial raider model*. This framework was later extended to include the six main updating mechanisms, analogous to those commonly used in evolutionary graph theory (Pattni et al. 2017). Incorporating these dynamics into the Broom-Rychtar framework offers a significant advantage, as it remains accessible to those familiar with evolutionary graph theory, ensuring continuity between the results from evolutionary graph theory and the Broom-Rychtar

framework.

Dynamics

BDB	$b_i = \frac{F_i}{\sum_n F_n}$,	$d_{ij} = \frac{w_{ij}}{\sum_n w_{in}}$	BDD	$b_i = \frac{1}{N}$,	$d_{ij} = \frac{w_{ij}F_j^{-1}}{\sum_n w_{in}F_n^{-1}}$
DBD	$d_j = \frac{F_j^{-1}}{\sum_n F_n^{-1}}$,	$b_{ij} = \frac{w_{ij}}{\sum_n w_{nj}}$	DBB	$d_j = \frac{1}{N}$,	$b_{ij} = \frac{w_{ij}F_i}{\sum_n w_{nj}F_n}$
LB	$\tau_{ij} = \frac{w_{ij}F_i}{\sum_{n,k} w_{nk}F_n}$		LD	$\tau_{ij} = \frac{w_{ij}F_j^{-1}}{\sum_{n,k} w_{nk}F_k^{-1}}$	

Table 1.2: Dynamics defined using the evolutionary graph $\mathbf{W}_t$ and fitnesses $F_{n,t}$.

1. *BDB or IP dynamics* (Lieberman et al. 2005): an individual is first selected for reproduction with probability proportional to its fitness and its offspring randomly replaces another member of the group.

2. *BDD dynamics* (Masuda 2009): an individual is first randomly chosen for reproduction and its offspring replaces another member of the group with probability inversely proportional to their fitness.

3. *DBD dynamics* (Antal & Scheuring 2006): an individual is first selected for death with probability inversely proportional to their fitness and is replaced by the offspring of another member of the group who is randomly chosen to reproduce.

4. *DBB dynamics* (Ohtsuki et al. 2006): an individual is first randomly chosen for death and is replaced by the offspring of another member of the group who is selected to reproduce with probability proportional to their fitness.

5. *LB dynamics* (Masuda & Ohtsuki 2009): each edge is considered separately in each direction, and weighted proportionally to its undirected weight and the fitness of the origin vertex. A weighted edge is then selected at random, with the origin individual replacing the destination one.

6. *LD dynamics* (Masuda & Ohtsuki 2009): each edge is considered separately in each direction, and weighted proportionally to its undirected weight and the inverse fitness of the destination vertex. A weighted edge is then selected at random, with the origin individual replacing the destination one.

1.7 The development of the Territorial Raider model

Different examples using the fully independent model were developed in Broom & Rychtar (2012). The most significant of these is the territorial raider model, see Fig1.4, which has been extensively explored (Broom et al. 2015, Pattni et al. 2017, Schimit et al. 2019, Erovenko et al. 2019, Schimit et al. 2022, Pires et al. 2023, Erovenko & Broom 2024). This model acts as the evolutionary setting for the work in this thesis.

1.7.1 Population structure

In the territorial raider model, there are N individuals, $I_1, ...I_N$ who can move and interact with other individuals at M places $P_1, ..., P_M$. It is assumed individual I_i lives at place P_m throughout the entire evolutionary process. In the original territorial raider model from Broom & Rychtar (2012) there was a one-to-one correspondence between individuals and places, although this was later generalised in Pattni et al. (2017) to include subpopulations of individuals at the same place, and further explored in Pires & Broom (2024). The amount of time an individual spends on their home vertex is governed by a global home fidelity parameter h, which is a measure of preference individuals have towards staying on their home vertex. The higher h is, the more likely individuals are to stay at home and, therefore, less likely to move and interact with other individuals and vice-versa. Given an individual I_i with m neighbouring places, the probability of I_i staying home is $h/(h+m)$ and moving is $m/(h+m)$. If $h = 1$, this represents an indifference individuals have between all reachable places and means that they are equally likely to visit any of them and if the base graph is the complete graph, this is a *completely mixed population.*

1.7.2 Evolutionary updating process

An evolutionary graph (Lieberman et al. 2005, Nowak 2006, Pattni et al. 2015, Voorhees & Murray 2013, Möller et al. 2019) is a graph with an associated weighted adjacency matrix $\mathbf{W} = (\mathbf{w_{ij}})$ where $w_{ij} \in [0, 1)$ is referred to as the replacement weight which governs which members of the population can replace each other. Every vertex v_n of the evolutionary graph is occupied by exactly one individual and if $w_{ij} > 0$, then the individual on v_i can replace the current individual on v_j by placing a copy of itself onto the vertex. The weights are often selected to ensure

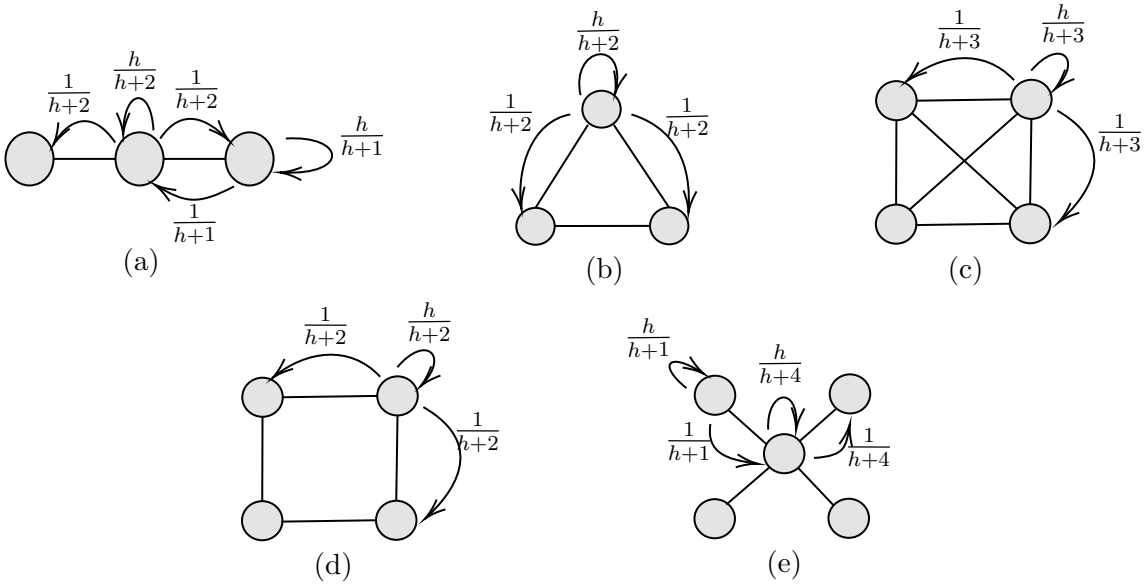

Figure 1.4: The population structures and apriori distributions for small graphs with three, four and five nodes. An individual remains on their home vertex with probability $\frac{h}{h+m}$ and moves to a neighbouring vertex with probability $\frac{1}{h+m}$, where m is the number of neighbours. (a) the line with three nodes. (b) the complete triangle graph. (c) the square with both diagonals connected i.e. the complete graph with four vertices. (d) the circle graph with four nodes. (e) the star graph with 5 nodes.

that the evolutionary graph is strongly connected i.e. there is a finite path between vertices v_i and v_j.

A general set of evolutionary dynamics for the Broom-Rychtář framework, analogous to the corresponding evolutionary graph theory dynamics (defined in section 1.6.3), were successfully adapted into the territorial raider model in Pattni et al. (2017) via the appropriate selection of the replacement weights.

The replacement weights within this framework are based on the assumption that an offspring of individual I_i will replace individual I_j with probability proportional to the time I_i and I_j spend together. The offspring of I_i can also replace its parent I_i, and it does so with probability proportional to the time I_i spends on its own. When $i \neq j$ The probability of individuals I_i and I_j meeting is given by summing all $\chi(m, \mathcal{G})$ over all m such that $I_i, I_j \in G$. We assume that I_i spends an equal amount of time with all other members of group $\mathcal{G}$, therefore we weight by $1/(|\mathcal{G}| - 1)$ as there are $|\mathcal{G}| - 1$ other members of the group. However, when $i = j$, we sum $\chi(m, \mathcal{G})$ over all m such that $\mathcal{G} = \{i\}$. Here there is no need to weight $\chi(m, \mathcal{G})$ because I_i is alone. The replacements weights are thus given as

$$w_{ij} = \begin{cases} \sum_m \sum_{\substack{G \\ i,j \in G}} \frac{\chi(m,G)}{|G|-1}, & i \neq j, \\ \sum_m \chi(m, \{i\}), & i = j. \end{cases} \tag{1.34}$$

1.7.3 The fixation probability

To determine the likelihood of the evolutionary success of a particular strategy within a finite population, we calculate its fixation probability. The fixation probability is regarded as the most significant quantity of a finite evolutionary process. To calculate the fixation probability of a type A mutant within a population of type B residents on a given spatial structure, the first step is to list all of the states that describe all of the possible distributions of individuals of both types on the different places throughout the evolutionary process, from the insertion of a type A mutant in a population of type B residents until its fixation or extinction. Not accounting for symmetries, a given population structure N individuals yields an evolutionary process with 2^N different states that are indexed by subsets $S \subset \{1, 2, ..., N\}$. State $\emptyset$ represents a population composed entirely of type B individuals, and state N represents a population composed of type A individuals only. Let $P_{SS'}$ denote the transition probability from state S to state S' during the evolutionary process.

$$P_{SS'} = \begin{cases} \sum_{i \notin S} b_i d_{ij}; & \text{if } S' = Sn\{j\} \text{ for some } j \in S \\ \sum_{i \in S} b_i d_{ij}; & \text{if } S' = S \cup \{j\} \text{ for some } j \notin S \\ 0 & \text{otherwise} \end{cases} \tag{1.35}$$

and, therefore,

$$P_{SS} = 1 - \sum_{S' \neq S} P_{SS'}. \tag{1.36}$$

The fixation probability of a type A mutant from state S is

$$\rho_S^A = \sum_{S \subset \{1,2,...,N\}} P_{SS'} \rho_{S'}^A. \tag{1.37}$$

with boundary conditions

$$\rho_\emptyset^A = 0, \tag{1.38}$$

$$\rho_N^A = 1. \tag{1.39}$$

The mean fixation probability of a type A mutant, will be a weighted average of the fixation probabilities from all states involving only one type A mutant.

1.7.4 Multiplayer games

Different multiplayer games can be used to model the interactions between individuals within the same group. For example, the Public Goods, Hawk-Dove and Stag-Hunt games shown in Figure 1.5. Each of the games describes a contest between two different types of individuals, $\mathcal{A}$ and $\mathcal{B}$. Using these games, we will describe an evolutionary process of a single type $\mathcal{A}$ individual within a population of $\mathcal{B}$s and vice-versa to determine the fixation probability for both types of individuals.

The Multiplayer Public Goods Game

The multiplayer public goods game consists of two types of individuals, cooperators ($\mathcal{A}$) and defectors ($\mathcal{B}$). The cooperator pays a cost of C which is shared among the rest of the group as a reward V but not shared among the individual who paid the cost. Defectors pay no cost and cooperators pay a cost even when they are alone. After a game is played between a group of a cooperators and b defectors, the payoffs for a cooperator and defector are respectively

$$R^{\mathcal{A}}_{a,b} = \begin{cases} R - C, & a = 1, \\ R - C + \left(\frac{a-1}{a+b-1}\right)V, & a > 1, \end{cases} \tag{1.40}$$

$$R^{\mathcal{B}}_{a,b} = \begin{cases} R, & a = 0, \\ R + \left(\frac{a}{a+b-1}\right)V, & a > 0. \end{cases} \tag{1.41}$$

where R is the background payoffs individuals receive unrelated to the games. The public good game presented here is one of many variations with other cooperative strategy games (Archetti & Scheuring 2012, Kurokawa & Ihara 2009, 2013, Santos et al. 2008*a*, Souza et al. 2009, Milinski et al. 2006, Li et al. 2016).

The Multiplayer Hawk-Dove Game

The Hawk-Dove game was developed by Maynard Smith & Price (1973) and attempts to explain the occasional use of violence in contests over valuable resources between animals such as in populations of red deer (Clutton-Brock & Albon 1979).

$\mathcal{A}$ represents the Hawk strategy, and $\mathcal{B}$ the Dove strategy. When individuals meet, they compete for a reward V. If all individuals in the group are Doves, then they all split the reward equally. If any hawks are present, then the doves concede and the hawks fight, with the winner receiving the reward of V while the losing hawks pay a cost of C. All individuals receive a background payoff of R, a reward gained from activities unrelated to the contests. In a group of a hawks and b doves, the average payoffs are given by

$$R^{\mathcal{A}}_{a,b} = R + \frac{V - (a-1)C}{a}, \tag{1.42}$$

$$R^{\mathcal{B}}_{a,b} = \begin{cases} R, & \text{if } a > 0, \\ R + \frac{V}{b}, & \text{if } a = 0. \end{cases} \tag{1.43}$$

The Multiplayer Stag-Hunt Game

The Stag-Hunt game (Pacheco et al. 2009, Broom et al. 2018) consists of two types of individuals, cooperators ($\mathcal{A}$) and defectors ($\mathcal{B}$). The payoff functions are step functions where $L > 1$ cooperators are required to group together for the public good to be produced. The cooperators always pay a cost C regardless of whether the threshold is met or not. In a group of x cooperators and y defectors, the payoffs are given by

$$R^{\mathcal{A}}_{x,y} = \begin{cases} R - C, & x < L \\ R - C + \left(\frac{x}{x+y}\right)V, & x \geq L \end{cases} \tag{1.44}$$

$$R^{\mathcal{B}}_{x,y} = \begin{cases} R, & x < L \\ R + \left(\frac{x}{x+y}\right)V, & x \geq L \end{cases} \tag{1.45}$$

1.8 History-dependence: Markov Movement Model

The Markov movement model was introduced to investigate whether cooperation can emerge in evolutionary settings where individuals can move strategically. In these models, individuals assess their current position, choosing to remain if it is advantageous or relocate otherwise. While similar strategic movement as been explored in previous studies (Aktipis 2004, 2011), these did not account for multiplayer interactions. Thus, the Markov movement model provides a deeper understanding of how strategic movement influences the evolution of cooperation in a multiplayer

Public-Goods game

	A	B
A	$R-C+V$	$R-C$
B	$R+V$	R

$$R^A_{a,b} = \begin{cases} R-C, & a=1 \\ R-C+[\frac{a-1}{a+b-1}]V, & a>1 \end{cases}$$

$$R^B_{a,b} = \begin{cases} R, & a=0 \\ R+[\frac{a}{a+b-1}]V, & a>1 \end{cases}$$

Hawk-Dove game

	A	B
A	$R+\frac{V-C}{2}$	$R+V$
B	R	$R+\frac{V}{2}$

$$R^A_{a,b} = R + \frac{V-(a-1)C}{a},$$

$$R^B_{a,b} = \begin{cases} R, & a>0 \\ R+\frac{V}{b}, & a=0 \end{cases}$$

Stag-Hunt game

	A	B
A	$R-C+V$	$R-C$
B	R	R

$$R^A_{a,b} = \begin{cases} R-C, & a<L \\ R-C+[\frac{a}{a+b}]V, & a\geq L \end{cases}$$

$$R^B_{a,b} = \begin{cases} R, & a<L \\ R+[\frac{a}{a+b}]V, & a\geq L \end{cases}$$

Figure 1.5: Payoffs for the pairwise and multiplayer versions of the Public Goods, Hawk–Dove, and Stag–Hunt games. In the Public Goods game, strategy A corresponds to cooperation and B to defection, with a denoting the number of cooperators and b the number of defectors in the group. In the Hawk–Dove game, A represents hawks and B represents doves, where a is the number of hawks and b the number of doves within the group. In the Stag–Hunt game, A corresponds to the cooperative strategy and B represents the defectors' strategy, with a denoting the number of cooperators and b the number of defectors in the group.

setting.

Building on this idea, Pattni et al. (2018) extended the territorial raider model to consider an evolutionary process in which the movement of individuals is history-dependent. That is, individuals explore their environment following a Markov process, moving through an exploration phase consisting of a fixed number of movement steps. During each movement step, all individuals independently decide whether to move or remain in the same position. Individuals that end up in the same position after a movement step play a multiplayer public goods game and receive a payoff (1.40) (1.41). At the end of the exploration phase, the payoffs are accumulated to give the individuals' fitness. All individuals then return to their home vertices, and the dynamic time step begins, during which reproduction and replacement occur (governed by a BDB process). The fitness values are then reset, and a new

exploration phase begins.

Each individual within the population has two traits: the interactive strategy used in the public goods game (cooperate or defect) and the exploration strategy (staying propensity). The staying propensity corresponds to the probability that an individual stays at their current location or moves, based on their exploration strategy and the current state of their environment.

During a movement step in the exploration phase, every individual evaluates the attractiveness of the group they are currently in. If the group is deemed attractive, the individual is more likely to remain within it. Otherwise, if the group is considered unattractive, the individual leaves and moves elsewhere. Let $\mathcal{G}_n(\mathbf{m}_{t-1})$ denote the group of individual I_n at time $t-1$. The attractiveness of the group to individual I_n (who is a member of the group) was defined as

$$\beta_{\mathcal{G}_n(\mathbf{m}_{t-1})n\{n\}} = \sum_{k \in \mathcal{G}_n(\mathbf{m}_{t-1})} \beta_k, \tag{1.46}$$

where β_k represents the attractiveness of group member I_k. The attractiveness of an individual depends on their interactive strategy and was defined as

$$\beta_k = \begin{cases} \beta_{\mathcal{C}}, \text{ if } I_k \text{ is a cooperator,} \\ \beta_{\mathcal{D}}, \text{ if } I_k \text{ is a cooperator,} \end{cases} \tag{1.47}$$

and the values $\beta_{\mathcal{C}} = 1$ and $\beta_{\mathcal{D}} = -1$ were used. α_n was denoted as the staying propensity of I_n. The probability $h_n(\mathcal{G}_n(\mathbf{m}_{t-1}))$ that individual I_n remained at its current location at time $t-1$, as a member of the group $\mathcal{G}_n(\mathbf{m}_{t-1})$, was expressed as a sigmoid function, given by

$$h_n(\mathcal{G}_n(\mathbf{m}_{t-1})) = \frac{\alpha_n}{\alpha_n + (1-\alpha_n)S^{\beta_{\mathcal{G}_n(\mathbf{m}_{t-1})n\{n\}}}}, \tag{1.48}$$

where $0 < S < 1$ represents the sensitivity to group composition. The greater the value of S, the less sensitive individuals are to group composition, meaning they are less likely to react to changes in their group's composition. The staying propensity α_n in the Markov model is analogous to the home fidelity parameter in the territorial raider model discussed in section 1.7. However, in the Markov movement model, the staying propensity is an evolving trait associated with individuals, whereas the home fidelity parameter in the territorial raider model is a fixed parameter of the model.

Every individual incurs a cost λ for every movement they make. The movement cost is carefully chosen to ensure it does not exceed the payoff individuals receive from the games, as this could result in a negative fitness.

Pattni et al. (2018) demonstrated that on complete networks, cooperation can evolve under BDB dynamics, despite the fact that traditional evolutionary graph theory does not support the evolution under such processes (Ohtsuki et al. 2006). This emphasises the crucial role of the Markov movement model in facilitating cooperative behaviour. Additionally, longer exploration times, lower movement costs and larger population sizes were found to further promote the evolution of cooperation. Another key finding was that the type of evolutionary dynamics governing population evolution had little impact on the outcome..

Erovenko et al. (2019) extended this process to consider heterogeneous structures, such as the circle and star graphs, which played a crucial role in evolutionary outcomes. The stability of cooperators within the population was determined by network structure. On complete networks, cooperators always resisted replacement from defectors if the population was sufficiently large. On the circle graph, there existed an intermediate movement cost threshold: lower costs promoted cooperation, while higher costs hindered it. In contrast, on the star graph, defectors always replaced cooperators.

This was further explored by Pires et al. (2023), who conducted a comprehensive analysis comparing six distinct evolutionary dynamics discussed in 1.6.3. Their findings demonstrated that different dynamics produced similar results, suggesting that network structure plays a more significant role than the specific dynamics considered.

1.9 Row-dependent movement

Coordinated movement is vital for the survival of many organisms, particularly in higher-order animals, where it is driven by various factors such as seasonal migration, resource acquisition and mating opportunities (Dingle 2006, Dingle & Drake 2007). The mechanisms underlying such movement patterns have long been studied (Dingle 2014). Social interactions often influence migration patterns, facilitating collective decision-making and synchronised movement among individuals (Petit & Bon 2010, Guttal & Couzin 2010) . Aggregation behaviours, observed in bird flocks, fish schools

and mammalian hunting groups, arise due to factors like safety, foraging efficiency and resource availability (Fretwell & Lucas 1969, Ford & Swearer 2013). These factors create a complex interplay between aggregation and interactive strategies.

A structured way to model coordinated movement is through row-dependent movement, where an individual's movement is influenced by the movement of others. Broom et al. (2020) introduced various row-dependent movement mechanisms to represent realistic herding and dispersal behaviours. Their work developed a general movement framework that integrates both well-established and novel concepts of aggregation and dispersal, accounting for how these processes depend on the presence of conspecifics. The models were designed to be adaptable, enabling integration into broader evolutionary modelling frameworks, particularly that of Broom & Rychtar (2012). The work of Broom et al. (2020) forms a fundamental basis for this thesis. Therefore, we provide a detailed explanation of the row-dependent models developed in their study.

The row-dependent movement models serve two purposes; firstly to represent certain movement mechanisms that lead to a particular distribution of individuals over the places, and secondly to model movement distributions with certain coordinated movement properties. In our analysis, we will consider a target *apriori* distribution, denoted by a_m, representing the probability of a randomly selected individual going to any particular place. Our processes will be designed to achieve this target whilst moving non-independently, for example to maximise herding or dispersal. Processes where the target distribution matches the apriori distribution were called *faithful* (Broom et al. 2020).

For example, for the territorial raider model on a complete graph with M vertices, the apriori distribution for any individual staying at home is $\frac{h}{h+M-1}$ and moving to a specific neighbouring vertex is $\frac{1}{h+M-1}$. More generally, we can select an appropriate apriori distribution to any given movement scenario.

Broom et al. (2020) also derived novel measures of aggregation. The most significant of these measures was denoted as T which is the probability of two individuals being together which is one of the most fundamental properties of any movement process, given by

$$T = \frac{1}{N(N-1)} \sum_{m=1}^{M} E[X_m(X_m - 1)], \tag{1.49}$$

where X_m denotes the number of individuals on place P_m.

We first consider two movement processes where individuals are placed sequentially based on their utility functions (Broom et al. 2020). It is assumed that there is a set of utility functions $\{U_m\}$ based upon several place characteristics. The form of the utility function U_m varies according to the movement distribution governing the evolutionary process. The first type of movement we consider is deterministic movement, where individuals simply move to the location which provides them with the most utility. The second is the stochastic counterpart, in the form of a polya-urn model, where an individual will have a higher probability of moving to a place that provides them with a larger utility. Then we consider a more novel type of movement, that simultaneously places all moving individuals.

1.9.1 Deterministic movement: follow the majority

In this process, individual allocation to places is decided sequentially. This represents a simultaneous movement of the group, however, so that the first step of the process is to assign the ordering uniformly at random over all possible orderings (or if simulating a large population, make selection among the remaining individuals at each step of the sequence with uniform probability).

The type of deterministic movement we consider is the *follow the majority* movement process where the first individual moves to a place according to its apriori distribution and subsequent individuals simply move to the location containing the largest number of individuals. This mathematically translates to any increasing function, but the simplest example was considered (Broom et al. 2020) which we also use. The utility an individual receives from place P_m is given by

$$U_m = Y_m + 1, \tag{1.50}$$

where Y_m is the current number of occupants on place P_m. Such herding movement has been observed in various animal groups, for example, in fish schools and bird flocks, the trajectories of individuals are influenced by their own preferences and the movement of their neighbours, which can result in collective movement towards a particular direction (Couzin et al. 2005, Hinz & de Polavieja 2017, Winklmayr et al. 2020). In particular, three-spine sticklebacks (Gasterosteus aculeatus) exhibit threshold movement responses, effectively implementing a majority rule dependent on the presence of conspecifics in their movement decisions (Ward et al. 2008).

For a well-mixed process (equivalent to a territorial raider model on a complete graph with $h = 1$) this leads to all individuals being in a single group, the location of which follows the apriori distribution. We note that if $h \neq 1$ we need a variant of this process to achieve the target apriori distribution, as we see in section 2.3.1.

1.9.2 Probabilistic movement: the Polya-urn

Here, we consider a stochastic counterpart to follow the majority, where individuals move to a place P_m with probability proportional to their utility function i.e. an individual moves to place P_m with probability $U_m / \sum_k U_k$. This probabilistic model is represented by a standard urn model (Johnson & Kotz 1977), where balls are numbered $1, 2, ..., M$ and placed into an urn and then sequentially drawn out at random. The n^{th} ball with number m being drawn out correspond to the n^{th} individual moving to place P_m. As utility positively correlates with place occupancy, an extra ball with the same number is placed back into the urn alongside the original ball. This is represented by the following utility function

$$U_m = Ba_m + Y_m, \tag{1.51}$$

where $B \in (0, \infty)$ corresponds to the initial number of balls in the urn, and a_m is the apriori probability distribution. The scaling parameter B moderates the dependency social aggregation has on population density. Ba_m represents the initial number of balls in the urn corresponding to place P_m. Note that as we are simply selecting the place following a probability distribution rather than actually picking out balls, there is no requirement for this number to be integer-valued.

This type of movement is commonly observed in ant colonies. Ants leave pheromones as they travel and can sense the concentration of pheromones present on different paths. When presented with several options, an ant is more likely to choose the path with a higher pheromone concentration. Consequently, a path frequently travelled by preceding ants, and therefore marked with a higher pheromone concentration, becomes the preferred route for subsequent ants (Deneubourg et al. 1990, Dorigo & Stützle 2004). Polya-urn processes have been used to model the movement and following behaviour of ants (Shah et al. 2010).

1.9.3 The wheel and base model

Whereas in the previous models, an underlying movement mechanism had sequentially allocated individuals onto the places, the wheel and base model assumes a simultaneous allocation of all individuals partaking in the movement process. We suppose a base disc of perimeter 1 is divided into M place $P_1, ..., P_M$ in the shape of wedges where P_m has perimeter length a_m (see Fig.1.6(a)) such that $\sum_m a_m = 1$. On top of the base disc, is an upper disc, the wheel representing the N individuals in the form of N spikes; see Fig.1.6(b). The angle between individuals I_i and I_j is given by $2\pi\theta_{ij}$, where $\theta_{ij} \in [-1/2, 1/2]$ can possibly be determined via a probability distribution. Note that $\theta_{ij} = -\theta_{ji}$. When the angles between the spikes have been set, the wheel is spun and rotates by an angle of θ selected uniformly at random. Then, individual I_i moves to place P_m if and only if the corresponding spike lands above the corresponding segment; see Fig.1.6(c). This movement mechanism offers the greatest flexibility and provides a clearer representation of complete aggregation amongst individuals ($\theta = 0$). For a well-mixed process (equivalent to a territorial

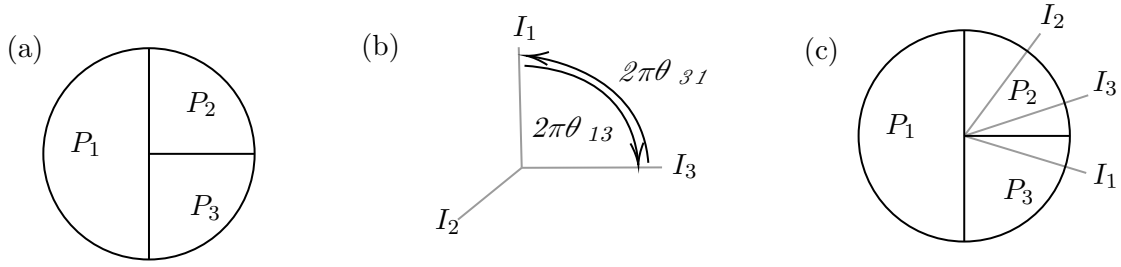

Figure 1.6: (a) $M = 3$ places with $a_1 = \frac{1}{3}, a_2 = \frac{1}{6}, a_3 = \frac{1}{2}$. (b) represents the $N = 3$ individuals as spikes. The angle between individuals I_i and I_j is given by $2\pi\theta_{ij}$. In this case, $\theta_{12} = \frac{1}{4} = -\theta_{21}$. (c) shows the simultaneous placement of all individuals after the upper disc is spun on top of the base. In this case, individuals I_1, I_2, I_3 move to places P_3, P_1, P_3 respectively.

raider model on a complete graph with $h = 1$), individuals move simultaneously, and θ can capture varying degrees of separation. This allows the model to represent realistic cases where individuals prefer specific distances of separation. For example, surf scoters rarely approach closer than one body length, typically maintaining around 1.45 body lengths apart (Lukeman et al. 2010).

1.10 Outline

We provide an outline of the research carried out in this thesis, pointing out published papers where applicable. In chapter 2, we develop a general movement

methodology that enables the embedding of any of the considered row-dependent movement mechanisms from section 1.9 into the evolutionary setting of the territorial raider model described in section 1.7. This work establishes a new direction in the territorial raider model by investigating the effects of coordinated movement on the evolution of cooperation. The results in this chapter were published in the *Journal of Mathematical Biology* (Haq et al. 2024). I developed the theory with my supervisor Mark Broom. I carried out the majority of the analysis and writing in this paper. The underlying theory was computationally translated by our collaborator, Pedro H. T. Schimit, who extended the simulation system used in previous work (Schimit et al. 2019, 2022) to incorporate our movement methodology. I then tested the system and used the system to conduct a numerical analysis.

In chapter 3, we build on the movement methodology developed in chapter 2 to investigate the effects of row-dependent movement on key predictors of fixation probability, namely, temperature and mean group size. We also implement the stag-hunt game into the model to examine a scenario where selection favours the evolution of cooperation within a well-mixed population. The work presented in this chapter was published in *Dynamic Games and Applications* (Haq et al. 2025). I developed the original theory with my supervisor, Mark Broom, and carried out the majority of the analysis and writing for this paper. The numerical analysis was conducted using the computational system developed by our collaborator, Pedro H. T. Schimit, as part of our earlier work (Haq et al. 2024).

In chapter 4, we extend our models to consider incomplete networks. We demonstrate that certain properties of our movement methodology developed in chapter 2 no longer hold under sequential movement processes. We also extend the wheel process for incomplete graph structures and develop an alignment algorithm to approximate herding behaviour. We also derive upper and lower bounds for a novel measure, T_{max} which quantifies the maximum probability of two individuals being together for any movement process. I developed the original theory with my supervisor, Mark Broom. The wheel alignment process for line and circle graphs was implemented by Pedro H. T. Schimit, and I carried out testing and analysis of the simulations. This work has not yet been published, but we intend to prepare a paper based on this chapter, for publication in the near future.

The final chapter explores hybrid models that combine row-dependent movement processes within the same evolutionary process. While work presented is prelimi-

nary, we believe it holds significant potential for future investigation. We provide analytical and numerical results under these hybrid models, offering a foundation for further exploration of their impact on evolutionary processes. Below, the table defines the parameters used and explored within this thesis.

Notation	*Description*
N	Size of the population
$I_1, \ldots, I_N$	List of individuals within population
M	Number of available places
$P_1, \ldots, P_M$	List of places
h	Home fidelity parameter
$\|G\|$	Size of group G
F_i	Fitness of Individual i
b_i	Probability of individual i reproducing
d_{ij}	Probability of individual i's offspring replacing individual j given individual i was selected to reproduce
τ_i	Temperature at vertex i
ρ_1^M	Fixation probability of a single mutant
B	Number of balls within the Polya-urn model that moderates social aggregation
θ	Represents the angle between the spikes in the wheel model
T	Probability of two individuals being together
T_{max}	The maximum possible probability of two individuals being together for all movement processes

Table 1.3: Notation used in subsequent chapters of the thesis.

Chapter 2

Extending the Territorial Raider Model to incorporate Row-dependent Movement

2.1 Introduction

This chapter consists of two parts. The first extends the territorial raider model by developing a generalised movement methodology that incorporates the row-dependent movement mechanisms developed in Broom et al. (2020) into the evolutionary setting of the territorial raider model. In this chapter, it is assumed that individuals reside within a N-sized, well-mixed population on a complete graph. This assumption significantly simplifies the analysis, providing useful insights in the mutant's fixation probability.

The second part applies this movement methodology to develop evolutionary models that investigate the effects of row-dependent movement on the evolution of cooperation. We implemented both analytical and computational methods and observed that these two approaches can yield different outcomes depending on the underlying dynamics. We published the work presented in this chapter in Haq et al. (2024).

2.2 The Model

Within this section, we define the evolutionary set-up for the analysis carried out in this chapter.

2.2.1 The population structure and distribution

The population structure is defined by the territorial raider model (refer to section 1.7). Since we assume that individuals reside on a complete graph, all members of the population have the same apriori distribution. For example, in the territorial raider model on a complete graph with M vertices, the apriori distribution for any individual staying at home is $\frac{h}{h+M-1}$ and moving to a specific neighbouring vertex is $\frac{1}{h+M-1}$. It is essential to ensure that when embedding the row-dependent movement mechanisms into the model, individuals adhere to their apriori distributions throughout the evolutionary process to maintain consistency within the model. As our work in this chapter is only focused on complete graphs, d_{ij} is the same for all individuals, as all individuals are equally likely to be replaced i.e. we can simply write d_{ij} as d (and sometimes as d_N, when we consider the influence of varying population size on d, since d depends upon N).

2.2.2 Evolutionary dynamics

The fitness of individuals and the replacement weights are calculated as in the territorial raider model (see section 1.7.2). In this chapter, all of the standard dynamics defined in Table 1.2 have been considered. However, we only present results under BDB and BDD dynamics. This is because it was shown in Pattni et al. (2017) that the results for BDB and DBD are identical (as are those for BDD and DBB). This is because the replacement structure $\mathbf{W}$ is doubly stochastic, therefore it is irrelevant whether birth or death occurs first. Also, it was shown in Pattni et al. (2015) that LB and LD dynamics are identical to the BDB and DBD dynamics, respectively.

We note that this process is an idealisation of the original evolutionary process described in Broom et al. (2015), which is represented by the simulations in subsequent chapters, allowing for analytical results to be considered. It was identified in Pires et al. (2023) that under certain circumstances, such as highly variable fitnesses or large self-weights, there can be significant differences between these outcomes for some dynamics, including BDD (but not BDB). We explore this in Chapter 3.

2.2.3 Fixation probability

As we consider only well-mixed populations, equivalent to a complete graph with $N = M$ on a territorial raider model. The fixation probability of a mutant ($\mathcal{M}$) in an N-sized, well-mixed population can be expressed by the standard formula (Karlin & Taylor 1975).

$$\rho_1^{\mathcal{M}} = \frac{1}{1 + \sum_{j=1}^{N-1} \prod_{k=1}^{j} \frac{\delta_k}{\beta_k}}. \tag{2.1}$$

Here β_K and δ_K are the respective birth and death rates of the mutant which depend on the game and dynamics.

2.3 Theoretical results

In this section, we consider our theoretical results. Initially, we describe a generalised movement method that ensures we can achieve our apriori target for $h \neq 1$. We then consider explicit fixation probability formulae for specific cases.

2.3.1 A generalised movement modelling approach

Our analysis aims to extend the existing territorial raider model to include other types of movement distributions whilst ensuring the other constituent parts of the model remain the same, that is, the population structure, the games played, and the evolutionary dynamics. By considering the home fidelity parameter and the number of connections an individual has on a complete graph, we can develop a general procedure that allows us to embed any of the considered row-dependent movement models into the evolutionary setting of the territorial raider model on complete networks. In the following, we describe a method of combining a movement process of the type described in section 1.9 (which we refer to as following the process) with a simple additional process to achieve our apriori targets.

The procedure involves deriving a probability distribution that accounts for the various movement choices available to individuals within the population. This includes both those who follow the process and those who do not, with the available actions for the latter group depending on the value of h. Specifically, if $h > 1$, this indicates a preference for remaining at home; $h = 1$ represents an indifference between an individual's home vertex and their neighbouring vertices; and $h < 1$ shows a preference for moving elsewhere. We incorporated these scenarios within

the probability distribution.

Consider a complete graph where there are M places.

- If $h > 1$, then an individual can either partake in the process and move via the movement mechanism with probability $\frac{M}{h+M-1}$ or they do not move and stay at their home vertex with probability $\frac{h-1}{h+M-1}$.
- If $h = 1$, then every member of the population plays the process.
- If $h < 1$, then an individual can either move via the process with probability $\frac{Mh}{h+M-1}$ or they move to a random non-home place with probability $\frac{(M-1)(1-h)}{h+M-1}$.

Naturally, this movement distribution is composed of parameters that affect the likelihood of movement, namely, the home fidelity parameter and the number of connections an individual has (equivalent to $M-1$ on a complete graph). Incorporating this probability distribution into the model ensures that all individuals within the population achieve the target distribution. We show how this distribution explicitly satisfies the apriori targets. If $h > 1$, the probability of an individual occupying their home vertex is $\frac{h-1}{h+M-1} + \frac{1}{M}(\frac{M}{h+M-1}) = \frac{h}{h+M-1}$ and the probability of an individual being elsewhere is $\frac{M}{h+M-1} - \frac{1}{M}(\frac{M}{h+M-1}) = \frac{M-1}{h+M-1}$. If $h < 1$, the probability of an individual occupying their home vertex is $\frac{1}{M}(\frac{Mh}{h+M-1}) = \frac{h}{h+M-1}$ and the probability of an individual being elsewhere is $\frac{(M-1)(1-h)}{h+M-1} + (\frac{Mh}{h+M-1} - \frac{1}{M}\frac{Mh}{h+M-1}) = \frac{M-1}{h+M-1}$.

As opposed to the wheel which simultaneously allocates all individuals participating in the movement process, ensuring the apriori targets are hit, sequential movement processes such as the polya-urn involve individuals moving later on in the process being influenced by preceding individuals. Assuming all individuals have the same distribution, it was proven that polya-urn process achieves the apriori targets (Broom et al. 2020), therefore this property naturally extends to our movement modelling approach. It is important to note that individuals who move via the movement mechanism are not influenced by the presence of individuals who did not move via the mechanism. This condition was important to add to our approach as it ensures the apriori targets are met. For example, an individual who moves via follow the majority, will not follow those who did not partake in the movement process. They may end up in the same place, but this will not be due to the movement mechanism process.

Regardless of the movement distribution chosen for the evolutionary model, we define a standard practice to follow when computing the fitnesses of mutants and

residents within a well-mixed population, which can be characterised as follows: First, outline the distribution that describes all conceivable ways in which members of a given population can move. For each specific movement case, establish the distribution that defines all potential groupings that can emerge as a result of the considered movement case. Then, average the payoffs from each case to obtain the average payoffs. These average payoffs are used to compute the necessary evolutionary metrics such as the fitnesses for deriving an analytical expression for the fixation probability.

As an example, we examined a well-mixed population of three individuals on a complete triangle graph. Using the methodology developed in section 2.3.1, we calculated average group distributions for each of the movement mechanisms. For $h > 1$, we show an example of the average group distribution for the follow the majority process (the polya-urn and the wheel can be found in the appendix).

- P(all individuals are together) $= \frac{9(h-1)}{(h+2)^3} + \frac{27}{(h+2)^3} = \frac{27+9(h-1)}{(h+2)^3}$,
- P(I_1 I_2 together, I_3 alone) = P(I_1 I_3 together, I_2 alone) = P(I_2 I_3 together, I_1 alone) $= \frac{2(h-1)^2}{(h+2)^3} + \frac{6(h-1)}{(h+2)^3} = \frac{2(h-1)^2+6(h-1)}{(h+2)^3}$,
- P(all individuals are alone) $= \frac{3(h-1)^2}{(h+2)^3} + \frac{(h-1)^3}{(h+2)^3} = \frac{3(h-1)^2+(h-1)^3}{(h+2)^3}$.

2.3.2 Fitness calculations

In our analysis, we evaluated the fitness of cooperators and defectors for any row-dependent movement distribution by considering the following scenario: in an N-sized, well-mixed population consisting of k cooperators and $N-k$ defectors, what proportion of reward V does a specific cooperator, denoted as C_1 receive on average?

First, we examined what fraction of V that C_1 receives from another cooperator in the population, denoted as C_2. We considered all possible groupings in which C_1 and C_2 could be together. We arbitrarily stated that the probability of C_1 and C_2 being together in a specific group with S others is γ_{S+2}. Therefore, C_1 receives precisely $\frac{1}{S+1}V$ from C_2 which is then weighted by the probability of the group forming, resulting in $V\frac{\gamma_{S+2}}{S+1}$. This quantity is then summed to consider all possible group sizes i.e. $V\sum_{S=0}^{N-2}\frac{\gamma_{S+2}}{S+1}$. This expression represents the total probability of C_1 and C_2 being in the same group, which is also a measure of how likely they are to interact, therefore, this was re-expressed as $\sum_{S=0}^{N-2}\frac{\gamma_{S+2}}{S+1} = d_N$. In other words, the

total proportion of V that C_1 receives from C_2 can be expressed as $d_N V$.

$$F_C = R - C + (k-1)Vd_N \text{ and } F_D = R + kVd_N. \tag{2.2}$$

(2.2) expresses the fitness of a cooperator and defector for any movement mechanism described in section 1.9, captured by the d_N term. The value of d_N, measures the likelihood of two individuals being in the same group, thus influencing their chances of receiving rewards from each other. A similar, more complex calculation for fitnesses in the Hawk-Dove game is provided in the appendix, assuming only independent movement for simplicity. In an N-sized, well-mixed population with k doves and $N-k$ hawks, the fitnesses for the dove and hawk are given by

$$R + \tau(h, N, k)V, \tag{2.3}$$

where

$$\tau(h,N,k) = \left(\left(\frac{h+N-2}{h+N-1} \right)^{N-k} - \left(\frac{(h+N-2)^{N-1}}{(h+N-1)^N} \right) \left(\frac{k(N-1)+(N-k)(N-1)}{k} \right) + \frac{(N-k)(N-1)(h+N-2)^{N-k-1}}{k(h+N-1)^{N-k}} \right)$$

and

$$R + \omega(h, N, k)V - \nu(h, N, k)C, \tag{2.4}$$

where

$$\omega(h,N,k) = \left(1 + \frac{k}{N-k} - \frac{(N-1)(h+N-2)^{N-k-1}}{(h+N-1)^{N-k}} - \frac{k(h+N-2)^{N-k}}{(N-k)(h+N-1)^{N-k}} \right),$$

$$\nu(h,N,k) = \left(\frac{k-N+1}{h+N-1} - \frac{k}{N-k} + \frac{h(N-k-1)+(N-k-1)(N-1)}{(h+N-1)^2} + \frac{k(h+N-2)^{N-k}}{(N-k)(h+N-1)^{N-k}} + \frac{(N-1)(h+N-2)^{N-k-1}}{(h+N-1)^{N-k}} \right).$$

(2.3) and (2.4) are the dove's and hawk's fitness respectively and the calculations for these can be found in the appendix given by (1) and (2).

2.3.3 General fixation probability formulae

In this section, we consider only well-mixed populations, equivalent to a complete graph with $N = M$ on a territorial raider model. The fixation probability of a

mutant ($\mathcal{M}$) in an N-sized, well-mixed population can be expressed by the standard formula (Karlin and Taylor 1975).

$$\rho_1^{\mathcal{M}} = \frac{1}{1 + \sum_{j=1}^{N-1} \prod_{k=1}^{j} \frac{\delta_k}{\beta_k}}. \tag{2.5}$$

Here β_K and δ_K are the respective birth and death rates of the mutant, the ratio of which we show to be equivalent to the fitnesses of the mutant and resident respectively under BDB dynamics. The birth rate of a mutant corresponds to an offspring of the mutant replacing a resident member of the population and vice-versa for the death rate. This mathematically translates to the following equation where there are k mutants ($\mathcal{M}$) and $N-k$ residents ($\mathcal{R}$).

$$\begin{aligned}
\frac{\delta_k}{\beta_k} &= \frac{P(\text{a resident replaces a mutant})}{P(\text{a mutant replaces a resident})} \\
&= \frac{\frac{F_{\mathcal{R}}(dk(N-k))}{kF_{\mathcal{M}}+(N-k)F_R}}{\frac{F_{\mathcal{M}}(dk(N-k))}{kF_{\mathcal{M}}+(N-k)F_R}} \\
&= \frac{F_{\mathcal{R}}}{F_{\mathcal{M}}}.
\end{aligned} \tag{2.6}$$

(2.5) now becomes

$$\rho_1^{\mathcal{M}} = \frac{1}{1 + \sum_{j=1}^{N-1} \prod_{k=1}^{j} \frac{F_{\mathcal{R}}}{F_{\mathcal{M}}}}. \tag{2.7}$$

This result means that under a complete graph and BDB dynamics, for any particular game, we need only substitute the average fitnesses of the mutant and resident to determine the fixation probability. Using a similar approach, if there are k individuals in the set of mutants $\mathbb{K}$, and $N-k$ in the set of residents $\mathbb{L}$ the corresponding ratio of the death and birth rates under BDD is

$$\begin{aligned}
\frac{\delta_k}{\beta_k} &= \frac{\mathrm{P}(\text{a resident replaces a mutant})}{\mathrm{P}(\text{a mutant replaces a resident})} \\
&= \frac{\left(\frac{\frac{1}{N} w_{ij} F_{\mathcal{M}}^{-1}(k(N-k))}{\sum\limits_{z\in\mathbb{K}} w_{iz} F_{\mathcal{M}}^{-1} + \sum\limits_{z\in\mathbb{L}} w_{iz} F_{\mathcal{R}}^{-1}} \right)}{\left(\frac{\frac{1}{N} w_{ji} F_{\mathcal{R}}^{-1}(k(N-k))}{\sum\limits_{z\in\mathbb{K}} w_{jz} F_{\mathcal{M}}^{-1} + \sum\limits_{z\in\mathbb{L}} w_{jz} F_{\mathcal{R}}^{-1}} \right)} \\
&= \frac{\left(N-k+(k+w^*)\frac{F_{\mathcal{R}}}{F_{\mathcal{M}}} \right)}{\left(k+(N-k+w^*)\frac{F_{\mathcal{M}}}{F_{\mathcal{R}}} \right)},
\end{aligned}$$

where $w = w_{ij} = w_{ji}$, $w_s = w_{ii} = w_{jj}$ and $w^* = \frac{w_s - w}{w}$.

Therefore, under BDD dynamics, the fixation probability of a single mutant (2.5) is expressed as

$$\rho_1^{\mathcal{M}} = \frac{1}{1 + \sum_{j=1}^{N-1} \prod_{k=1}^{j} \frac{(N-k+(k+w^*)\frac{F_{\mathcal{R}}}{F_{\mathcal{M}}})}{(k+(N-k+w^*)\frac{F_{\mathcal{M}}}{F_{\mathcal{R}}})}}. \tag{2.8}$$

With the fitnesses calculated, we can directly substitute them into the fixation probability of a mutant on a complete N-sized network under BDB dynamics (2.7) and BDD dynamics (2.8). By substituting (2.2) and (2.3) into (2.7) respectively, we have that the fixation probability of a mutant cooperator and dove under BDB dynamics are respectively given by

$$\rho_1^{A} = \frac{1}{1 + \sum_{j=1}^{N-1} \prod_{k=1}^{j} \frac{R+kVd_N}{R-C+(k-1)Vd_N}}, \tag{2.9}$$

$$\rho_1^{B} = \frac{1}{1 + \sum_{j=1}^{N-1} \prod_{k=1}^{j} \frac{R+\omega V-\nu C}{R+\tau V}}. \tag{2.10}$$

Similarly, by substituting (2.2) and (2.3) into (2.8), the fixation probability of a mutant cooperator and dove, under BDD dynamics are respectively given by

$$\rho_1^{\mathcal{A}} = \frac{1}{1 + \sum_{j=1}^{N-1} \prod_{k=1}^{j} \frac{(N-k+(k+w^*)\frac{R+kVd_N}{R-C+(k-1)Vd_N})}{(k+(N-k+w^*)\frac{R-C+(k-1)Vd_N}{R+kVd_N})}}, \tag{2.11}$$

$$\rho_1^{\mathcal{B}} = \frac{1}{1 + \sum_{j=1}^{N-1} \prod_{k=1}^{j} \frac{(N-k+(k+w^*)\frac{R+\omega V-\nu C}{R+\tau V})}{(k+(N-k+w^*)\frac{R+\tau V}{R+\omega V-\nu C})}}. \tag{2.12}$$

2.3.4 Weak selection

The concept of selection intensity to consider situations in which the game exerts a minor influence on the evolutionary process was considered and the *rule of* 1/3 was established (Taylor et al. 2004) and states that selection favours type A fixating if the internal equilibrium point is less than 1/3. This general rule was considered for the Hawk-Dove game and it was found that if $\frac{V}{C} > \frac{2}{3}$, then selection favours the fixation of the dove. It is worth noting that this analysis only considered pairwise contests between individuals therefore, we have extended this analysis to encompass the multiplayer Hawk-Dove game from our model, allowing us to explore the effects multiplayer interactions have on the evolution of cooperation. We considered the

effect weak selection has on the fixation formulae in section 2.3.3 by assuming R is very large compared to V and C i.e. the game has little influence in the evolutionary process. This is a similar approach to Ohtsuki et al. (2006), where assuming small w implies weak selection which is equivalent to $R = \frac{1-w}{w}$.

The Public Goods game

We first considered the cooperator's fixation probability under BDB. Consider the expression inside the product term of (2.9).

$$\frac{R + kVd_N}{R - C + (k-1)Vd_N} \approxeq 1 + \frac{Vd_N + C}{R}, \tag{2.13}$$

so (2.9) now becomes

$$\frac{1}{1 + \sum_{j=1}^{N-1} (1 + \frac{Vd_N + C}{R})^j}. \tag{2.14}$$

The term inside the summation can be approximated by the following,

$$\left(1 + \frac{Vd_N + C}{R}\right)^j \approxeq 1 + j\left(\frac{Vd_N + C}{R}\right). \tag{2.15}$$

Therefore, (2.14) becomes

$$\frac{1}{1 + \sum_{j=1}^{N-1} (1 + j(\frac{Vd_N + C}{R}))}, \tag{2.16}$$

which simplifies to

$$\begin{aligned} \frac{1}{N + (\frac{Vd_N + C}{R}) \sum_{j=1}^{N-1} (j)} &= \frac{1}{N}\left(\frac{1}{1 + \frac{N-1}{2R}(Vd_N + C)}\right) \\ &\approxeq \frac{1}{N}\left(1 - \frac{N-1}{2R}(Vd_N + C)\right). \end{aligned} \tag{2.17}$$

From (2.17), as the parameter d_N increases, the situation becomes increasingly unfavourable for the mutant cooperator due to the defector's advantageous position. The defector can receive an additional reward without incurring any cost because, from their perspective, there is an extra cooperator within the population from whom they will receive this benefit. Conversely, the cooperator does not have this advantage as they receive no share from their own contributions. With the growing

value of d_N, the likelihood of the mutant cooperator interacting with defectors rises, further reinforcing the defector's advantageous position.

We also considered the cooperator's fixation probability under BDD dynamics. By applying similar weak selection methods to (2.11), we have

$$\frac{1}{N}\left(1-\frac{(N+2w^*)(N-1)}{2R(N+w^*)}(Vd_N+C)\right). \tag{2.18}$$

(2.18) is an approximation of the fixation probability of the mutant cooperator under BDD dynamics.

The Hawk-Dove game

We carried out a similar, more complicated calculation for considering the dove's fixation probability which can be found in the appendix. Using the dove's fixation probability (2.10), a calculation was done to determine the dove's neutrality condition by setting the dove's fixation probability to equal $\frac{1}{N}$ i.e. $\rho_1^B = \frac{1}{N}$. This corresponds to neutral selection, where the mutant strategy has no selective advantage or disadvantage, and its fixation is solely random.

$$V = \frac{(\frac{1}{2}-\frac{1}{\mathrm{e}})}{(\frac{1}{\mathrm{e}}(\gamma-1-f(h))+1)}C, \tag{2.19}$$

where $f(h) = H[N-1, \left(\frac{h+N-1}{h+N-2}\right)^k] - \ln(N-1)$ and $H[N-1,a] = \sum_{k=1}^{N-1}\frac{a^k}{k}$.

For varying h, the neutrality condition is approximately given by $C = 1.11V$ which means that under our models, hawks are generally worse off compared to doves as the cost does not need to be raised as significantly in the classical models for hawks and doves to be doing equally well. This intuitively makes sense as larger groups are generally bad for hawks who are more likely to encounter competition and, therefore, incur a greater cost due to a larger presence of other hawks in their game interactions. We also applied weak selection methods to the dove's fixation probability under BDD dynamics which can be found in the appendix. We saw that the dynamics do not affect the dove's neutrality condition.

The BDD approximations for the fixation probabilities of the cooperator (2.18) and dove (21) have a similar form to their respective BDB approximations (2.17), (9). If $w^* = 0$, then the approximations are equal. In other words, if the self-weights are equal to all other weights, then under weak selection, the fixation probability of

a mutant cooperator or dove is the same regardless of whether selection acts on the first or second event. Other dynamics were considered and their functionality was explained in Pattni et al. (2017), such as the DBD dynamics where death acts first and selection acts on this event. It was found that the results of DBD and BDB were identical. If the self-weights are the same as all other weights, then implementing DBD is equivalent to BDD; therefore, BDD is the same as BDB.

A general condition for the fixation probability of a type A mutant in a type B population is greater than the fixation probability of a type B mutant in a type A population was established in Tarnita et al. (2009) given by

$$\sigma a + b > c + \sigma d. \tag{2.20}$$

where σ is the *structure coefficient* of the process. The value of σ depends on both the graph and the updating rule, but not on the values a, b, c and d (which are the payoffs to the pairwise matrix game) for example. For regular graphs with degree k and $N \gg k$, we have $\sigma = \frac{k+1}{k-1}$. Using this analysis for the pairwise Hawk-Dove game, it was shown that in an infinite, well-mixed population ($k \to \infty$), hawks and doves do equally well when $V = 2C$. We also extended this analysis to our models under the assumption of an infinite, well-mixed population, where hawks and doves interact with one another in arbitrary group sizes rather than limiting pairwise interactions.

By considering the fitness of a dove and hawk in an infinite, well-mixed population with a proportion of p doves, we were able to extend the analysis from Tarnita et al. (2009) by introducing a multiplayer Hawk-Dove game. By using the substitution $p = \frac{k}{N}$, and then assuming $N \to \infty$, the fitnesses of a dove (2.3) and hawk (2.4) are respectively given by

$$R + \left(\frac{e^p - 1}{ep}\right)V, \tag{2.21}$$

$$R + \left(\frac{1 - e^{p-1}}{1 - p}\right)V - \left(\frac{e^{p-1} - p}{1 - p}\right)C. \tag{2.22}$$

By equating these two fitnesses together and solving for $\frac{V}{C}$, we have

$$\frac{V}{C} = \frac{ep(e^{p-1} - p)}{(1 - e^{p-1})(ep) - (e^p - 1)(1 - p)}. \tag{2.23}$$

For each value of p, (2.23) provides the corresponding equilibrium ratio of $\frac{V}{C}$. Our point of interest is at $p = \frac{1}{2}$ where both doves and hawks are doing equally well. This equilibrium condition is given by $\frac{V}{C} = 0.688$ i.e. $C = 1.453V$ which supports our previous neutrality condition for a dove (2.19), that in a multiplayer game context, hawks are generally doing worse than in the traditional pairwise game analysis.

2.4 Numerical results

For considering higher populations on larger graphs, we carried out computational methods to simulate such processes as analytically carrying them out would be impractical. The computational methods are the same as the ones carried out in Schimit et al. (2019) except here, the simulations are carried out on much simpler, complete networks, and individuals move via our approach developed in section 2.3.1.

One simulation is defined as follows:

- The chosen complete network is formed using the iGraph library (Csardi & Nepusz 2006).
- The mutant is randomly placed on one of the nodes.
- Every individual probabilistically moves (or not) from their home vertex according to the parameters of the model. Groups are formed and multiplayer games are played where $R = 10, C = 1$ and $V = 2$ for both of the considered games.
- Individuals return to their home places.
- Each individual moves (or not) and groups are formed. Here, no games are played, instead, the dynamic process occurs. One individual is selected to reproduce an offspring that will replace another random member of the group (or its parent if the parent is alone). Selection either acts on the birth or death even according to the chosen dynamics.
- The simulation terminates once the population is entirely composed of a single type of individual.
- This process is averaged over $1,000,000$ runs to minimise statistical variability.

As discussed in section 1.7.2, the assumptions in this section are slightly different to section 2.3. In the simulations, a single step is used in the contests and in the dynamic process i.e. individuals only move once. The theoretical section assumes average weights corresponding to where individuals move many times to accrue average fitnesses and weights.

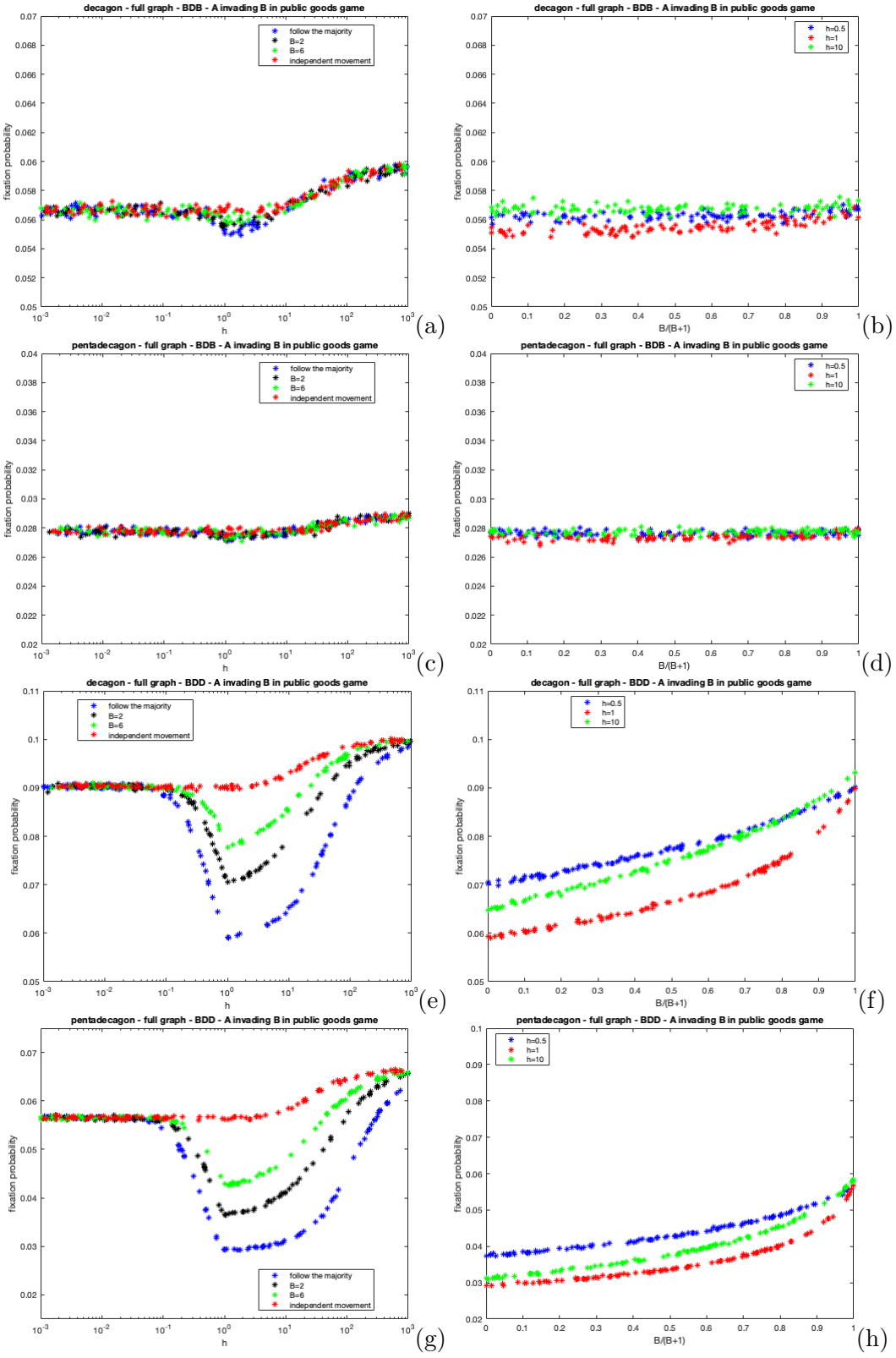

Figure 2.1: The fixation probability of a mutant cooperator in a population of defectors on complete decagon and pentadecagon graphs under BDB and BDD dynamics for varying h under distinct polya-urn movement processes, For (a), (c), (e) and (g), we set $B = 0$ (follow the majority), $B = 2$, $B = 6$ and $B = 10{,}000$ (a sufficiently large value to mirror independent movement). For (b), (d), (f) and (h) we set $h = 0.5$, $h = 1$, and $h = 10$ and vary B.

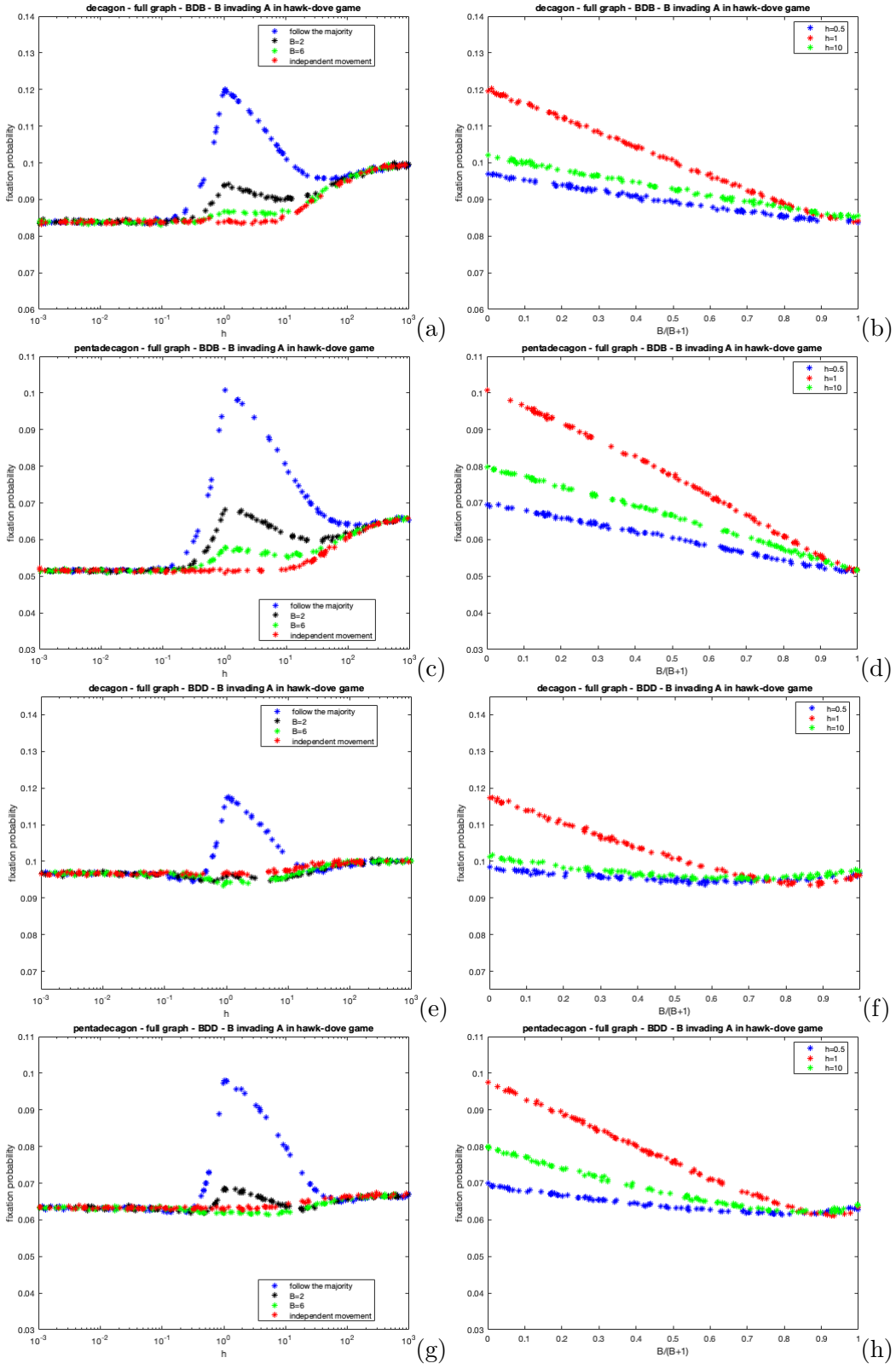

Figure 2.2: The fixation probability of a mutant dove in a population of hawks on complete decagon and pentadecagon graphs under BDB and BDD dynamics for varying h under distinct polya-urn movement processes, For (a), (c), (e) and (g), we set $B = 0$ (follow the majority), $B = 2$, $B = 6$ and $B = 10{,}000$ (a sufficiently large value to mirror independent movement). For (b), (d), (f) and (h) we set $h = 0.5$, $h = 1$ and $h = 10$ and vary B.

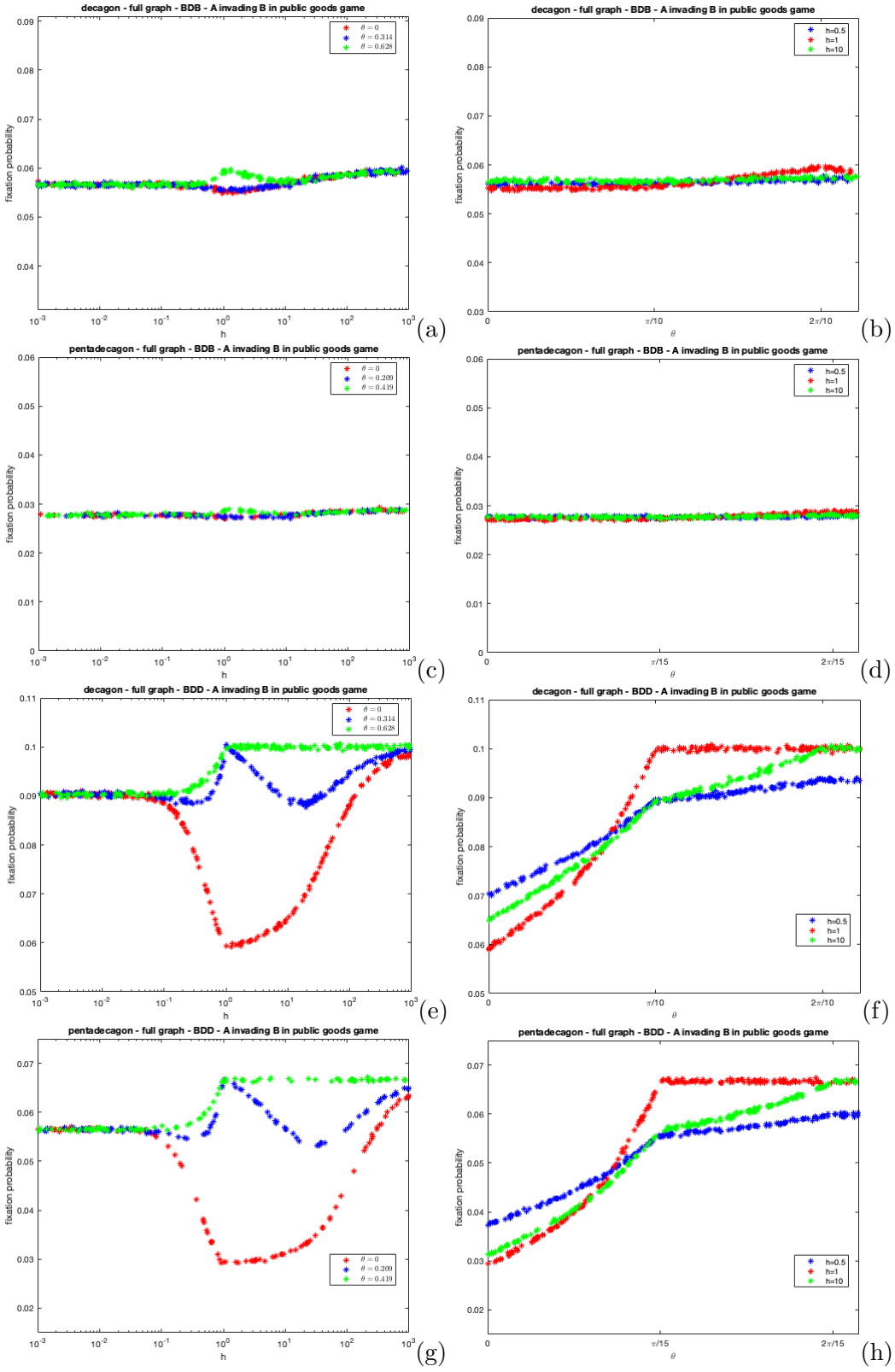

Figure 2.3: The fixation probability of a mutant cooperator in a population of defectors on complete decagon and pentadecagon graphs under BDB and BDD dynamics for varying h under distinct wheel movement processes, For (a), (c), (e) and (g), we set $\theta = 0$ (follow the majority), $\theta = \frac{2\pi}{N}$ (represents a near complete dispersal process), $\theta = \frac{\pi}{N}$. For (b), (d), (f) and (h) we set $h = 0.5$, $h = 1$ and $h = 10$ and vary θ.

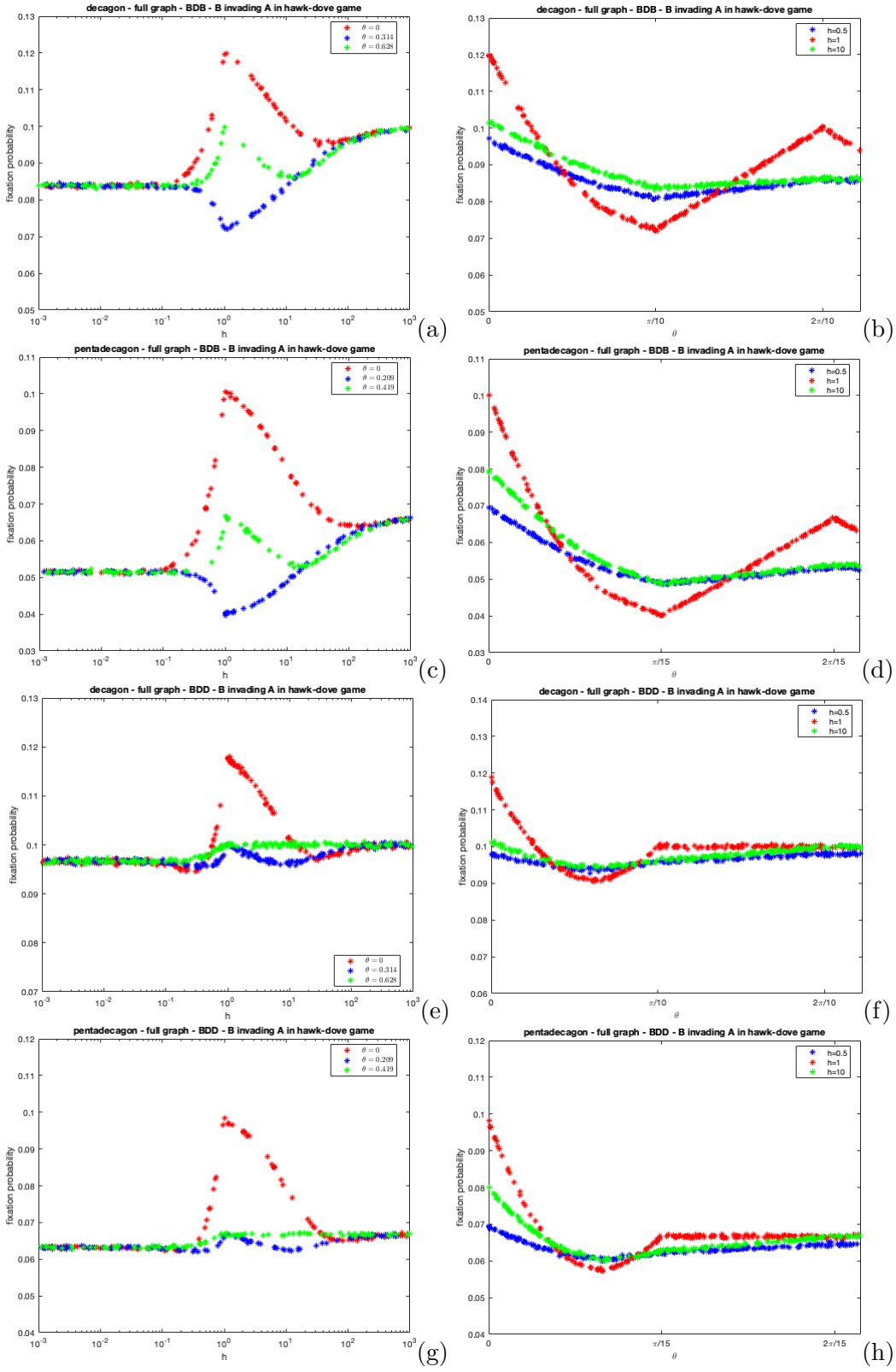

Figure 2.4: The fixation probability of a mutant dove in a population of hawks on complete decagon and pentadecagon graphs under BDB and BDD dynamics for varying h under distinct wheel movement processes, For (a), (c), (e) and (g), we set $\theta = 0$ (follow the majority), $\theta = \frac{2\pi}{N}$ (represents a near complete dispersal process), $\theta = \frac{\pi}{N}$. For (b), (d), (f) and (h) we set $h = 0.5$, $h = 1$, and $h = 10$ and vary θ.

Figure 2.1 illustrates the fixation probability of a mutant cooperator under polya-urn processes for BDB and BDD dynamics on complete decagon and pentadecagon graphs. As h approaches 0.1, the fixation probability remains constant, attributed to individuals randomly moving to non-home places.

The cooperator's fixation probability reaches its lowest point when $h = 1$ where all members of the population must participate in the movement process, leading to the formation of groups of varying sizes (depending on the type of movement governing the process). Recall that from section 2.3.1, the movement methodology states that when $h = 1$, all members of the population must participate in the movement process as all individuals are indifferent to their home vertex and neighbouring vertices. This high level of movement is disadvantageous for cooperators as they are more likely to encounter defectors due to the high levels of movement within the population. The "follow the majority" process is the worst type of movement for cooperators as it ensures all individuals partaking in the movement process, herd together at the same place; therefore, ensuring that defectors receive rewards from cooperators.

As h tends to larger values, regardless of the movement process, the cooperator's fixation probability gradually increases because individuals are more likely to remain on their own therefore, cooperators are highly unlikely to interact with defectors, thus increasing their relative fitness.

Fig. 2.1 also shows plots of the fixation probability of the cooperator against B (scaled to $\frac{B}{B+1}$). As B increases, the cooperator's fixation probability increases. This is attributed to the gradual shift in the movement mechanism from a deterministic type ($B = 0$), where individuals simply move to the place containing the largest number of individuals, to an independent type ($B \to \infty$) where individuals move randomly, without influence from other individuals. As B increases, individuals are less likely to herd together therefore the relative difference in the average cooperator's and defector's fitness gradually decreases, thus increasing the cooperator's fixation probability.

The cooperator's fixation probability is higher under BDD dynamics because selection affects the second event. During the birth event, the probability of the co-operator reproducing is simply $\frac{1}{N}$ as opposed to the less favourable BDB dynamics where the probability is proportional to the cooperator's fitness. For large h, the fixation probability tends to $\frac{1}{N}$ shown in Fig. 2.1(e) and Fig. 2.1(g). Here, individ-

uals are mostly alone or occasionally with another individual. If an alone individual is randomly selected to reproduce, then its offspring will replace them. Suppose an individual within a pair is randomly selected to reproduce. In that case, the other individual within the pair is guaranteed to be replaced, thus rendering the influence of selection within the replacement process irrelevant.

Furthermore, Fig. 2.1 shows that row-dependent movement has a more prominent effect on the cooperator's fixation probability when selection acts on the second event. In Fig. $2.1(e)-(h)$, there is a greater disparity in the fixation probabilities between the different movement processes compared to Fig. $2.1(a)-(d)$ where there is a smaller effect. Under BDD dynamics, even though cooperators are more likely to reproduce, they are also more likely to be replaced (depending on the movement mechanism governing the process). For instance, if individuals are moving via follow the majority and $h = 1$, then all individuals herd together and cooperators are more likely to be replaced because of selection acting on the replacement event. Whereas under BDB dynamics, all individuals within the group are equally likely to be replaced.

Figure 2.2 portrays the fixation probability of a mutant dove under distinct polya-urn processes for BDB and BDD dynamics on the complete decagon and pentadecagon. In these figures, as h approaches one, the dove's fixation probability increases and reaches its maximum when $h = 1$.

As all members of the population partake in the movement process when $h = 1$, hawks are more likely to interact with one another, incurring greater costs, thus reducing their relative fitness. Therefore, in this game, follow the majority is the most beneficial movement process for doves because this process forces all hawks partaking in the movement process to interact with each other. As h increases, the dove's fixation probability decreases because hawks are more likely to stay on their home vertices and, therefore, less likely to interact with each other, increasing their relative fitness. As h becomes infinitely large, the dove's fixation probability tends to $\frac{1}{N}$ regardless of the dynamics. Hawks and doves will have the same fitness if they are always alone therefore, selection does not affect the process. Also, Fig. 2.2 shows that as B increases, the dove's fixation probability falls. This occurs because as B increases, hawks are no longer forced to group, thus their relative fitness gradually increases alongside B.

Furthermore, if selection acts on the second event, independent movement is no

longer the worst type of movement for doves. Instead, a polya-urn process (close to independent movement) is the worst type of movement as shown in Fig. 2.2(f) and Fig. 2.2(h), where the value of $\frac{B}{B+1}$ reaches its lowest point slightly below 1 but begins to increase after. This occurs due to the combined effects of the game and dynamics but this effect is largely insignificant.

Figure 4.4 shows the fixation probability of a mutant cooperator under the wheel process for both BDB and BDD dynamics on the complete decagon and pentadecagon. The chosen values of theta remain consistent for each graph. $\theta = 0$ represents the follow the majority process, while $\theta = \frac{2\pi}{N}$ signifies a near complete dispersal process where all individuals are separated. Note that in our simulations, theta is rounded to three decimal places to allow for a minimal degree of pairwise interaction between individuals under this angle. Without this adjustment, the simulation would fail to complete as individuals would only replace themselves if they were always separated, thus the evolutionary process would never reach extinction or fixation. $\theta = \frac{\pi}{N}$ corresponds to an intermediary angle between complete herding and separation.

The trends depicted in Fig. 4.4 resemble those observed in the polya-urn in Fig. 2.1, particularly concerning the influences of herding, dynamics, and the level of h have on the cooperator's fixation probability. However, the key finding from these figures is that $\theta = \frac{2\pi}{N}$, provides the maximum fixation probability for the mutant cooperator for all h. When $h = 1$ and $\theta = \frac{2\pi}{N}$, all individuals are nearly always alone. This leads to an increase in the cooperator's relative fitness, as they rarely provide any rewards to defectors. Consequently, the fixation probability rises significantly at this point. Fig. 4.4(e) and Fig. 4.4(g) show that when $\theta = \frac{2\pi}{N}$ or $\theta = \frac{\pi}{N}$ and $h = 1$, the fixation probability is $\frac{1}{N}$ because individuals are either alone or in a pair rendering selection insignificant as fitness is negligible in these cases due to selection acting on the second event.

Figure 2.4 depicts the fixation probability of a mutant dove under the wheel process for both BDB and BDD dynamics on the complete decagon and pentadecagon.

Fig. 2.4($a-d$) show that when $h = 1$ and $\theta = \frac{2\pi}{N}$, the dove's fixation probability is $\frac{1}{N}$ despite selection acting on the first event. This occurs as nearly every member of the population is separated, therefore individuals do not compete with each other over resources. Therefore, both hawks and doves have the same fitness rendering selection insignificant. When $h = 1$ and $\theta = \frac{\pi}{N}$, the fixation probability is at its

lowest. Under this angle, there are at most pairwise groups which is beneficial for hawks who incur very small costs from the game interactions.

Also, Fig. 2.4 shows that follow the majority ($\theta = 0$) gives a fixation probability greater than $\frac{1}{N}$. As there is a large native hawk population, they herd together leading to them incurring significant costs, greatly reducing their relative fitness, therefore, increasing the dove's fixation probability. In the Hawk-Dove Game, it is clear that herding favours the evolution of cooperation more than dispersal.

Below, we show a table summarising how the different movement processes generally affect the mutant cooperator's and dove's fixation probability (FP).

	Cooperator's FP	**Dove's FP**
Follow the majority ($B = 0$)	Minimum	Maximum
Polya-Urn (increasing B)	Increases	Decreases
Random movement ($B \to \infty$)	Increases	Minimum
The wheel (separation angle)	Maximum	Increases

Table 2.1: Fixation probabilities (FP) of cooperators and doves under different movement processes: follow the majority ($B = 0$), polya-urn (increasing B), random movement ($B \to \infty$), and the wheel (separation angle).

2.5 Discussion

In this chapter, we have developed the framework from Broom & Rychtar (2012), by considering the evolution of structured populations on complete networks involving multiplayer interactions where individuals move in a coordinated manner (row-dependent movement). Specifically, we have extended the territorial raider model developed by Broom et al. (2015) as we have devised a methodology to model an evolutionary process where individuals move in a coordinated manner described by the movement mechanisms developed by Broom et al. (2020). In previous models, (Broom et al. 2015, Schimit et al. 2019, 2022) individuals moved independently irrespective of how other individuals moved. Other models (Pattni et al. 2018, Erovenko et al. 2019, Pires et al. 2023, Erovenko & Broom 2024) involved the development of a Markov movement model, where the movement of individuals depends upon the population's history. Hence, the model in this chapter provides a different perspective on the movement of individuals. In particular, we explored the relation between row-dependent movement and the evolution of cooperation.

The main objective of this chapter was to embed realistic coordinated movement systems into a complete evolutionary setting and use different social dilemma games

to illustrate this as this has previously not been considered in modelling the evolution of structured populations. In Krieger et al. (2017) the effects of an abstract type of motion on the evolution of cooperation in structured populations were explored. In the context of evolutionary graph theory, individuals swap or shuffle vertices on the graph structure, independent of the reproductive events. They demonstrated that the presence of motion can amplify or suppress selection depending on the graph structure. For instance, motion suppresses selection on the cycle graph. However, it was also shown that this type of motion did not change the population's configuration on the complete graph and, therefore, has no effects on the evolutionary dynamics. This, however, differs from our results in this chapter focused on complete graphs as we have illustrated the several effects the movement mechanisms have on the evolution of cooperation. However, the work done in this chapter is largely different as individuals move more realistically and can form multiplayer groups. More importantly, in the models developed in this chapter, individuals have a preference towards their unique home vertex, governed by the home fidelity parameter. When $h \neq 1$, individuals do not share the same movement distribution due to the bias towards their home vertex. This represents a significant disparity to evolutionary graph theory models involving complete graphs, where individuals typically have identical distributions in well-mixed populations (when the weights are equal). By using the Broom-Rychtar framework, we are able to further investigate the mutant cooperator's fixation probability and capture the realistic influence of territorial preference on complete graph structures.

In the context of the Public Goods game, we demonstrated that herding hinders the evolution of cooperation as aggregation provides defectors with opportunities to exploit cooperators in their contest interactions. Dispersal, however, increases the likelihood of cooperative behaviour evolving as defectors are less likely to be in groups containing cooperators and, therefore, cannot receive a benefit from their presence. Ohtsuki et al. (2006) showed that, in general, birth-death processes do not favour the evolution of cooperation. Consequently, in the Public Goods game, the cooperator's fixation probability is always under $1/N$, even with the implementation of the movement mechanisms. However, in the Hawk-Dove Game, aggregation benefits the evolution of cooperation. In Broom et al. (2015), it was shown that the dove's fixation probability can occasionally exceed $1/N$ if the reward is adjusted. However, the results in this chapter show that even if the reward

remains constant, the movement distributions, particularly follow the majority, have a stronger effect in increasing the dove's fixation probability above $1/N$ as hawks are forced to herd together. This forces hawks to interact with one another, incurring a greater cost, thus decreasing their relative fitness. While dispersal also benefits doves, herding has a stronger effect.

Moreover, we derived analytical expressions for the fixation probabilities of the cooperator and dove in both BDB and BDD dynamics. By applying weak selection methods, we extended previous analyses (Tarnita et al. 2009, Taylor et al. 2004) by producing neutrality and equilibrium conditions for the Hawk-Dove game. These conditions align with our expectations, indicating that, in the models developed in this chapter, hawks generally perform worse than in the traditional evolutionary graph theory models. The work in this chapter accounts for a more realistic multi-player game scenario compared to the limiting pairwise case. Notably, larger group sizes negatively impact the hawk's fixation probability as expected.

Chapter 3

Predictors of Fixation Probability under Coordinated Movement Systems

3.1 Introduction

In the previous chapter, the effects of the row-dependent movement mechanisms on the evolution of cooperation in the Public Goods and Hawk-Dove games on complete networks were extensively explored. However, it has been previously shown that measures such as mean group size and temperature are strong predictors of fixation probability, with temperature often being the stronger predictor (Broom et al. 2015, Schimit et al. 2019, 2022). The purpose of this chapter is to extend the previous analysis by using the evolutionary model developed in the previous chapter to investigate how the row-dependent movement mechanisms affect the predictors of fixation probability, and whether the measures retain their significance as strong predictors of fixation. We also consider the Stag-Hunt game as this has not been previously considered in our models, to investigate the effects of row-dependent movement in a social dilemma game where selection can potentially favour cooperation. We published the work presented in this chapter in Haq et al. (2025).

3.2 The Model

The evolutionary model in this chapter follows the same formulation as presented in Chapter 2 (refer to section 2.2). For clarity, the key assumptions are briefly summarised below, with references to relevant sections where necessary.

The population structure is defined as before in section 2.2.1 via the territorial raider model. Similarly, this chapter only considers complete networks. Due to this assumption, all individuals have the same temperature (1.12) and this can be expressed as

$$\tau_N = (N-1)d_N. \tag{3.1}$$

We also considered BDB and BDD dynamics, the same as in section 2.2.2.

3.3 Results

In this section, we first demonstrate how to calculate significant evolutionary predictors of fixation probability. We then present simulation results on fixation probabilities for mutant cooperative strategies from the games defined in Section 1.7.4, under the coordinated movement mechanisms described in section 1.9, and their relationships with mean group size and temperature in a well-mixed population on the complete decagon. This is followed by an analytical explanation for certain trends observed in the simulations.

3.3.1 Evolutionary measures impacting the fixation probability

We first considered how T (1.49) relates to the expected group size. From (1.30), the expected group size is given by

$$E[|G|] = \frac{E[X_m^2]}{E[X_m]} = E[X_m^2]. \tag{3.2}$$

As we only considered well-mixed populations on complete graphs where each individual resides within their unique home vertex, the expected number of individuals on a given place is one i.e. $E[X_m] = 1$. By substituting (3.2) into (1.49) and simplifying,

$$T = \frac{1}{N-1}(E[|G|] - 1). \tag{3.3}$$

(3.3) demonstrates that the aggregation measure T is directly related to the mean group size and if either T or $E[|G|]$ is known, the other can be calculated. We analytically calculated the evolutionary measures considered in this chapter on an N-sized complete network, for $h > 1$, under the follow the majority, independent and wheel processes. As an example, we show how we calculated the mean group size under follow the majority.

$$\begin{aligned}
|G| &= \sum_{L=0}^{N} (\lambda)^L (1-\lambda)^{N-L} \binom{N}{L} \Bigg(\frac{N-L}{N} \Bigg(\frac{(L+1)^2 + N - L - 1}{N} \Bigg) \\
&\quad + \frac{N}{L} \Bigg(\frac{L^2 + N - L}{N} \Bigg) \Bigg), \\
&= \sum_{L=0}^{N} (\lambda)^L (1-\lambda)^{N-L} \Bigg(\binom{N}{L} + \frac{1}{N} \binom{N}{L-1} + \frac{L^2(N-2)}{N} \binom{N}{L} \Bigg), \\
&= 1 + \lambda \Bigg(1 + (1 - \frac{2}{N})((N-1)\lambda + 1) \Bigg), \qquad (3.4)
\end{aligned}$$

where $\lambda = \frac{N}{h+N-1}$. By using similar methods, the mean group size under independent movement is given by

$$|G| = 1 + \lambda \Bigg(2 - \frac{1}{N}(2 + \lambda N - \lambda) \Bigg), \qquad (3.5)$$

and the mean group size for the wheel is given by

$$\begin{aligned}
|G| = 1 + \frac{1}{N} \Bigg(\Bigg(\sum_{\lfloor \frac{2\pi}{N\theta} \rfloor}^{N} \Bigg(\lfloor \frac{2\pi}{N\theta} \rfloor^2 + \frac{1}{2} (\lfloor \frac{2\pi}{N\theta} \rfloor^2 + \lfloor \frac{2\pi}{N\theta} \rfloor) \Bigg(\frac{N\theta}{2\pi} (1 - \lfloor \frac{2\pi}{N\theta} \rfloor) - 1 \Bigg) \\
+ \sum_{L=2}^{\lfloor \frac{2\pi}{N\theta} \rfloor - 1} \Bigg(L^2 + \frac{L^2 + L}{2} (\frac{N\theta}{6\pi}(1-L) - 1) \Bigg) \Bigg) (\lambda)^L (1-\lambda)^{N-L} \binom{N-2}{L-2} \\
+ \frac{2(\lambda - \lambda^2)}{N} \Bigg). \qquad (3.6)
\end{aligned}$$

The calculations for (3.5) and (3.6) can be found in the appendix leading to the above, labelled (22) and (25). By using (3.3), we were able to calculate T for the movement processes by using (3.4), (3.5) and (3.6). For the follow the majority process

$$T = \frac{1}{N-1} \lambda \Bigg(1 + (1 - \frac{2}{N})((N-1)\lambda + 1) \Bigg). \qquad (3.7)$$

Similarly, T under independent movement is given by

$$T = \frac{1}{N-1}\lambda\bigg(2 - \frac{1}{N}(2 + \lambda N - \lambda)\bigg), \tag{3.8}$$

and T for the wheel is

$$\begin{aligned} T = \frac{1}{N(N-1)}\Bigg(\Bigg(\sum_{\lfloor\frac{2\pi}{N\theta}\rfloor}^{N}\Bigg(\lfloor\frac{2\pi}{N\theta}\rfloor^2 + \frac{1}{2}(\lfloor\frac{2\pi}{N\theta}\rfloor^2 + \lfloor\frac{2\pi}{N\theta}\rfloor)\Bigg(\frac{N\theta}{2\pi}(1 - \lfloor\frac{2\pi}{N\theta}\rfloor) - 1\Bigg) \\ + \sum_{L=2}^{\lfloor\frac{2\pi}{N\theta}\rfloor - 1}\Bigg(L^2 + \frac{L^2+L}{2}(\frac{N\theta}{6\pi}(1-L) - 1)\Bigg)\Bigg)(\lambda)^L(1-\lambda)^{N-L}\binom{N-2}{L-2} \\ + \frac{2(\lambda - \lambda^2)}{N}\Bigg). \end{aligned} \tag{3.9}$$

To calculate the temperature, we considered an N-sized, well-mixed population and all of the possible ways two individuals I_i and I_j can replace each other within an L-sized group and used the relation $\tau_N = (N-1)d_N$. We show how we calculated this measure under the follow the majority process (the calculations for independent movement and the wheel can be found in the appendix leading to (26), (27) and (28)). A group of size L can form in one of three ways:

- I_i and I_j move with $L-2$ individuals to an empty vertex;
- I_i moves with $L-2$ individuals to I_j's home vertex or vice-versa;
- I_i and I_j move with $L-3$ individuals to a place containing an individual.

We then obtain the following expression where the first summation represents the first two cases and the second summation represents the third case.

$$\begin{aligned} \tau_N = N - 1\Bigg(\sum_{L=2}^{N}(\lambda)^{L-2}(1-\lambda)^{N-L}\binom{N-2}{L-2}\Bigg(\frac{1}{N}\Bigg)\Bigg(\frac{L}{L-1}(\lambda)^2 + 2\lambda(1-\lambda)\Bigg) \\ + \sum_{L=3}^{N}(\lambda)^{L-1}(1-\lambda)^{N-L+1}\binom{N-2}{L-3}\Bigg(\frac{1}{L-1} - \frac{1}{N}\Bigg)\Bigg), \end{aligned}$$

where $\lambda = \frac{N}{h+N-1}$. By expanding the summations and simplifying, the temperature for follow the majority process on a complete N-sized network is given by

$$\tau_N = \lambda + \frac{1-\lambda}{N} - \frac{(1-\lambda)^{N-1}}{N}. \tag{3.10}$$

Using similar methods, the temperature under independent movement is given by equation (3.11), while the temperature for the wheel is provided in equations (3.12) and (3.13).

$$\tau_N = 1 - \frac{(N + N\lambda(\lambda-1) - \lambda^2)(N-\lambda)^{N-2}}{N^{N-1}}. \tag{3.11}$$

$0 \leq \theta \leq \frac{\pi}{N}$:

$$\begin{aligned}\tau_N = 1 - \Bigg(&\frac{1}{N}(N-1)(1-\lambda)(1-(1-\lambda)^{N-1}) + (1-\lambda)^N \\ &+ \frac{\theta}{\pi}\Bigg(\lambda + \frac{1}{2}((1-\lambda)(1-(1-\lambda)^{N-1}) + (N-1)(\lambda-1)(\lambda))\Bigg)\Bigg).\end{aligned} \tag{3.12}$$

$\frac{\pi}{N} \leq \theta \leq \frac{2\pi}{N}$:

$$\begin{aligned}\tau_N = 1 - \Bigg(&\frac{1}{N}\Bigg(-1 + (1-\lambda)^N + \lambda(\lambda+2) - N(\lambda^2+\lambda-1)\Bigg) \\ &- \frac{\theta}{2\pi}\Bigg(-1 + (1-\lambda)^N + \lambda(N + 3\lambda - 3N\lambda)\Bigg)\Bigg).\end{aligned} \tag{3.13}$$

The detailed calculations for (3.11), (3.12) and (3.13) can be found in the appendix (26), (27) and (28).

In Broom et al. (2015), it was identified that temperature and fixation probability share a linear relationship. This was observed under conditions of high home fidelity and independent movement. However, our analysis in section 3.3.2 demonstrates that this result generalises across all values of h and for all movement processes. To support this analytically, Haq et al. (2024) showed that the fixation probability of a mutant cooperator on a complete N-sized network under BDB dynamics is given by (2.9). Using the definition of the temperature from (1.12), we can re-express (2.9) in terms of the temperature

$$\rho_1^{\mathcal{A}} = \frac{1}{1 + \sum_{j=1}^{N-1}\prod_{k=1}^{j}\frac{R + kV(\frac{\tau_N}{N-1})}{R - C + (k-1)V(\frac{\tau_N}{N-1})}}. \tag{3.14}$$

(3.14) shows that by simply knowing the temperature, the cooperator's fixation probability can be calculated, without knowing the governing movement mechanism. Therefore, in the models considered in this paper for the Public Goods game, temperature matters more than the governing movement mechanism and is the most significant measure in the evolutionary process.

In Haq et al. (2024), it was shown that under independent movement, the fixation probability of a mutant dove under BDB dynamics on a complete N-sized network is given by (2.10). It is clear that unlike (2.9), the fitnesses cannot be expressed in terms of d_N and, therefore, cannot be re-expressed in terms of the temperature. This implies that the governing movement procedure plays a more significant role in the Hawk-Dove game than in the Public Goods game, hence the presence of the non-linear trends in Figure 7. A similar analysis holds for the Stag-Hunt game, where the fitnesses will not simply depend on d_N, but other significant factors such as the threshold value.

3.3.2 Numerical results

In this section, we conducted similar simulation methods to those used in the second chapter to investigate evolutionary processes involving the games defined in section 1.7.4 and whether mean group size (1.30) and temperature (1.12) continue to serve as strong predictors of fixation, under models involving row-dependent movement.

One simulation is delineated as follows:

- The decagon complete network is formed using the iGraph library (Csardi and Nepusz 2006).
- The mutant is randomly placed on one of the vertices.
- Every individual moves (or not) from their home vertex according to the model as described in section 2.3.1. Groups are formed and multiplayer games are played.
- Individuals return to their home places.
- Each individual moves (or not) and groups are formed and the dynamic process occurs. No games are played. Instead, one individual is selected to reproduce an offspring that will replace another random member of the group (or its parent if the parent is alone) explained in section 1.7.2.
- The simulation ends once the mutant fixates in the population or becomes extinct.
- This process is averaged over 1,000,000 cases to minimise statistical variability.

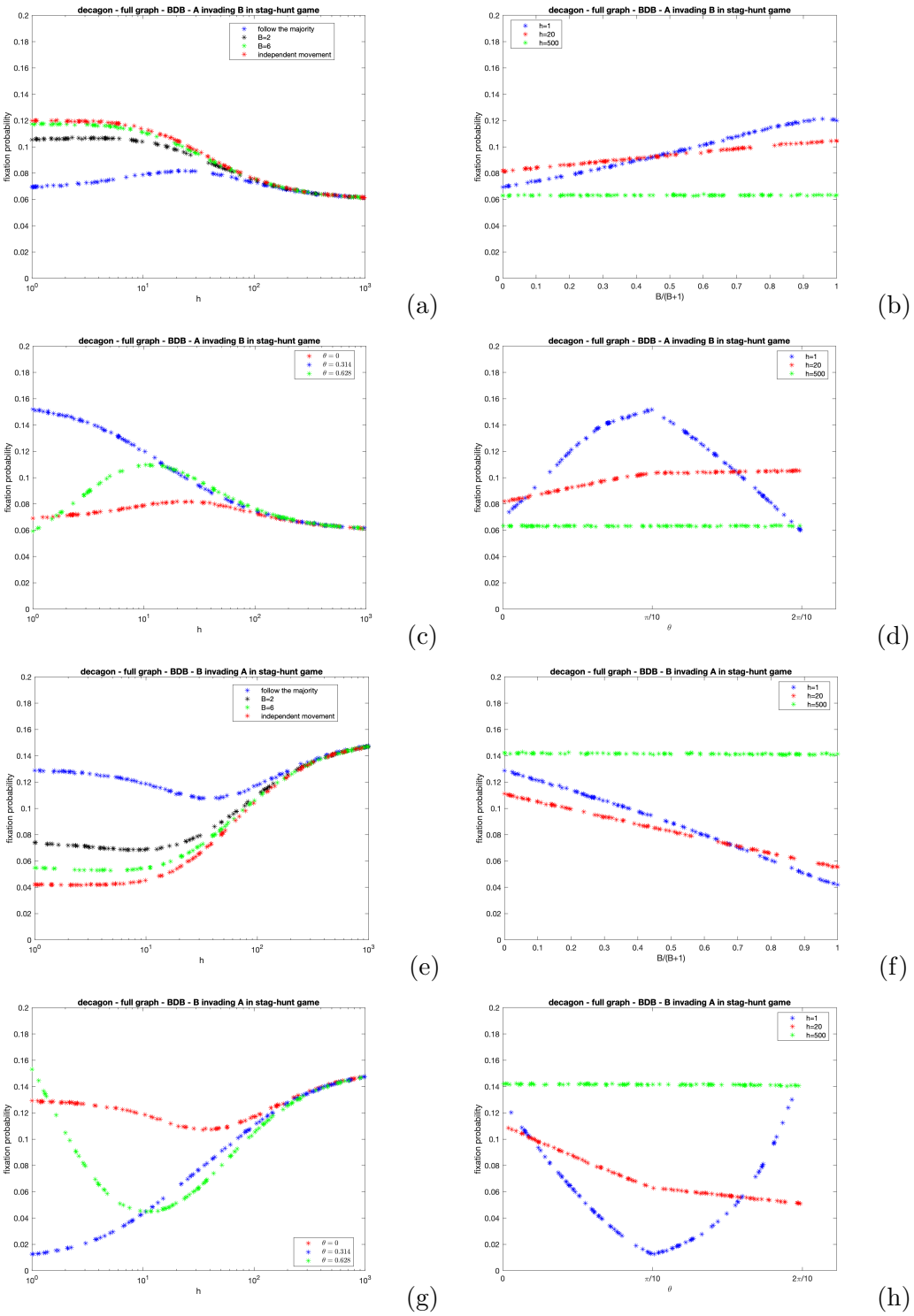

Figure 3.1: The fixation probabilities of the cooperator and defector in the Stag-Hunt game on the complete decagon under the Polya-urn and wheel processes. (the payoffs are set as $R = 10, C = 1, V = 12$ and $L = 2$). (a), (b), (c) and (d) show the fixation probability of a mutant cooperator in a population of defectors and vice-versa for (e), (f), (g) and (h). Figures (a), (b), (c) and (d) represent the cooperator's fixation probability and figures (e), (f), (g) and (h) represent the defector's. For the Polya-urn, in (a) and (e) we set $B = 0$ (follow the majority), $B = 2$, $B = 6$ and $B =$ 10,000 (a sufficiently large value to mirror independent movement). For the wheel, in (c) and (g) we set $\theta = 0$ (follow the majority), $\theta = \frac{2\pi}{N}$ (represents a near complete dispersal process), $\theta = \frac{\pi}{N}$. For (b) and (f), we plot the fixation probability against B (for the Polya-urn) and set $h = 1$, $h = 20$ and $h = 500$. For (d) and (h), we plot the fixation probability against θ (for the wheel) and set $h = 1$, $h = 20$ and $h = 500$.

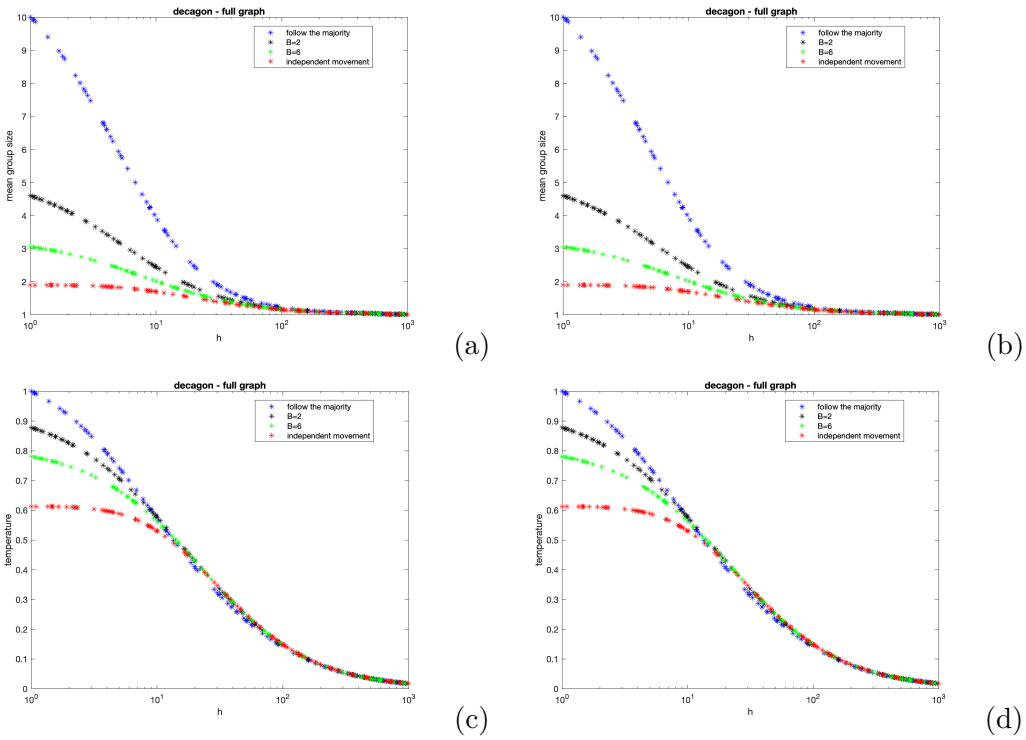

Figure 3.2: The mean group size and temperature of individuals within the a well-mixed population on the complete decagon for varying h under distinct Polya-urn processes and wheel processes. (a) and (b) show the mean group size and (c) and (d) show the temperature. We set $B = 0$ (follow the majority), $B = 2$, $B = 6$ and $B = 10{,}000$ (a sufficiently large value of B representing independent movement). We also set $\theta = 0$ (follow the majority), $\theta = \frac{2\pi}{N}$ (represents a near complete dispersal process) and $\theta = \frac{\pi}{N}$.

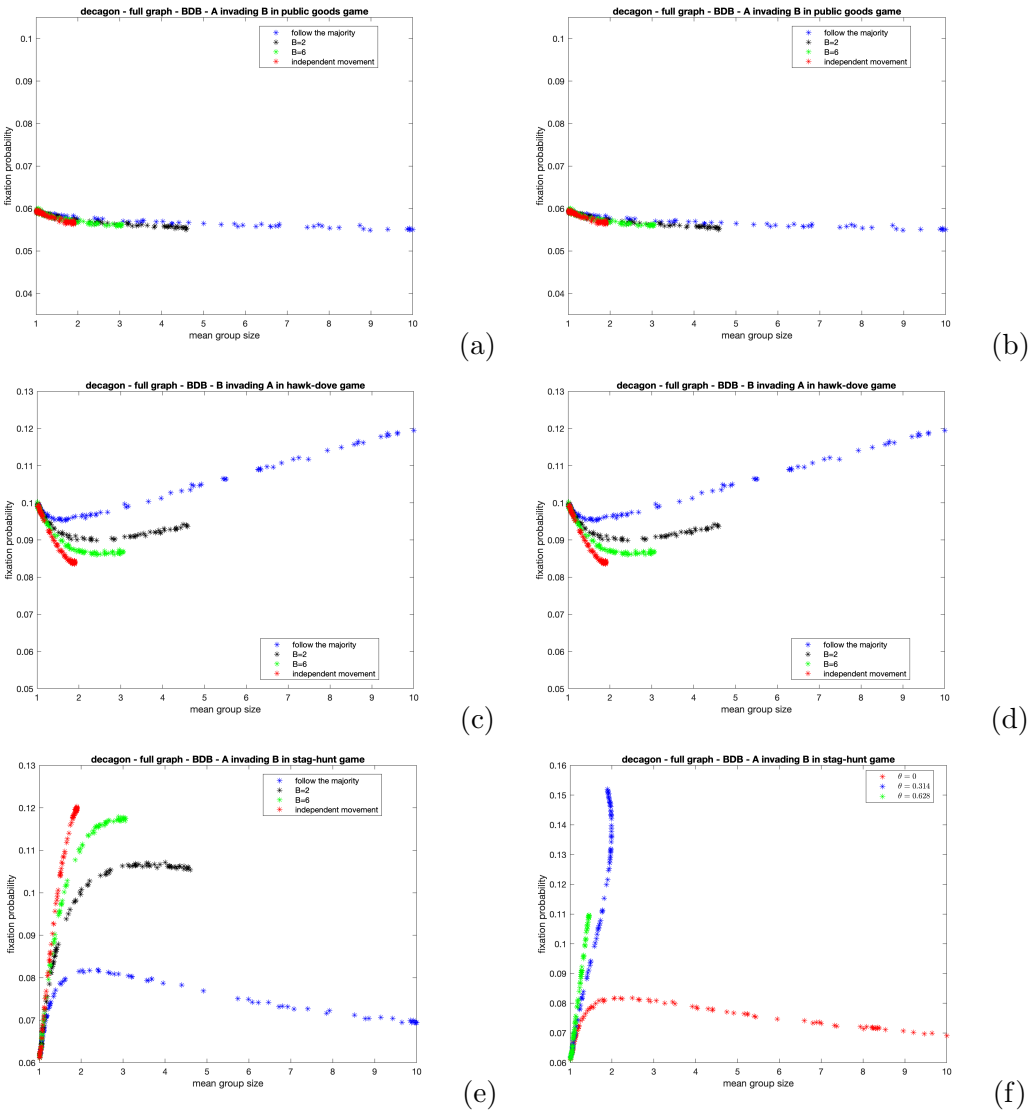

Figure 3.3: The fixation probability plotted against the mean group size for a well-mixed population in the Public Goods, Hawk-Dove and Stag-Hunt games on the complete decagon graph. As we vary h, we plot the corresponding fixation probability and mean group size values against each other. Figures (a), (c) and (e) illustrate Polya-urn processes where we set $B = 0$ (follow the majority), $B = 2$, $B = 6$ and $B = 10{,}000$ (a sufficiently large value of B representing independent movement). (b), (d) and (f) show wheel processes where we set $\theta = 0$ (follow the majority), $\theta = \frac{2\pi}{N}$ (represents a near complete dispersal process) and $\theta = \frac{\pi}{N}$.

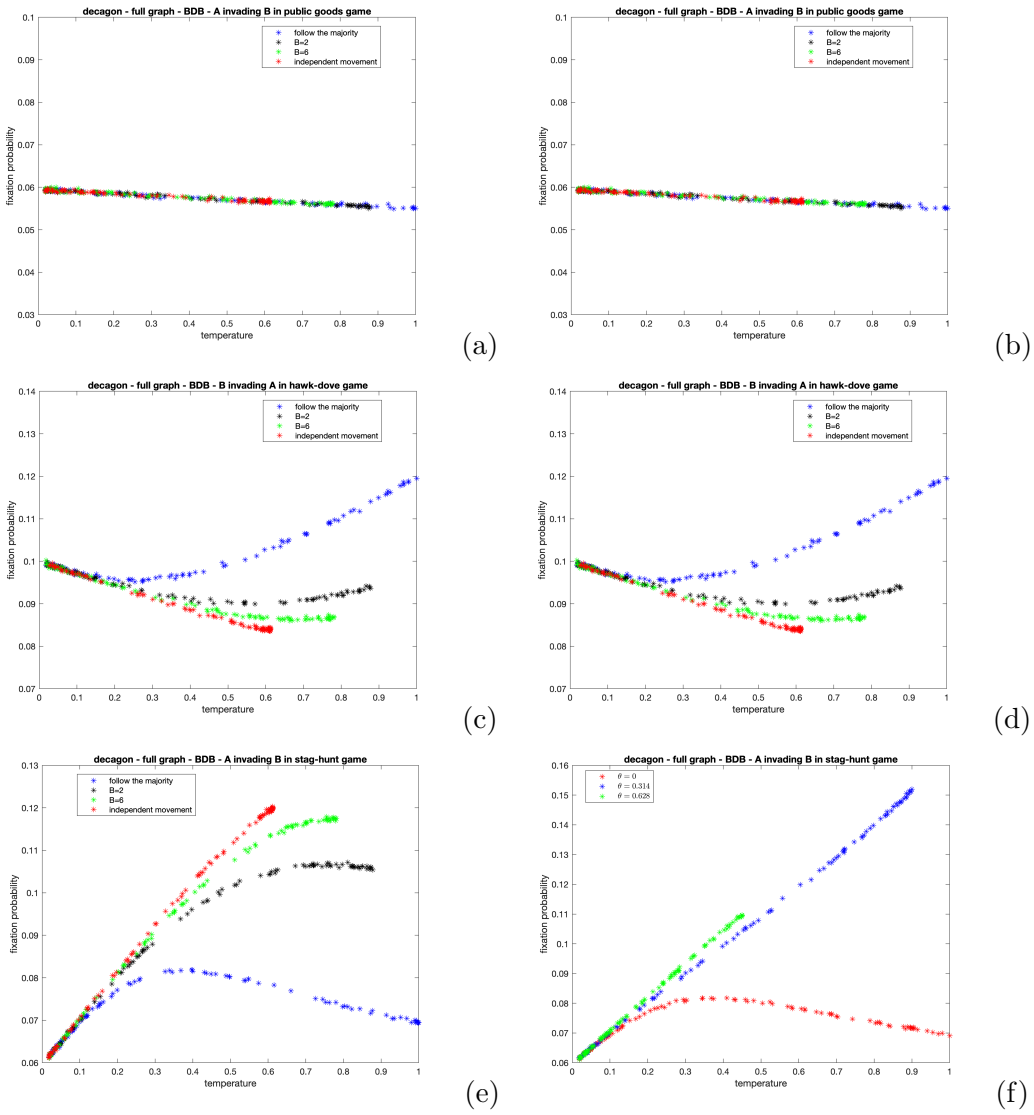

Figure 3.4: The fixation probability plotted against the temperature for a well-mixed population in the Public Goods, Hawk-Dove and Stag-Hunt games on the complete decagon graph. As we vary h, we plot the corresponding fixation probability and temperature values against each other. Figures (a), (c) and (e) illustrate Polya-urn processes where we set $B = 0$ (follow the majority), $B = 2$, $B = 6$ and $B = 10{,}000$ (a sufficiently large value of B representing independent movement). (b), (d) and (f) show wheel processes where we set $\theta = 0$ (follow the majority), $\theta = \frac{2\pi}{N}$ (represents a near complete dispersal process) and $\theta = \frac{\pi}{N}$.

Figure 3.1 illustrates the fixation probability of a mutant cooperator and defector in the Stag-Hunt game under the Polya-urn and wheel processes on the complete decagon. Figures 3.1(a) and 3.1(b) show that for the Polya-urn processes where $B \neq 0$, the cooperator's fixation probability reaches its maximum when $h = 1$, meaning that all members of the population participate in the movement process. This leads to the formation of groups of varying sizes that reach the threshold, enabling members to share the reward among themselves. At this point, the cooperator's fixation probability exceeds $1/N = 0.1$, whereas Figure 3.1(e) indicates that the corresponding fixation probability for the defector remains below $1/N$. This demonstrates the significant impact of row-dependent movement in the Stag-Hunt game, as it can raise the cooperator's fixation probability not only above neutrality but also above the defector's, thereby facilitating the evolution of cooperation. Corresponding figures are shown in Haq et al. (2024) for the Public Goods game. It was shown that under this social dilemma game, cooperation is always below neutrality for all movement processes. However, the results in the Stag-Hunt game demonstrate a stronger influence of the movement mechanisms, as these can raise the cooperator's fixation probability not only above neutrality, but also above the defector's. This is due to the nature of the Stag-Hunt game, where cooperators can generate rewards when in groups that reach the threshold. However, in the Public Goods game, defectors always benefit from the presence of cooperators, regardless of whether the threshold is met, thereby undermining the advantages of cooperative behaviour.

We see a similar trend in Figures 3.1(c) and 3.1(g) which show an important example where the wheel process significantly influences the evolution of cooperation. When $h = 1$ and $\theta = \pi/10$, the cooperator's fixation probability is above 0.15, whereas the defector's corresponding fixation probability is below 0.02. This angle proves very beneficial for cooperators and allows them to meet each other in pairwise groups that meet the threshold to produce the reward. Under these conditions, defectors mostly find themselves in pairwise groups that either contain another defector or a single cooperator, in either case, the reward cannot be produced and the defector's fitness remains relatively low. Therefore, there is a significant disparity between the cooperator's and defector's fixation probabilities.

As h increases, the cooperator's fixation probability gradually decreases. This is due to individuals being more likely to remain on their home vertex and, therefore,

less likely to move and interact with one another. Therefore, the likelihood of cooperators being in groups where the threshold is reached diminishes, while defectors have a higher relative fitness when all individuals are alone, thereby reducing the cooperator's fixation probability.

For the follow the majority process ($B = 0$), the cooperator's fixation probability is at its lowest compared to the other movement processes. This is due to all members partaking in the movement process aggregating on the same vertex, allowing defectors to exploit cooperators by receiving a share of the produced reward without incurring any cost. Under this movement process, defectors have a greater relative fitness than cooperators, thereby minimising the cooperator's fixation probability. An important result in this context is that herding proves quite detrimental to cooperators, as it reduces their fixation probability below the neutral benchmark of $\frac{1}{N}$ and raises the defector's above this level, thereby favouring the evolution of defection. As h rises, the fixation probability gradually rises, as individuals are more likely to be in smaller groups, until h reaches a level where individuals are most inclined to remain on their home vertex. As h continues to increase, the fixation probability falls as cooperators are always alone and continue to pay a cost, unlike defectors who do not and, therefore, maintain a higher relative fitness.

Figure 3.2 illustrates the mean group size and temperature under distinct Polya-urn and wheel processes for varying values of h on the complete decagon graph. In Figure 4a, the mean group size reaches its maximum when $h = 1$ across all movement processes. This is because all individuals participate in the movement process at this value of h, meaning that under the follow the majority process, the mean group size is equal to the population size. However, as the value of B increases, the value of the mean group size decreases. This is due to the movement process gradually shifting from a deterministic type to a stochastic process, eventually becoming a completely random movement process as the number of balls in the urn increases. The trends in Figure 3.2(b) for the wheel process are largely similar to the Polya-urn, except when the angle between the spikes is approximately $\frac{2\pi}{N}$ and $h = 1$. At this point, all individuals within the population are nearly always alone. Given the significant effects of the movement processes on the mean group size, we considered the impact of mean group size on the fixation probability of cooperative strategies, as shown in Figure 3.3.

Figure 3.3 illustrates the fixation probabilities of cooperative strategies plotted

against the mean group size under the Polya-urn and wheel processes on the complete decagon. Figures 3.3(a) and 3.3(b) show the fixation probability of a mutant cooperator in the Public Goods game. As the mean group size increases, the cooperator's fixation probability decreases for all movement processes. This result is expected, as larger group sizes lead to interactions between cooperators and defectors, allowing defectors to gain rewards and thereby reducing the relative fitness of cooperators. Figures 3.3(c) and 3.3(d) depict the fixation probability of a mutant dove. In contrast, as the mean group size increases, the fixation probability also increases. This occurs because hawks are more likely to be grouped together as the group size grows, causing them to endure greater costs, which lowers their relative fitness and, consequently, raises the dove's fixation probability. Figures 3.3(e) and 3.3(f) represent the cooperator's fixation probability in the Stag-Hunt game. Initially, as the mean group size increases, the fixation probability rises until the mean group size reaches the threshold level (set as $L = 2$). This benefits cooperators, as they either find themselves in groups with another cooperator, enabling them to produce and share the reward, or with a defector, in which case the reward cannot be produced. Other values of L would change the mean group size where the maximum fixation probability occurs, constrained by the group formations of the considered movement process. However, as the mean group size continues to increase, the fixation probability declines. This is because larger group sizes do not provide significant additional benefits to cooperators beyond the threshold level and instead allow defectors to join cooperative groups and receive a share of the reward.

Figures 3.2(c) and 3.2(d) show the temperature for various Polya-urn (c) and wheel (d) processes for varying values of h on the complete decagon graph. The trends observed here are very similar to those in Figures 3.2a and 3.2b, as it has been previously demonstrated that temperature increases with mean group size (Broom et al. 2015). This unsurprisingly holds under the considered movement processes. Low values of h correspond to high levels of movement within the population, therefore when $h = 1$, the temperature is at its highest, as individuals are more likely to be replaced by others due to frequent interactions (except for the case where $\theta = \frac{2\pi}{N}$, as individuals are nearly always alone, the temperature is at its lowest). As h increases, individuals are less likely to move and, therefore, less likely to interact with one another, leading to a decrease in temperature across all of the movement processes.

Figure 3.4 depicts the fixation probabilities of cooperative strategies plotted against the temperature under the Polya-urn and wheel processes on the complete decagon. Figures 3.4(a) and 3.4(b) show the fixation probability of a mutant cooperator in the Public Goods game. As the temperature increases, the cooperator's fixation probability decreases for all movement processes. This is because higher temperatures indicate greater levels of mixing between cooperators and defectors, enabling defectors to gain rewards from cooperators. Notably, the different movement processes overlap, indicating that, regardless of the movement mechanism, the temperature consistently predicts the cooperator's fixation probability. In other words, the temperature is the most significant predictor in the Public Goods evolutionary process as shown in table 3.1.

Furthermore, from Figures 3.4(c) and 3.4(d), we observe that in the Hawk-Dove game, as the temperature increases, the dove's fixation probability increases. High temperature levels correspond to low values of h and, therefore, high levels of interaction between doves and hawks. As hawks interact with one another, they incur greater costs, which reduces their relative fitness and, consequently, increases the dove's fixation probability. Additionally, the relationship between temperature and the dove's fixation probability is linear for small temperature values but breaks down as temperature increases, particularly for the follow the majority process. Low temperatures, correspond to high values of h, meaning many individuals are not partaking in the movement process and are either alone or in small pairwise groups. As temperature increases, more individuals become mobile, leading to the formation of groups of various sizes, particularly for the follow the majority process, which significantly disadvantages hawks and causes the linearity breakdown. Thus, in the Hawk-Dove game, at higher temperatures, the governing movement process holds an important role in the evolutionary process.

Furthermore, from Figures 3.4(e) and 3.4(f), we observe that in the Stag-Hunt game, the cooperator's fixation probability increases as the temperature rises, until it reaches a level where the fixation probability begins to decrease. Low temperature values indicate limited interaction between individuals. Consequently, the relationship between temperature and fixation probability is linear, similar to that observed in the Hawk-Dove game. As temperature increases, individuals are more likely to move and interact in pairwise groups, when cooperators interact with at least one other cooperator, they can produce the reward, leading to an increase in fixation

probability. When $B = 0$ or $\theta = 0$, the fixation probability declines rapidly as temperature rises, due to the deterministic nature of the movement process, which causes individuals to herd together. This herding effect is disadvantageous to cooperators, reducing their relative fitness and, consequently, their fixation probability. When $B \neq 0$ or $\theta \neq 0$, the decrease in fixation probability is more gradual, as cooperators move probabilistically and can still engage in beneficial pairwise interactions.

Below, we present table 3.1 summarising how effective the evolutionary measures are at predicting fixation probability for each of the games considered, and when the movement mechanism holds a more influential role.

Game	**Mean group size**	**Temperature**
Public-Goods	Strong predictor at low values, the effect diminishes for larger groups.	Strongest predictor across all temperatures.
Hawk–Dove	Strong predictor at low mean group size values.	Strong predictor for low temperatures.
Stag–Hunt	fixation is dependent on the movement mechanism and threshold value (L).	Strong predictor for low temperatures.

Table 3.1: Summary of the relative effectiveness of mean group size and temperature in predicting fixation probability across the Public-Goods, Hawk–Dove and Stag–Hunt games under BDB dynamics.

3.3.3 Differences between processes

In the Public Goods game, the fixation probability of a mutant cooperator under BDD dynamics, expressed in terms of the temperature, is given by

$$\rho_1^{\mathcal{A}} = \frac{1}{1 + \sum_{j=1}^{N-1} \prod_{k=1}^{j} \frac{(N-k+(k-N+\frac{1}{\tau_N}(N-1))\frac{R+kV(\frac{\tau_N}{N-1})}{R-C+(k-1)V(\frac{\tau_N}{N-1})})}{(k+(\frac{1}{\tau_N}(N-1)-k)\frac{R-C+(k-1)V(\frac{\tau_N}{N-1})}{R+kV(\frac{\tau_N}{N-1})})}}. \tag{3.15}$$

This equation has a similar structure to that of the BDB case (3.14). In both cases, the temperature plays a more significant role in determining the fixation probability than the governing movement mechanism. This pattern is illustrated in Figure 3.4(a), where, under BDB dynamics, a fixed temperature value results in approximately identical fixation probabilities across all movement processes. This suggests that the temperature alone is sufficient to determine the fixation probability in the Public-Goods game.

However, Figure 3.5 demonstrates a different relationship under BDD dynamics. Specifically, for a fixed temperature value, the different movement processes yield varying fixation probabilities. Unlike in the BDB case, the analytical predictions and simulations do not match. The difference arises because the theoretical process assumes that individuals effectively participate in an infinite number of games, which is the same process as in Broom et al. (2015) and Pattni et al. (2017). However, the simulations assume that individuals only play a single game before the dynamic time step, which is consistent with the process in Schimit et al. (2019) (2022).

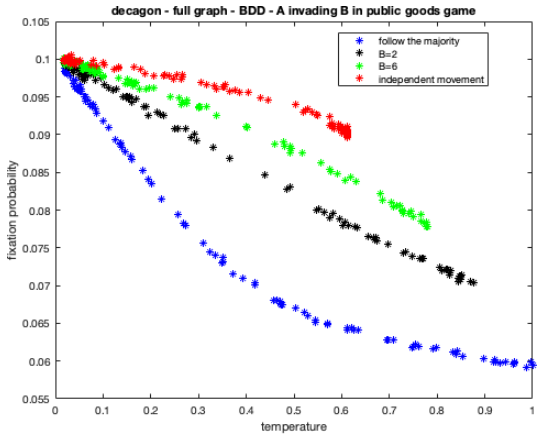

Figure 3.5: The fixation probability plotted against the temperature in the Public Goods games on the complete decagon graph under BDD dynamics for distinct Polya-urn processes. We set $B = 0$ (follow the majority), $B = 2$, $B = 6$ and $B = 10,000$ (a sufficiently large value of B representing independent movement).

These two processes might be expected to produce the same results, however, under certain updating rules, they yield differing outcomes due to three key averaging effects: payoff averaging, weight averaging and averaging of reciprocals of fitness. As Broom, Cressman & Křivan (2019) discussed, the expectation of a ratio, $E[a/b]$, is not equal to the ratio of expectations, $E[a]/E[b]$.

This distinction between the expectation of a ratio and the ratio of expectations manifests differently across the updating rules, occasionally leading to different outcomes between the two processes. For example, under BDB dynamics, the simulations, an extension of Schimit et al. (2019), assume

$$E[b_i] = E\left[\frac{F_i}{\sum_k^N F_k}\right], \tag{3.16}$$

whereas the theoretical analysis, an extension of Broom et al. (2015) and Pattni

et al. (2017) assume,

$$E[b_i] = \frac{E[F_i]}{E\left[\sum_k^N F_k\right]}. \tag{3.17}$$

Although this discrepancy can lead to differences between the two processes, the error becomes negligible under BDB dynamics when the background payoff is high or the population size is large. This averaging effect is present under all dynamics, but its influence varies depending on the specific updating rule.

A further averaging issue occurs when considering the weights under dynamics where selection acts on the second event (such as BDD and DBB), introducing an additional layer of difference between the two processes. For example, when h is large, the self weight dominates the others, emphasising this effect. However, under dynamics where selection acts on the first event (such as BDB and DBD), the denominator in the replacement event sums to one, therefore removing this additional issue of averaging.

The third averaging issue occurs in dynamics where selection acts on the replacement event (such as DBD and BDD). These dynamics involve terms with reciprocals of individuals' fitnesses, which further contributes to the differences between the two processes.

Consequently, for BDD dynamics, the analytical and simulation results do not coincide, as they are derived from different processes based on different assumptions. Table 3.2 shows that all three effects are present in BDD dynamics. For this reason, we did not compare the analytical results with the simulations in Chapter 2.

Below, we present a table summarising these three factors and their presence in the different dynamics.

Dynamics	**Payoff Averaging**	**Weight Averaging**	**Fitness Inverses**
BDB	✓	x	x
BDD	✓	✓	✓
DBD	✓	x	✓
DBB	✓	✓	x

Table 3.2: Summary of the three effects across different dynamics. A tick (✓) represents the presence of the effect, whereas a cross (x) indicates its absence.

3.4 Discussion

In this chapter, we have extended the modelling framework developed in Broom & Rychtar (2012), by utilising the evolutionary model introduced in Haq et al. (2024) to not only examine the effects of row-dependent movement (Broom et al. 2020) on predictors of fixation probability, but also to implement the multiplayer Stag-Hunt game within the evolutionary context of the territorial raider model. In previous models, (Broom et al. 2015, Pattni et al. 2017, Schimit et al. 2019) individuals moved independently, meaning that only random movement was considered in the prior analysis of predictors of fixation probability. Also, individuals primarily interacted via the Public Goods, Hawk-Dove or Fixed Fitness Games. We have considered a different social dilemma in the form of the multiplayer Stag-Hunt game, where selection can favour the evolution of cooperation depending on the movement mechanism governing the process (unlike in the Public Goods game, where cooperation cannot evolve in well-mixed populations).

We first demonstrated in section 3.3.1 how previously defined measures of aggregation from Broom et al. (2020), specifically T (1.49) relate to the mean group size and showed how T, mean group size and temperature can be calculated. Previous work by Broom et al. (2015) and Schimit et al. (2019) explained the importance of these predictors, and our aim was to demonstrate that these measures not only hold theoretical significance, but can also be practically calculated for various movement processes. In section 3.3.2, we examined the Stag-Hunt game and showed that herding can be significantly detrimental to the evolution of cooperation, to the extent that selection opposes its evolution. However, other movement processes raise the cooperator's fixation probability above that of the defector and above the neutral benchmark, thereby supporting the evolution of cooperation. A significant example of this was shown in the wheel process. In the Stag-Hunt game, row-dependent movement plays a more influential role than in the Public Goods game considered by Haq et al. (2024). Dispersal can also be detrimental to cooperators as it ensures cooperators partaking in the movement process, do not interact with each other, reducing their chances of being in a group that meets the threshold.

We also considered the effects of various movement processes on the mean group size and temperature and, in turn, their influence on fixation probability and have observed patterns in our model that have not been previously observed in evolu-

tionary graph theory (Pattni et al. 2015, Traulsen et al. 2007). In the Public Goods game, we demonstrated that temperature is a stronger predictor of fixation than mean group size across all levels of h, regardless of the movement process. Our findings indicated that temperature maintains a linear relationship with fixation probability for all movement processes, signifying its importance as the most crucial parameter in the evolutionary process. This was first identified by Broom et al. (2015) but only for high levels of home fidelity and independent movement. Our analysis extends this work by incorporating more complex movement mechanisms, demonstrating that temperature's predictive property remains robust even when individuals move in a coordinated manner. In the Hawk-Dove game, we showed that temperature continues to be a stronger predictor of fixation. However, due to the greater complexity of the game compared to the Public Goods game, the linear relationship between temperature and fixation breaks down as the temperature rises, with a similar pattern observed in the Stag-Hunt game. We provided an analytical analysis of this relationship, highlighting that while temperature is generally a reliable predictor, the nature of the game and the governing movement process play significant roles in determining the relationship between temperature and fixation.

In addition to examining the impact of the row-dependent movement mechanisms, we also investigated the differences between two modelling processes used in the territorial raider model (Broom et al. 2015, Pattni et al. 2017, Schimit et al. 2019, 2022). One process assumes that individuals effectively participate in an infinite number of games per time step, an assumption underlying the process from Broom et al. (2015) and Pattni et al. (2017). The other process assumes that individuals play a single game before each update, often assumed in the simulations such as in Schimit et al. (2019, 2022). Although these processes might appear equivalent, we identified three averaging issues, payoffs, weights and reciprocal fitness terms that can lead to different outcomes depending on the evolutionary dynamics governing the process. Although the simulation process from Schimit et al. (2019, 2022) can be seen as extensions of the theoretical process from Broom et al. (2015) and Pattni et al. (2017), under BDB dynamics, this equivalence does not generally hold under other dynamics. Schimit et al. (2019) considered the territorial raider model involving complex networks which could be revisited using an approach where individuals play a large number of games per time step, but this would involve significant computational resources.

Chapter 4

Extending the Movement Methodology to Incomplete Networks

4.1 Introduction

In the previous chapters, we analysed the effects of row-dependent movement on the evolution of cooperation, focusing on complete graphs. In such settings, tracking the level of herding among individuals is relatively straightforward. For example, under the follow the majority process with $h = 1$, all individuals are located at the same place. On incomplete graphs, however, perfect aggregation is no longer guaranteed. To address this, we begin by extending T (1.49) by establishing upper and lower bounds on the maximum possible aggregation for all movement processes on a given graph structure.

An important question is whether the generalised movement methodology developed in section 2.3.1 retains its faithful property when applied to incomplete graphs. In chapter 2, we showed that this methodology ensures all individuals achieve the target apriori distribution. In this chapter, however, we provide a simple counterexample demonstrating that the property can fail on incomplete graphs for sequential movement processes. This result motivates our focus on the wheel process, where we extend the mechanism to incomplete graphs and develop an alignment algorithm to approximate maximum herding. We intend to submit the results in this chapter as a publication.

4.2 The Model

The evolutionary set-up in this chapter uses the same underlying framework discussed in chapters 2 and 3 (refer to sections 2.2 and 3.2). The population structure is again defined by the territorial raider model (refer to section 2.2.1). However, in this chapter, we consider cases where the underlying network is incomplete. As a result, certain assumptions that held in the previous chapters no longer apply. For instance, some individuals in the population no longer have access to all locations, meaning the movement methodology developed in section 2.3.1 may no longer ensure the movement mechanisms remain faithful i.e. a given target distribution may not be achieved. Additionally, individuals in the same population no longer share the same temperature, that is, equation (3.1) does not hold globally. As before, we consider both BDB and BDD dynamics, consistent with the dynamics in chapters 2 and 3.

4.3 Results

In this section, we first establish upper and lower bounds for measures introduced by Broom et al. (2020). These bounds provide insight into the maximum achievable aggregation on incomplete graphs because, unlike complete graphs considered in chapters 2 and 3, total aggregation is not guaranteed on incomplete graphs, which motivates this direction.

We then show that the movement methodology developed in Section 2.3.1 no longer guarantees the faithfulness of sequential movement processes (follow the majority and Polya-urn), by providing a simple counterexample where this property fails. This demonstrates a limitation of the methodology when applied to incomplete graphs and motivates our focus on the wheel process.

Next, we extend the wheel process to incomplete networks and introduce an alignment algorithm designed to approximate maximal aggregation. We provide illustrative examples of the alignment algorithm and conclude with simulations investigating how the extended wheel process affects the evolution of cooperation on complete networks.

4.3.1 Upper and lower bounds on T_{max}

In section 1.9, T (1.49) was defined as the probability of two individuals being together under a particular movement process. Then, T_{max} is the maximum possible probability over all movement processes on a particular structure. In this section, we provide upper and lower bounds on T_{max}. To determine an upper bound for T_{max}, we present a step-by-step explanation leading to (4.1). Consider an arbitrary number of individuals who have moved to I_i's home vertex, denoted by k_i+1, where k_i is the number of I_i's neighbours and the $+1$ accounts for I_i, remaining on their home place to maximise aggregation. The number of pairs that can form within this group is given by $\binom{k_i+1}{2}$. An upper bound for the probability of this group forming is determined by the minimum number of connections I_i or one of its neighbours possesses. Accordingly, this probability is bounded above by $\frac{1}{k_{i,min}+1}\binom{k_i+1}{2}$, where $k_{i,min}$ denotes the minimal degree among I_i's neighbours. To capture this across the entire network, we sum over all vertices, yielding, $\sum_{i=1}^{N}\frac{1}{k_{i,min}+1}\binom{k_i+1}{2}$. Hence, the upper bound for T_{max} is given by

$$\frac{1}{\binom{N}{2}}\sum_{i=1}^{N}\frac{1}{k_{i,min}+1}\binom{k_i+1}{2}. \tag{4.1}$$

Similarly, to determine a lower bound for T_{max}, we weight by $1/N$ as we can coordinate I_i and all of their neighbours to meet on I_i's home place by partitioning the probability into N segments, one per place, and move all that can go there to that place. Therefore, we can achieve an expected number of pairs given by $\sum_{i=1}^{N}\frac{1}{N}\binom{k_i+1}{2}$. Therefore, a lower bound for T_{max} is given by

$$\frac{1}{\binom{N}{2}}\sum_{i=1}^{N}\frac{1}{N}\binom{k_i+1}{2}. \tag{4.2}$$

Alternatively, one might naturally consider a potentially tighter lower bound for T_{max} by weighting by $1/(k_{i,max}+1)$, where $k_{i,max}$ denotes the maximal degree among I_i and their neighbours. This leads to the expression:

$$\frac{1}{\binom{N}{2}}\sum_{i=1}^{N}\frac{1}{k_{i,max}+1}\binom{k_i+1}{2}. \tag{4.3}$$

However, we show that this proposed lower bound can fail. Consider a cycle graph with four nodes. Under maximum alignment, three individuals aggregate at a single

location while the remaining individual is alone. In this case, there are three possible pairs of individuals who are together and three other possible pairs that are not resulting in $T_{max} = \frac{1}{2}$. Applying the expression in (4.3), we obtain: $\frac{1}{6}(\frac{4}{3}\binom{3}{2}) = \frac{2}{3}$, which overestimates the true value. In contrast, using (4.2), we find $\frac{1}{6}\frac{1}{4}(4\binom{3}{2}) = \frac{1}{2}$. This example illustrates that while (4.3) may seem like a natural alternative, it does not always provide a valid lower bound. The failure arises because, under these higher probabilities, we cannot always achieve the same level of coordination between individuals that was guaranteed in the previous case.

Consider an N-sized, regular graph with k degree, then the upper and lower bounds of T_{max} are given by

$$\frac{1}{\binom{N}{2}}\sum_{i=1}^{N}\frac{1}{N}\binom{k+1}{2} \leq T_{max} \leq \frac{1}{\binom{N}{2}}\sum_{i=1}^{N}\frac{1}{k+1}\binom{k+1}{2},$$

$$\frac{1}{\binom{N}{2}}\frac{k(k+1)}{2} \leq T_{max} \leq \frac{1}{\binom{N}{2}}\frac{Nk}{2},$$

$$\frac{k(k+1)}{N(N-1)} \leq T_{max} \leq \frac{k}{N-1}. \tag{4.4}$$

4.3.2 Example of an unfaithful process

In chapter 2, we developed a general movement methodology with two main purposes. Firstly, it embedded the row-dependent movement mechanisms of Broom et al. (2020) into the evolutionary framework of the territorial raider model introduced by Broom et al. (2015). Secondly, it ensured that individuals within the population achieve a specified target distribution, given by the apriori distribution. This property also held in chapter 3, as the graphs considered were all complete.

A natural next step is to ask whether this methodology extends to incomplete graph structures, which represent more realistic and complex population networks. Faithfulness was a key property intended in the previous chapters, and it is important to determine whether it holds in this broader setting. We demonstrate, however, through a simple counterexample that faithfulness can fail under sequential movement processes (follow the majority and Polya-urn). Specifically, we examined a line graph with three nodes and individuals, illustrated in Figure 4.1, where movement is governed by the follow the majority process.

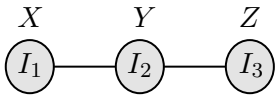

Figure 4.1: The line graph for three individuals. I_1 resides on place X, I_2 resides on place Y, I_3 resides on place Z.

The apriori distribution for I_1 is given by: $P(I_1$ is on their home vertex$) = h/(h+1)$ and $P(I_1$ is not on their home vertex$) = 1/(h+1)$. Assuming $h > 1$, the probability that I_1 partakes in the movement process is $P($ I_1 partakes in the movement process$) = 2/(h+1)$, while the probability that I_1 does not move and, therefore, remains on their home vertex is $P($ I_1 does not partake in the movement process$) = (h-1)/(h+1)$. Using the movement methodology developed, we considered all the possible ways in which I_1 remains on their home vertex to determine whether the target distribution aligns with their apriori distribution.

The probability that only I_1 partakes in the movement process and returns to their home vertex $(h-1)^2/(h+2)(h+1)^2$. If only I_2 moves, then I_1 must remain on their home vertex; the same holds if only I_3 moves. The probability of these cases occurring is $5(h-1)^2/(h+2)(h+1)^2$. If both I_1 and I_2 move, the probability of I_1 being on their home vertex is $3(h-1)/(h+2)(h+1)^2$. If I_2 and I_3 partake in the movement process, then I_1 must remain on their home vertex, with probability $6(h-1)/(h+2)(h+1)^2$. If only I_1 and I_3 move, the probability of I_1 being on their home vertex is $3(h-1)/2(h+2)(h+1)^2$. If all individuals move, then the probability of I_1 being on their home vertex is $29/6(h+2)(h+1)^2$. If no one moves, then the probability of I_1 being on their home vertex is $(h-1)^3/(h+2)(h+1)^2$. Hence, the total probability of I_1 being on their home vertex is $6(h-1)^2/(h+2)(h+1)^2 + 21(h-1)/2(h+2)(h+1)^2 + 29/6(h+2)(h+1)^2 + (h-1)^3/(h+2)(h+1)^2$. To determine the correct value of h' that achieves the target apriori distribution, we must solve for h' in the following equation

$$\frac{h'}{h'+1} = \frac{12(h-1)^2 + 21(h-1)}{2(h+2)(h+1)^2} + \frac{29}{6(h+2)(h+1)^2} + \frac{(h-1)^3}{(h+2)(h+1)^2}. \tag{4.5}$$

By carrying out a very similar calculation for the probability of I_2 being on their home vertex, we must also solve for h' in the following equation

$$\frac{h'}{h'+2} = \frac{5(h-1)^2 + 9(h-1)}{(h+2)(h+1)^2} + \frac{35}{6(h+2)(h+1)^2} + \frac{(h-1)^3}{(h+2)(h+1)^2}. \tag{4.6}$$

Equations (4.5) and (4.6) show that two distinct values of h' are required to ensure that I_1 and I_2 meet their respective target distributions. In other words, each individual would require their unique value home fidelity value. Therefore, in our models with a single global home fidelity parameter, individuals following sequential processes on incomplete networks may not always achieve their target distributions.

However, this result may be expected, particularly in heterogeneous graph structures, where the evolutionary setting is governed by a single global home fidelity parameter. In such models, collective movement becomes increasingly constrained by factors such as spatial connectivity. As a result, individual movement choices are not solely governed by the row-dependent movement mechanism but are also influenced by structural limitations and the ordering of others within the movement process, making it difficult to achieve a target distribution that aligns with the apriori. In a more complex model where each individual has their unique home fidelity parameter, it may be possible to achieve the apriori distribution as a target.

It is important to note that, unlike the sequential movement processes, the wheel continues to be a faithful movement process due to its mechanism. For instance, consider an incomplete graph where there are M places. Suppose individual I_i has $d-1$ neighbours. Then their target apriori distribution is: P(at home vertex) $= \frac{h}{h+d-1}$, P(elsewhere) $= \frac{d-1}{h+d-1}$. Assuming $h > 1$, I_i engages in the wheel process with probability $\frac{d}{h+d-1}$, their wheel is split into d evenly-sized segments, therefore the probability I_i is at their home place is $\frac{h-1}{h+d-1} + \frac{1}{d}(\frac{d}{h+d-1}) = \frac{h}{h+d-1}$. The probability they are elsewhere is $(1-\frac{1}{d})(\frac{d}{h+d-1}) = \frac{d-1}{h+d-1}$. Both of these match the target apriori distribution exactly.

This agreement occurs because the wheel allocates individuals simultaneously, preserving the intended distribution. However, sequential movement processes introduce dependence on the order in which individuals move. Once the first individual moves, it can alter the marginal distribution of the next individual, potentially altering the achieved distribution away from the intended target. This makes it difficult for all individuals to simultaneously satisfy the apriori distribution on incomplete networks. For this reason, we focus on the wheel process for the remainder of the chapter.

4.3.3 Extending the wheel to incomplete graph structures

The sequential movement processes can be implemented on incomplete graphs, but, as demonstrated, they may fail to preserve faithfulness, making them unsuitable for maintaining target distributions. However, the wheel process is faithful on incomplete graphs, but it must be extended to function on incomplete graphs where individuals may have access to unique locations. On a complete graph, individuals within a well-mixed population have access to all locations, allowing them to be represented as spikes on the same wheel. On an incomplete graph, however, individuals may have unique apriori distributions granting them access to specific locations unavailable to others, so a single shared wheel is generally no longer possible.

To address this, we modified the wheel procedure from section 1.9. The first step involves identifying all individuals participating in the movement process, followed by stacking their corresponding wheels on top of each other, ensuring that each individual's spike is aligned above their respective wheel, as illustrated in Figure 4.2.

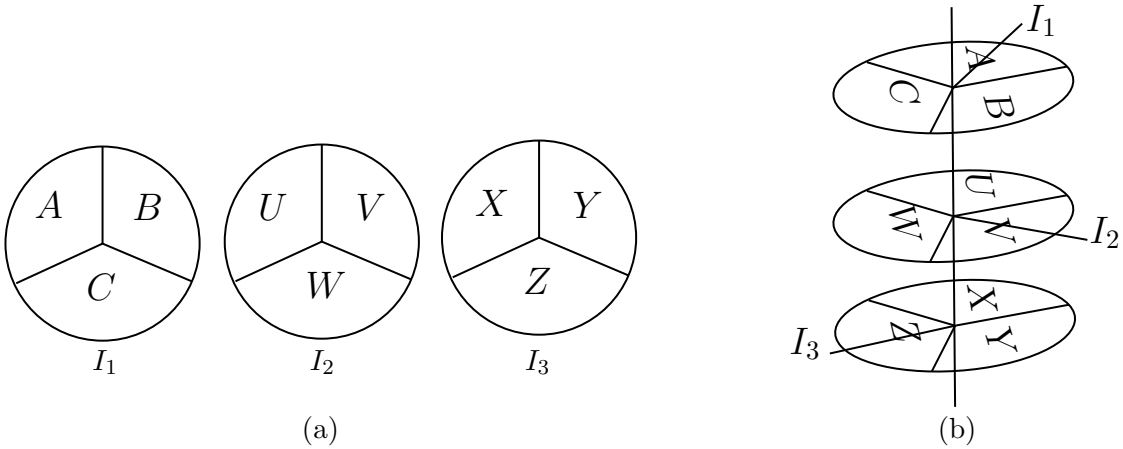

Figure 4.2: The wheel process for incomplete graphs. (a) The wheels for different individuals, where each wheel represents the accessible locations for each individual. Individual I_1 can move to places A, B and C, I_2 can move to U, V and W and I_3 can move to X, Y and Z. (b) represents the wheel stacking procedure. Each individual's spike is positioned above their respective wheel, ensuring that movements are correctly carried out on incomplete graph structures.

4.3.4 The wheel alignment process

The wheel was introduced in previous chapters as a simple, idealised model of simultaneous allocation, designed to construct distributions with specific properties while preserving faithfulness. For instance, in a well-mixed population, when $h = 1$ and $\theta = 2\pi/N$, all individuals in the population are alone, representing a movement

process where all individuals simultaneously move and eventually become separated. One could imagine a population of animals dispersing from a central location with particular requirements for levels of separation from others. When $h = 1$ and $\theta = 0$, all individuals within the population occupy the same place, representing a movement process where all individuals prefer to move simultaneously and aggregate at the same location. These examples highlight the wheel's ability to capture both dispersal and herding behaviours.

An important consideration is to ensure that the fundamental behaviours captured in earlier chapters, such as aggregation when $\theta = 0$, remain consistent when the wheel is applied on an incomplete graph. To address this, we developed an alignment algorithm to approximate maximal aggregation by rotating the stacked wheels in such a way that it enables as many individuals as possible herd together at the same location $\theta = 0$.

Consider an N-sized population on an incomplete graph. The alignment procedure is defined as follows:

- Construct an N x N matrix, where the (i, j)-entry represents the probability of individual I_i moving to the j^{th} place.

- Identify the column with the least zero entries. Within this column, subtract the minimum non-zero value from all non-zero entries. This step is referred to as the *primary alignment.*

- Record the alignment in a table. Each column label corresponds to a location where individuals aggregate. For example, $P_1 : A$ implies that the individuals within the first primary alignment are aligned to place A. The entries within each column will either be the value subtracted during the primary alignment, or its negative. A negative value indicates that the corresponding individual cannot move to that place and will instead be aligned elsewhere.

- If a column in the alignment table contains any negative entries, examine the corresponding rows in the matrix to determine whether another column can group at least some of these individuals during the previous primary alignment. If so, repeat the same procedure as the primary alignment. This step is referred to as the *secondary alignment.*

- Ensure that the secondary alignment does not interfere with subsequent pri-

mary alignments, as the objective is to maximise aggregation. If there is a conflict, carry out the secondary alignment if it aligns more individuals than the next primary alignment.

- Once the cumulative total of all primary alignments sums to one, then the alignment process is complete. Any remaining secondary alignments can now be managed accordingly.

To illustrate this process, we present two examples. The first example considers a simple line graph with three nodes, offering an intuitive understanding of how the primary alignment operates in a straightforward setting. The second example explores a more complex and heterogeneous structure, demonstrating the importance of secondary alignments when full alignment between all individuals is not achieved during the primary step. This allows us to observe how our alignment methodology handles more complex networks and ensures that approximately the maximum number of individuals are grouped together.

The first example considers a line graph with three nodes (see figure 4.1). Assuming $h = 1$, the corresponding matrix for this graph is given by

$$\begin{bmatrix} \frac{1}{2} & \frac{1}{2} & 0 \\ \frac{1}{3} & \frac{1}{3} & \frac{1}{3} \\ 0 & \frac{1}{2} & \frac{1}{2} \end{bmatrix} \tag{4.7}$$

The second column has the least zero entries, therefore, we apply the primary alignment to this column aligning $1/3$ of each individual's wheels to location Y. The matrix then becomes

$$\begin{bmatrix} \frac{1}{2} & \frac{1}{6} & 0 \\ \frac{1}{3} & 0 & \frac{1}{3} \\ 0 & \frac{1}{6} & \frac{1}{2} \end{bmatrix} \tag{4.8}$$

The alignment table is updated as follows:

	$P_1 : Y$
I_1	$\frac{1}{3}$
I_2	$\frac{1}{3}$
I_3	$\frac{1}{3}$

Each column now contains one zero, therefore, a primary alignment can be applied

to any of them. For simplicity, we perform the alignment in the first column, aligning $1/3$ of I_1's and I_2's wheel to location X. I_3 will be aligned elsewhere in the secondary alignment step.

$$\begin{bmatrix} \frac{1}{6} & \frac{1}{6} & 0 \\ 0 & 0 & \frac{1}{3} \\ 0 & \frac{1}{6} & \frac{1}{2} \end{bmatrix} \tag{4.9}$$

The alignment table is updated as follows:

	$P_1 : Y$	$P_2 : X$
I_1	$\frac{1}{3}$	$\frac{1}{3}$
I_2	$\frac{1}{3}$	$\frac{1}{3}$
I_3	$\frac{1}{3}$	$\frac{-1}{3}$

(4.10)

Only one negative value has appeared as a result of the primary alignment. Therefore, we do no need to consider the secondary alignment yet and can proceed with the next primary alignment step. The final primary alignment is carried out in the third column. We align $1/3$ of I_2's and I_3's wheels are aligned to location Z, while I_1 is aligned elsewhere. Note that the alternative approach would have been to subtract $1/6$ from the second column and then another $1/6$ from the third column. However, both methods are equivalent and yield the same results in terms of aggregation.

$$\begin{bmatrix} \frac{1}{6} & \frac{1}{6} & 0 \\ 0 & 0 & 0 \\ 0 & \frac{1}{6} & \frac{1}{6} \end{bmatrix} \tag{4.11}$$

The alignment table is updated as follows:

	$P_1 : Y$	$P_2 : X$	$P_3 : Z$
I_1	$\frac{1}{3}$	$\frac{1}{3}$	$\frac{-1}{3}$
I_2	$\frac{1}{3}$	$\frac{1}{3}$	$\frac{1}{3}$
I_3	$\frac{1}{3}$	$\frac{-1}{3}$	$\frac{1}{3}$

(4.12)

We can now include the secondary alignments in the table,

	$P_1:Y$	$P_2:X$	$P_3:Z$	$S_2:Y$	$S_2:Z$	$S_3:X$	$S_3:Y$
I_1	$\frac{1}{3}$	$\frac{1}{3}$	$\frac{-1}{3}$	0	0	$\frac{1}{6}$	$\frac{1}{6}$
I_2	$\frac{1}{3}$	$\frac{1}{3}$	$\frac{1}{3}$	0	0	0	0
I_3	$\frac{1}{3}$	$\frac{-1}{3}$	$\frac{1}{3}$	$\frac{1}{6}$	$\frac{1}{6}$	0	0

(4.13)

Using the results from the final alignment table, we interpret, for example, the $P_2 : X$ column to imply that I_1 and I_2 each have $1/3$ of their wheels aligned to location X. Similarly, columns $S_2 : Y$ and $S_2 : Z$ shows that I_3 has $1/6$ of their wheel aligned to both locations Y and Z, respectively. The formulation for each individual's wheel is illustrated in Figure 4.3. By using (4.1), we calculated that on this network, the

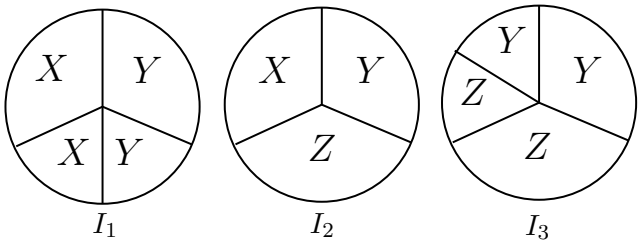

(a)

Figure 4.3: The alignments for each individual on the line graph with three nodes

upper bound of T_{max} is

$$\frac{1}{\binom{3}{2}}\left(\frac{1}{3}\binom{2}{2}+\frac{1}{3}\binom{3}{2}+\frac{1}{3}\binom{2}{2}\right)=\frac{13}{18}. \tag{4.14}$$

Similarly, by using (4.2), the lower bound of T_{max} is

$$\frac{1}{\binom{3}{2}}\frac{1}{3}\left(\binom{2}{2}+\binom{3}{2}+\binom{2}{2}\right)=\frac{5}{9}. \tag{4.15}$$

Calculating the actual value of T under the wheel alignment process gives

$$T=\frac{1}{\binom{3}{2}}\left(\frac{1}{3}\binom{3}{2}+\frac{1}{3}\binom{2}{2}+\frac{1}{3}\binom{2}{2}\right)=\frac{5}{9}. \tag{4.16}$$

The actual value of T coincides with the lower bound of T_{max} on this network.

We also examined the application of the alignment process on a complex graph structure to investigate factors that influence when it is necessary to perform a secondary alignment before proceeding with the next primary alignment. The graph

structure used for this analysis is shown in figure 4.4.

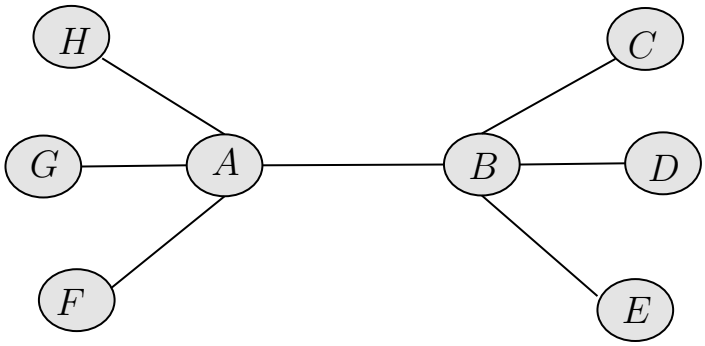

Figure 4.4: A graphical representation of a network considered in the alignment process.

Assuming $h = 1$, the corresponding matrix for the graph in Figure 4.4 is given by

$$\begin{bmatrix} \frac{1}{5} & \frac{1}{5} & 0 & 0 & 0 & \frac{1}{5} & \frac{1}{5} & \frac{1}{5} \\ \frac{1}{5} & \frac{1}{5} & \frac{1}{5} & \frac{1}{5} & \frac{1}{5} & 0 & 0 & 0 \\ 0 & \frac{1}{2} & \frac{1}{2} & 0 & 0 & 0 & 0 & 0 \\ 0 & \frac{1}{2} & 0 & \frac{1}{2} & 0 & 0 & 0 & 0 \\ 0 & \frac{1}{2} & 0 & 0 & \frac{1}{2} & 0 & 0 & 0 \\ \frac{1}{2} & 0 & 0 & 0 & 0 & \frac{1}{2} & 0 & 0 \\ \frac{1}{2} & 0 & 0 & 0 & 0 & 0 & \frac{1}{2} & 0 \\ \frac{1}{2} & 0 & 0 & 0 & 0 & 0 & 0 & \frac{1}{2} \end{bmatrix} \tag{4.17}$$

By carrying out the first primary alignment in the first column, aligning $1/5$ of the five individuals' wheels to place A.

$$\begin{bmatrix} 0 & \frac{1}{5} & 0 & 0 & 0 & \frac{1}{5} & \frac{1}{5} & \frac{1}{5} \\ 0 & \frac{1}{5} & \frac{1}{5} & \frac{1}{5} & \frac{1}{5} & 0 & 0 & 0 \\ 0 & \frac{1}{2} & \frac{1}{2} & 0 & 0 & 0 & 0 & 0 \\ 0 & \frac{1}{2} & 0 & \frac{1}{2} & 0 & 0 & 0 & 0 \\ 0 & \frac{1}{2} & 0 & 0 & \frac{1}{2} & 0 & 0 & 0 \\ \frac{3}{10} & 0 & 0 & 0 & 0 & \frac{1}{2} & 0 & 0 \\ \frac{3}{10} & 0 & 0 & 0 & 0 & 0 & \frac{1}{2} & 0 \\ \frac{3}{10} & 0 & 0 & 0 & 0 & 0 & 0 & \frac{1}{2} \end{bmatrix} \tag{4.18}$$

The alignment table is updated as:

	$P_1 : A$
I_1	$\frac{1}{5}$
I_2	$\frac{1}{5}$
I_3	$\frac{-1}{5}$
I_4	$\frac{-1}{5}$
I_5	$\frac{-1}{5}$
I_6	$\frac{1}{5}$
I_7	$\frac{1}{5}$
I_8	$\frac{1}{5}$

Before the next primary alignment in the second column of the matrix, we address the negative values that appear in rows $3, 4$ and 5 of the alignment table. These three individuals can be secondarily aligned using $1/5$ of the apriori probability in the second column of the matrix. While the first five individuals are aligned to place A, the remaining three are secondarily aligned to place B to maximise aggregation. This secondary alignment does not interfere with the next primary alignment.

$$\begin{bmatrix} 0 & \frac{1}{5} & 0 & 0 & 0 & \frac{1}{5} & \frac{1}{5} & \frac{1}{5} \\ 0 & \frac{1}{5} & \frac{1}{5} & \frac{1}{5} & \frac{1}{5} & 0 & 0 & 0 \\ 0 & \frac{3}{10} & \frac{1}{2} & 0 & 0 & 0 & 0 & 0 \\ 0 & \frac{3}{10} & 0 & \frac{1}{2} & 0 & 0 & 0 & 0 \\ 0 & \frac{3}{10} & 0 & 0 & \frac{1}{2} & 0 & 0 & 0 \\ \frac{3}{10} & 0 & 0 & 0 & 0 & \frac{1}{2} & 0 & 0 \\ \frac{3}{10} & 0 & 0 & 0 & 0 & 0 & \frac{1}{2} & 0 \\ \frac{3}{10} & 0 & 0 & 0 & 0 & 0 & 0 & \frac{1}{2} \end{bmatrix} \tag{4.19}$$

and the alignment table is updated as:

	$P_1 : A$	$S_1 : B$
I_1	$\frac{1}{5}$	0
I_2	$\frac{1}{5}$	0
I_3	$\frac{-1}{5}$	$\frac{1}{5}$
I_4	$\frac{-1}{5}$	$\frac{1}{5}$
I_5	$\frac{-1}{5}$	$\frac{1}{5}$
I_6	$\frac{1}{5}$	0
I_7	$\frac{1}{5}$	0
I_8	$\frac{1}{5}$	0

The next primary alignment is carried out in the second column, which contains fewer zero entries than the other columns. The smallest non-zero entry in this column is $\frac{1}{5}$. This value is subtracted from all non-zero entries in the column.

$$\begin{bmatrix} 0 & 0 & 0 & 0 & 0 & \frac{1}{5} & \frac{1}{5} & \frac{1}{5} \\ 0 & 0 & \frac{1}{5} & \frac{1}{5} & \frac{1}{5} & 0 & 0 & 0 \\ 0 & \frac{1}{10} & \frac{1}{2} & 0 & 0 & 0 & 0 & 0 \\ 0 & \frac{1}{10} & 0 & \frac{1}{2} & 0 & 0 & 0 & 0 \\ 0 & \frac{1}{10} & 0 & 0 & \frac{1}{2} & 0 & 0 & 0 \\ \frac{3}{10} & 0 & 0 & 0 & 0 & \frac{1}{2} & 0 & 0 \\ \frac{3}{10} & 0 & 0 & 0 & 0 & 0 & \frac{1}{2} & 0 \\ \frac{3}{10} & 0 & 0 & 0 & 0 & 0 & 0 & \frac{1}{2} \end{bmatrix} \tag{4.20}$$

	$P_1 : A$	$S_1 : B$	$P_2 : B$
I_1	$\frac{1}{5}$	0	$\frac{1}{5}$
I_2	$\frac{1}{5}$	0	$\frac{1}{5}$
I_3	$\frac{-1}{5}$	$\frac{1}{5}$	$\frac{1}{5}$
I_4	$\frac{-1}{5}$	$\frac{1}{5}$	$\frac{1}{5}$
I_5	$\frac{-1}{5}$	$\frac{1}{5}$	$\frac{1}{5}$
I_6	$\frac{1}{5}$	0	$\frac{-1}{5}$
I_7	$\frac{1}{5}$	0	$\frac{-1}{5}$
I_8	$\frac{1}{5}$	0	$\frac{-1}{5}$

Following the same reasoning as before, a secondary alignment to place A can be

carried out during this primary alignment.

$$\begin{bmatrix} 0 & 0 & 0 & 0 & 0 & \frac{1}{5} & \frac{1}{5} & \frac{1}{5} \\ 0 & 0 & \frac{1}{5} & \frac{1}{5} & \frac{1}{5} & 0 & 0 & 0 \\ 0 & \frac{1}{10} & \frac{1}{2} & 0 & 0 & 0 & 0 & 0 \\ 0 & \frac{1}{10} & 0 & \frac{1}{2} & 0 & 0 & 0 & 0 \\ 0 & \frac{1}{10} & 0 & 0 & \frac{1}{2} & 0 & 0 & 0 \\ \frac{1}{10} & 0 & 0 & 0 & 0 & \frac{1}{2} & 0 & 0 \\ \frac{1}{10} & 0 & 0 & 0 & 0 & 0 & \frac{1}{2} & 0 \\ \frac{1}{10} & 0 & 0 & 0 & 0 & 0 & 0 & \frac{1}{2} \end{bmatrix} \tag{4.21}$$

	$P_1 : A$	$S_1 : B$	$P_2 : B$	$S_2 : A$
I_1	$\frac{1}{5}$	0	$\frac{1}{5}$	0
I_2	$\frac{1}{5}$	0	$\frac{1}{5}$	0
I_3	$\frac{-1}{5}$	$\frac{1}{5}$	$\frac{1}{5}$	0
I_4	$\frac{-1}{5}$	$\frac{1}{5}$	$\frac{1}{5}$	0
I_5	$\frac{-1}{5}$	$\frac{1}{5}$	$\frac{1}{5}$	0
I_6	$\frac{1}{5}$	0	$\frac{-1}{5}$	$\frac{1}{5}$
I_7	$\frac{1}{5}$	0	$\frac{-1}{5}$	$\frac{1}{5}$
I_8	$\frac{1}{5}$	0	$\frac{-1}{5}$	$\frac{1}{5}$

The next primary alignment can be in the first or second columns. For simplicity, we choose the first,

$$\begin{bmatrix} 0 & 0 & 0 & 0 & 0 & \frac{1}{5} & \frac{1}{5} & \frac{1}{5} \\ 0 & 0 & \frac{1}{5} & \frac{1}{5} & \frac{1}{5} & 0 & 0 & 0 \\ 0 & \frac{1}{10} & \frac{1}{2} & 0 & 0 & 0 & 0 & 0 \\ 0 & \frac{1}{10} & 0 & \frac{1}{2} & 0 & 0 & 0 & 0 \\ 0 & \frac{1}{10} & 0 & 0 & \frac{1}{2} & 0 & 0 & 0 \\ 0 & 0 & 0 & 0 & 0 & \frac{1}{2} & 0 & 0 \\ 0 & 0 & 0 & 0 & 0 & 0 & \frac{1}{2} & 0 \\ 0 & 0 & 0 & 0 & 0 & 0 & 0 & \frac{1}{2} \end{bmatrix} \tag{4.22}$$

	$P_1 : A$	$S_1 : B$	$P_2 : B$	$S_2 : A$	$P_3 : A$
I_1	$\frac{1}{5}$	0	$\frac{1}{5}$	0	$\frac{-1}{10}$
I_2	$\frac{1}{5}$	0	$\frac{1}{5}$	0	$\frac{-1}{10}$
I_3	$\frac{-1}{5}$	$\frac{1}{5}$	$\frac{1}{5}$	0	$\frac{-1}{10}$
I_4	$\frac{-1}{5}$	$\frac{1}{5}$	$\frac{1}{5}$	0	$\frac{-1}{10}$
I_5	$\frac{-1}{5}$	$\frac{1}{5}$	$\frac{1}{5}$	0	$\frac{-1}{10}$
I_6	$\frac{1}{5}$	0	$\frac{-1}{5}$	$\frac{1}{5}$	$\frac{1}{10}$
I_7	$\frac{1}{5}$	0	$\frac{-1}{5}$	$\frac{1}{5}$	$\frac{1}{10}$
I_8	$\frac{1}{5}$	0	$\frac{-1}{5}$	$\frac{1}{5}$	$\frac{1}{10}$

The next primary alignment is in the second column where three individuals can be aligned to place B, however, this can be slotted in a secondary alignment to the previous primary alignment.

$$\begin{bmatrix} 0 & 0 & 0 & 0 & 0 & \frac{1}{5} & \frac{1}{5} & \frac{1}{5} \\ 0 & 0 & \frac{1}{5} & \frac{1}{5} & \frac{1}{5} & 0 & 0 & 0 \\ 0 & 0 & \frac{1}{2} & 0 & 0 & 0 & 0 & 0 \\ 0 & 0 & 0 & \frac{1}{2} & 0 & 0 & 0 & 0 \\ 0 & 0 & 0 & 0 & \frac{1}{2} & 0 & 0 & 0 \\ 0 & 0 & 0 & 0 & 0 & \frac{1}{2} & 0 & 0 \\ 0 & 0 & 0 & 0 & 0 & 0 & \frac{1}{2} & 0 \\ 0 & 0 & 0 & 0 & 0 & 0 & 0 & \frac{1}{2} \end{bmatrix} \tag{4.23}$$

	$P_1 : A$	$S_1 : B$	$P_2 : B$	$S_2 : A$	$P_3 : A$	$S_3 : B$
I_1	$\frac{1}{5}$	0	$\frac{1}{5}$	0	$\frac{-1}{10}$	0
I_2	$\frac{1}{5}$	0	$\frac{1}{5}$	0	$\frac{-1}{10}$	0
I_3	$\frac{-1}{5}$	$\frac{1}{5}$	$\frac{1}{5}$	0	$\frac{-1}{10}$	$\frac{1}{10}$
I_4	$\frac{-1}{5}$	$\frac{1}{5}$	$\frac{1}{5}$	0	$\frac{-1}{10}$	$\frac{1}{10}$
I_5	$\frac{-1}{5}$	$\frac{1}{5}$	$\frac{1}{5}$	0	$\frac{-1}{10}$	$\frac{1}{10}$
I_6	$\frac{1}{5}$	0	$\frac{-1}{5}$	$\frac{1}{5}$	$\frac{1}{10}$	0
I_7	$\frac{1}{5}$	0	$\frac{-1}{5}$	$\frac{1}{5}$	$\frac{1}{10}$	0
I_8	$\frac{1}{5}$	0	$\frac{-1}{5}$	$\frac{1}{5}$	$\frac{1}{10}$	0

The other two secondary alignments for the remaining two individuals can also be

done now as they do not interfere with the next primary alignments.

$$\begin{bmatrix} 0 & 0 & 0 & 0 & 0 & \frac{1}{10} & \frac{1}{5} & \frac{1}{5} \\ 0 & 0 & \frac{1}{10} & \frac{1}{5} & \frac{1}{5} & 0 & 0 & 0 \\ 0 & 0 & \frac{1}{2} & 0 & 0 & 0 & 0 & 0 \\ 0 & 0 & 0 & \frac{1}{2} & 0 & 0 & 0 & 0 \\ 0 & 0 & 0 & 0 & \frac{1}{2} & 0 & 0 & 0 \\ 0 & 0 & 0 & 0 & 0 & \frac{1}{2} & 0 & 0 \\ 0 & 0 & 0 & 0 & 0 & 0 & \frac{1}{2} & 0 \\ 0 & 0 & 0 & 0 & 0 & 0 & 0 & \frac{1}{2} \end{bmatrix} \tag{4.24}$$

	$P_1:A$	$S_1:B$	$P_2:B$	$S_2:A$	$P_3:A$	$S_3:B$	$S_3:F$	$S_3:C$
I_1	$\frac{1}{5}$	0	$\frac{1}{5}$	0	$\frac{-1}{10}$	0	$\frac{1}{10}$	0
I_2	$\frac{1}{5}$	0	$\frac{1}{5}$	0	$\frac{-1}{10}$	0	0	$\frac{1}{10}$
I_3	$\frac{-1}{5}$	$\frac{1}{5}$	$\frac{1}{5}$	0	$\frac{-1}{10}$	$\frac{1}{10}$	0	0
I_4	$\frac{-1}{5}$	$\frac{1}{5}$	$\frac{1}{5}$	0	$\frac{-1}{10}$	$\frac{1}{10}$	0	0
I_5	$\frac{-1}{5}$	$\frac{1}{5}$	$\frac{1}{5}$	0	$\frac{-1}{10}$	$\frac{1}{10}$	0	0
I_6	$\frac{1}{5}$	0	$\frac{-1}{5}$	$\frac{1}{5}$	$\frac{1}{10}$	0	0	0
I_7	$\frac{1}{5}$	0	$\frac{-1}{5}$	$\frac{1}{5}$	$\frac{1}{10}$	0	0	0
I_8	$\frac{1}{5}$	0	$\frac{-1}{5}$	$\frac{1}{5}$	$\frac{1}{10}$	0	0	0

The remaining alignments are essentially all equivalent, consisting of a pair of individuals grouped together while all others are aligned alone elsewhere. The purpose of this example was to provide an example of the decision-making process involved in carrying out a secondary alignment.

By using (4.1), we calculated that on this network, the upper bound of T_{max} is

$$\frac{1}{\binom{8}{2}}\left(\binom{5}{2}+\frac{6}{5}\binom{2}{2}\right)=\frac{2}{5}. \tag{4.25}$$

Similarly, by using (4.2), the lower bound of T_{max} is

$$\frac{1}{\binom{8}{2}}\frac{1}{8}\left(2\binom{5}{2}+6\binom{2}{2}\right)=\frac{13}{112}. \tag{4.26}$$

Calculating the actual value of T under the wheel alignment process gives

$$T = \frac{1}{\binom{8}{2}}\left(\frac{2}{5}\binom{5}{2} + \frac{3}{5}\binom{3}{2} + \binom{2}{2}\right) = \frac{17}{70}. \tag{4.27}$$

The actual value of T lies within the upper and lower bounds of T_{max}.

We also derived a general rule that explicitly describes the alignment of each individual's wheel on a line or circle graph of size N. On these graphs, each individual has access to three locations: their own home place or their two connected neighbour's (except for the two individuals at either end of the line graph, who only have access to two locations, their own or their neighbour's). Consider a wheel model divided into three equally sized segments of $2\pi/3$ (illustrated in figure 4.2 (a)). Assuming a general wheel, with labels A, B and C, the alignment rule on an N-sized circle or line graph is given by table 4.1.

	A	B	C
I_{3k}	3k-1	3k	3k+1
I_{3k+1}	3k+2	3k	3k+1
I_{3k+2}	3k+2	3k+3	3k+1

Table 4.1: Alignment rule for individuals on a line or circle graph of size N, where each individual's wheel is divided into three equal segments. The table shows how individuals indexed I_{3k}, I_{3k+1}, and I_{3k+2} align to locations A, B, and C based on their relative positions in the network.

It is important to note that at the endpoints of the line graph, individuals have access to two locations. Therefore, one of their wheel segments is equally redistributed between the two accessible places. Also, this result does not provide the most optimal alignment for circle graphs of size $3k + 1$ where $k \in \mathbb{Z}$. For example, consider a circle graph with four vertices, the alignment rule gives the following alignments presented in Figure 4.5.

In figure 4.5 (b), it is clear that a better, more optimal alignment can be achieved by swapping "1" and "4" on I_4's wheel. However, this result does yield the most optimal alignment for all other sizes on the circle graph and all sizes on the line graph.

4.4 Simulations

In this section, we conducted similar simulation methods to those used in the previous chapters to demonstrate that the alignment method developed in section 4.3.4

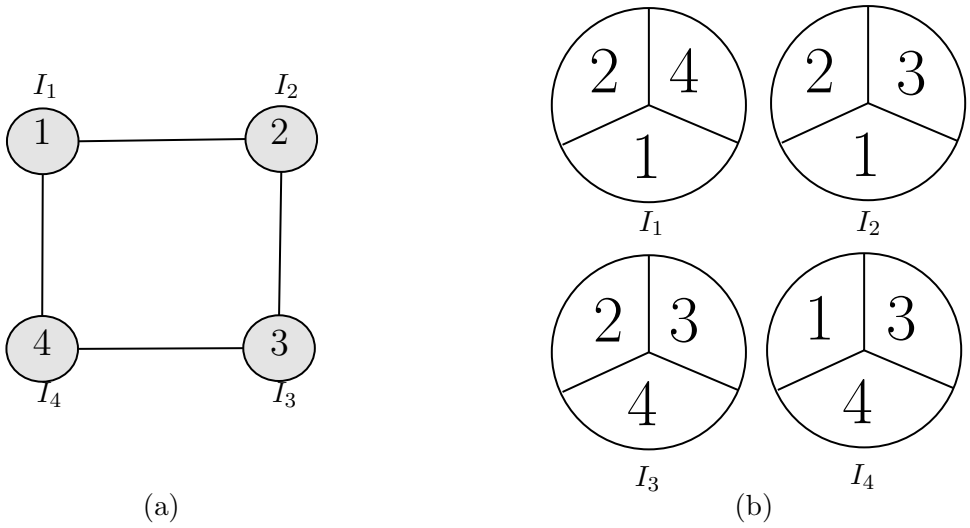

Figure 4.5: The alignments for four individuals on the circle graph. (a) shows the circle graph with four individuals $I_1, I_2.I_3$ and I_4 with vertices labelled as $1, 2, 3$ and 4. (b) shows the wheel alignments for each individual.

can be successfully implemented within the evolutionary setting.

One simulation is delineated as follows:

- The chosen network is formed using the iGraph library (Csardi and Nepusz 2006).
- The mutant is randomly placed on one of the vertices.
- Every individual moves (or not) from their home vertex according to the model as described in section 2.3.1 under the wheel alignment process discussed in section 4.3.4. Groups are formed and multiplayer games are played where $R = 10, C = 1$ and $V = 2$ for both of the considered games.
- Individuals return to their home places.
- Each individual moves (or not) and groups are formed and the dynamic process occurs. No games are played. Instead, one individual is selected to reproduce an offspring that will replace another random member of the group (or its parent if the parent is alone) explained in section 1.7.2.
- The simulation ends once the mutant fixates in the population or becomes extinct.
- This process is averaged over 25,000 cases to balance computational efficiency and low statistical variability.

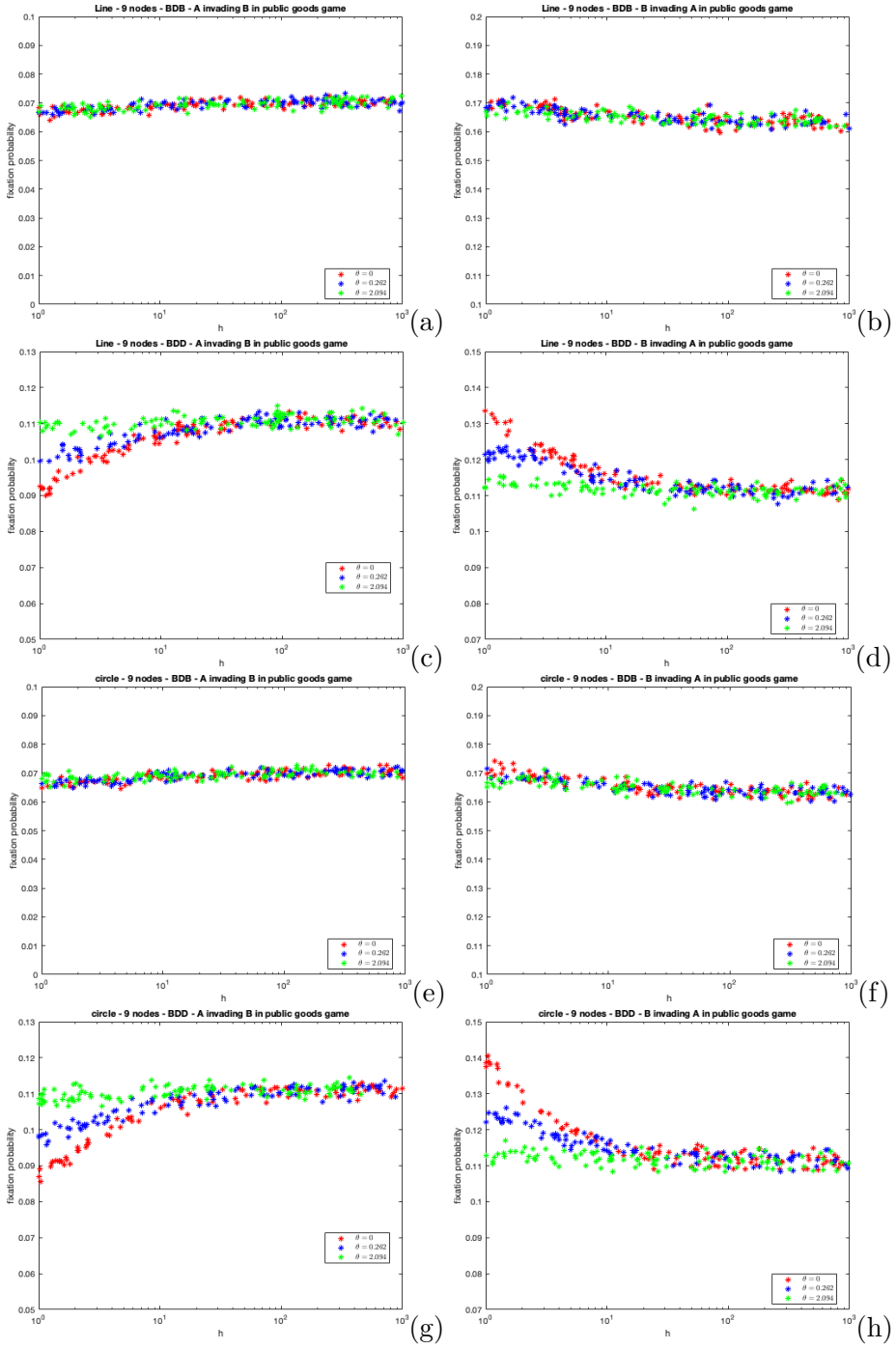

Figure 4.6: The fixation probability of a mutant cooperator and defector plotted against the home fidelity parameter, h in the Public Goods game under the wheel alignment process on the line and circle graphs with nine nodes. (a), (c), (e) and (g) show the cooperator's fixation probability and (b), (d), (f) and (h) show the defector's fixation probability. For the wheel process, we set $\theta = 0$, $\frac{\pi}{12}$ and $\frac{2\pi}{9}$ (to represent a near dispersal process).

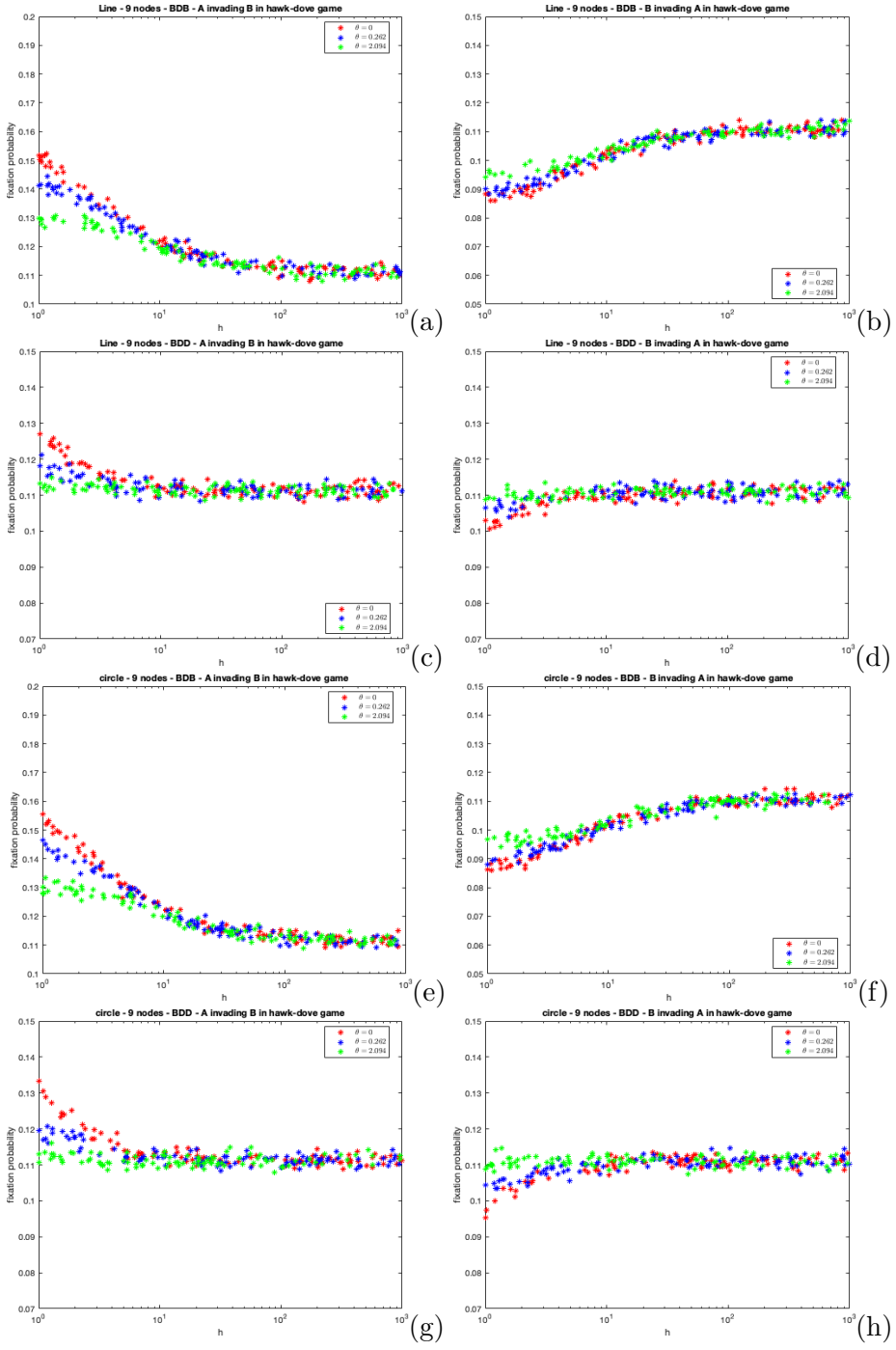

Figure 4.7: The fixation probability of a mutant dove and hawk plotted against the home fidelity parameter, h in the Public Goods game under the wheel alignment process on the line and circle graphs with nine nodes. (a), (c), (e) and (g) show the hawk's fixation probability and (b), (d), (f) and (h) show the dove's fixation probability. For the wheel process, we set $\theta = 0$, $\frac{\pi}{12}$ and $\frac{2\pi}{9}$ (to represent a near dispersal process).

Figure 4.6 illustrates the fixation probabilities of a mutant cooperator and defector in the Public Goods game under wheel alignment processes on line and circle graphs with nine nodes. Figure 4.6 (a), (b), (e) and (f) show that the angle θ has minimal effect on fixation probability under BDB dynamics. This contrasts

to results on complete graphs, such as in Figure in chapter 2, where much larger group sizes, up to the size of the population can form, enabling the row-dependent movement process to have a more influential effect.

The limited impact of θ under BDB dynamics occurs due to the incomplete structure of the line and circle graphs, where the maximum group size achievable is only three. As BDB dynamics involve selection on the birth event, and cooperators generally have a lower average fitness than defectors in the Public Goods game, their fixation probability is below $1/N$. Furthermore, the restricted group sizes imposed by the graph structure limit the influence of the row-dependent movement mechanisms on the evolutionary outcome. As h increases, the cooperator's (defector's) fixation probability slightly increases (decreases). This is because individuals are more likely to be alone, reducing opportunities for cooperators to interact with defectors and provide them with rewards. Therefore, the relative fitness between cooperators and defectors reduces, thereby slightly increasing the cooperator's fixation probability.

Figure 4.6 (c), (d), (g) and (h) illustrate the fixation probabilities of the mutant cooperator and defector under BDD dynamics, where the angle θ has a more influential effect on the evolutionary outcome. When h is small, individuals are more likely to partake in the movement process, resulting in the formation of groups of size 2 or 3. Under BDD dynamics, each individual has probability $1/N$ of being chosen to reproduce. If a cooperator reproduces in a pairwise group, the other group member is guaranteed to be replaced. This mechanism allows cooperators to achieve higher fixation probabilities than under the corresponding BDB dynamics, making the role of θ more significant.

As expected, the angle $\theta = 2\pi/3$ yields the highest fixation probability when $h = 1$ as it allows for the greatest degree of separation between individuals. At this point, many individuals are alone, and the cooperator's fixation probability reaches $1/N = 1/9$, remaining at this level as h increases. However, $\theta = 0$ results in the lowest fixation probability, as it maximises aggregation and increases the likelihood of cooperators interacting with defectors, which negatively impacts cooperation. A similar trend was observed in chapter 2 in Figure .

Figure 4.7 illustrates the fixation probabilities of a mutant hawk and dove in the Hawk-Dove game under wheel alignment processes on line and circle graphs with nine nodes. These figures show that, regardless of the evolutionary dynamics, θ

plays a more influential role here than in the Public Goods game.

When $\theta = 0$, individuals are more likely to herd together. In chapter 2, Figure 2.4, we observed that such aggregation was detrimental for hawks and beneficial for doves, as hawks were more likely to be in larger groups and incur significant costs. However, due to the incomplete structure of the line and circle graphs, the maximums group size is restricted to just two or three individuals. This structural limitation means hawks do not experience the same level of costly interactions as they would on complete graphs, where the risk of multiple hawks interacting is much larger. Therefore, aggregation positively impacts the hawks fixation probability in this evolutionary setting, since he presence of just a single hawk in a group is sufficient to deny all doves a share of the reward, lowering their relative fitness and, therefore, the dove's fixation probability.

4.5 Discussion

In this chapter, we have developed the framework of Broom & Rychtar (2012) by examining the evolution of structured populations on incomplete networks involving multiplayer interactions, where individuals move in a coordinated (row-dependent) manner. While previous models, such as those presented in chapters 2 and 3 (Haq et al. 2024, 2025) focused on complete graphs, this chapter marks the first step in applying those models to more complex, incomplete graphs. This extension allows us to test whether the dynamics and insights established in the previous chapters continue to hold in more complex settings.

Earlier studies on incomplete networks (Broom et al. 2015, Schimit et al. 2019, 2022) assumed independent movement. However, our model retains the coordinated movement process introduced in earlier chapters, ensuring continuity of methodology while exploring their under new structural constraints. Building on the aggregation measure T (1.49) from Broom et al. (2020), which was examined in chapter 3, we investigated its maximum value, T_{max}, and established upper and lower bounds. These bounds provide insight into the maximum level of aggregation that can be achieved on a heterogeneous structure.

An important motivation behind the development of the general movement methodology in Section 2.3.1 was faithfulness, ensuring the movement processes preserved the intended apriori distributions. In chapter 2, we showed that while the

sequential movement processes guaranteed faithfulness on complete networks, this property no longer holds on incomplete graphs. This represents a fundamental difference between the two settings, emphasising the need for alternatives that ensure faithfulness, such as the wheel process. The wheel's mechanism was extended in this chapter to incomplete networks via the development of an alignment algorithm designed to approximate maximal herding. Importantly, the equivalence between $\theta = 0$ and follow the majority, observed in complete graphs in chapters 2 and 3, breaks down in this chapter due to network constraints. This demonstrates that for the sequential movement processes, properties that hold for complete networks do not necessarily hold on incomplete graph structures.

We then explored the evolutionary implications of the wheel alignment process in the Public-Goods and Hawk-Dove games. In the context of the Public Goods game, we showed that under BDB dynamics, the wheel alignment process has minimal effect on the evolution of cooperation. This is due to the restrictive group sizes permitted by the underlying network structure. In other words, network topology exerts a stronger influence than the movement rules. Ohtsuki et al. (2006) demonstrated that, in general, birth-death processes do not support the evolution of cooperation. Therefore, in the Public Goods game, our results show that the cooperator's fixation probability typically remains below $1/N$. Under BDD, however, the wheel's herding effect becomes more pronounced, again reflecting but also extending earlier findings on complete graphs in chapter 2.

In the Hawk-Dove game, we showed that herding benefits hawks, contrary to the previous analysis in chapter 2 (Haq et al. 2024), where herding hindered their evolutionary success. This reversal is attributed to the limiting group sizes that can be formed on circle and line graphs. These limitations benefit the hawk as they do not incur significant costs from large group interactions, therefore improving the hawk's fixation probability and worsening the dove's chances of fixating. In Broom et al. (2015), it was shown that the dove's fixation probability could exceed $1/N$ if the reward was adjusted and in chapter 2, it was demonstrated that even without altering the reward, the row-dependent movement mechanisms, particularly follow the majority, can raise the dove's fixation probability above $1/N$ due to hawks being forced to herd together in large groups. However, our results show that on the considered incomplete networks, similar movement processes now favour hawks, emphasising the significant role of the underlying network structure in influencing

evolutionary outcomes.

Overall, this chapter bridges the gap between the complete graph analysis in chapters 2 and 3 and the more complex setting of incomplete graph structures considered in this chapter. Whereas the earlier chapters established the foundations of coordinated movement and analysed their evolutionary consequences in well-mixed populations, here we extended these ideas to structured populations where access to locations is restricted. In doing so, we showed that some properties from the complete case, such as the applicability of the aggregation measure T, remain robust, while others, such as the faithfulness of sequential movement processes, break down once network constraints are introduced. This finding emphasises why the wheel continues to serve as a flexible model of coordinated movement as it is able to ensure an achievable target distribution.

Chapter 5

Hybrid models

5.1 Introduction

The previous chapters examined models in which all individuals within the population followed the same movement mechanism throughout the evolutionary process. This chapter, however, focuses exclusively on hybrid movement models, extending the methodology developed in chapter 2 to incorporate several movement mechanisms within a single population. Broom et al. (2020) introduced these models to capture situations in which individuals adapt their mobility in response to external factors such as predator presence, resource availability, or the search for potential mates.

By formally embedding the hybrid models into the evolutionary setting, this chapter investigates how varying movement mechanisms influence evolutionary outcomes in simulations. The analysis provides a direct extension of the work carried out in chapter 2, which focused on developing the theory to model a single movement process and complements chapter 4's analysis by further broadening the scope of movement modelling.

This is a relatively short chapter, presenting preliminary results and outlining the initial progress made in extending evolutionary analysis to include hybrid models.

5.2 Hybrid type 1

In Broom et al. (2020), the hybrid type 1 model was defined as follows: assume there are R movement procedures and R non-negative numbers $s_1, s_2, ..., s_R$ with $\sum_{r}^{R} s_r = 1$. The movement process is then governed by the following probabilistic

rule: with probability s_r, all members of the population follow the r^{th} movement procedure.

This hybrid model can be incorporated into the evolutionary setting at two distinct levels. The first level of hybridisation consists of selecting a movement procedure being probabilistically selected that the entire population follows throughout the entire evolutionary process. We denote this level of hybridisation as *hybrid type* $1, 1$. For example, suppose a single mutant has a fixation probability of x under the follow the majority process and a fixation probability of y under the independent movement process. If the population follows the follow the majority process with probability p or follows the independent movement process with probability $1 - p$, then the mutant's fixation probability under the hybrid type $1, 1$ is simply a weighted average given by

$$\rho_1^{\mathcal{M}} = (p)(x) + (1 - p)(y).$$

The second level of hybridisation occurs at the dynamic time steps. At each time step, a new movement procedure is probabilistically selected for the entire population to follow. While this process may seem more complex, its intuition is straightforward. Since the movement distribution is chosen at each time step, the transition probabilities from all considered movement procedures must be weighted accordingly. These averaged transition probabilities are then used to compute the fixation probability. We denote this model as *hybrid type* $1, 2$.

5.3 Hybrid type 2

In Broom et al. (2020), the hybrid type 2 model was defined as follows: assume there are R movement procedures, each associated with a non-negative weight $s_1, s_2, \ldots, s_R$, such that $\sum_r^R s_r = 1$. In this model, each individual independently follows the r^{th} movement procedure with probability s_r.

Within this hybrid model, we do not consider the first level of hybridisation i.e. *hybrid type* $2, 1$. In such a setting, where each individual probabilistically selects a movement procedure at the start of the evolutionary process and adheres to it throughout, it becomes necessary to track each individual's movement. Analytically, this process is highly complex and requires advanced computational methods to

solve. Moreover, additional important complications arise when considering how new offspring should behave after reproduction. For instance, whether they should choose a row-dependent movement process at random, inherit the same movement mechanism as their parent, or adopt the same movement strategy from the previous location owner. These considerations further increase the complexity of the model, making this level of hybridisation increasingly difficult to be analytically tractable and, therefore, less preferable to currently consider.

For *hybrid type* $2, 2$, at each time step, individuals independently select a new movement procedure. Unlike the previous case, where individuals commit to a fixed movement process throughout the entire evolutionary process, here, tracking the replacement of individuals is unnecessary because all members of the population probabilistically select a new movement procedure at each dynamic time step.

5.4 Simulations

In this section, we present preliminary simulations of the hybrid models to demonstrate that various approaches to hybridisation discussed in this chapter can be successfully implemented within the evolutionary setting.

One simulation is defined as follows:

- The complete decagon network is formed using the iGraph library (Csardi and Nepusz 2006).
- The mutant is randomly placed on one of the vertices.
- Every individual moves (or not) from their home vertex according to the movement methodology described in section 2.3.1 except here, the movement of individuals is hybridised and governed by the wheel process $\theta = \pi/10$ with probability $1/2$ or the follow the majority process with probability $1/2$. Following this, groups are formed and multiplayer games are played.
- Individuals return to their home places.
- Each individual moves (or not) and groups are formed and the dynamic process occurs. No games are played. Instead, one individual is selected to reproduce an offspring that will replace another random member of the group (or its parent if the parent is alone) explained in section 1.7.2.

- The simulation ends once the mutant fixates in the population or becomes extinct.

- This process is averaged over 25,000 cases to balance computational efficiency and low statistical variability.

Figure 5.1 illustrates the fixation probabilities of a mutant cooperator and defector in the Public Goods game under the wheel ($\theta = 2\pi/N$) and follow the majority ($B = 0$) processes on the complete decagon. The figures illustrate three hybrid levels $1,1$, $1,2$ and $2,2$. Figures 4.6 (a) and (b) implement BDB dynamics and the figure portrays that the three hybrid models have very little effect on the evolutionary outcomes. In the Public Goods game, under BDB processes where the network is sufficiently large, the row-dependent movement mechanisms have little effect on the fixation probability, therefore it makes sense that regardless of the hybrid model, fixation is approximately the same for all of the models considered.

Figure 5.1 (c) and (d) show the cooperator's and defector's fixation probability under BDD dynamics. Notably, the hybrid $1,2$ model gives the lowest fixation probability compared to hybrid $1,1$ which gives the highest. The key difference between hybrid type $1,1$ and type $1,2$ is in the frequency at which the movement process is selected. In type $1,1$, a single movement process is probabilistically selected at the start and fixed throughout the evolutionary process. This means that when the dispersal process is selected (with probability $1/2$), cooperators benefit from a fixed environment that favours their strategy. However, type $1,2$, involves randomly selecting the movement process at each time step. Although each movement process is equally likely at every time step, cooperators may not experience extended periods of beneficial separation before the movement process switches to herding again. This lack of sustained separation weakens the mutant cooperator's prospects of fixating. Therefore, the hybrid type $1,2$ gives a lower fixation probability for the cooperator than hybrid type $1,1$. This demonstrates that perhaps consistency in dispersal and separation plays a pivotal role in the evolutionary success of cooperation.

Figure 5.2 illustrates the fixation probabilities of a mutant hawk and dove in the Hawk-Dove game under the wheel ($\theta = 2\pi/N$) and follow the majority ($B = 0$) processes on the complete decagon. The figures illustrate three hybrid types $1,1$, $1,2$ and $2,2$.

In the Hawk-Dove game, the hybrid type $1,1$ gives the lowest fixation probability

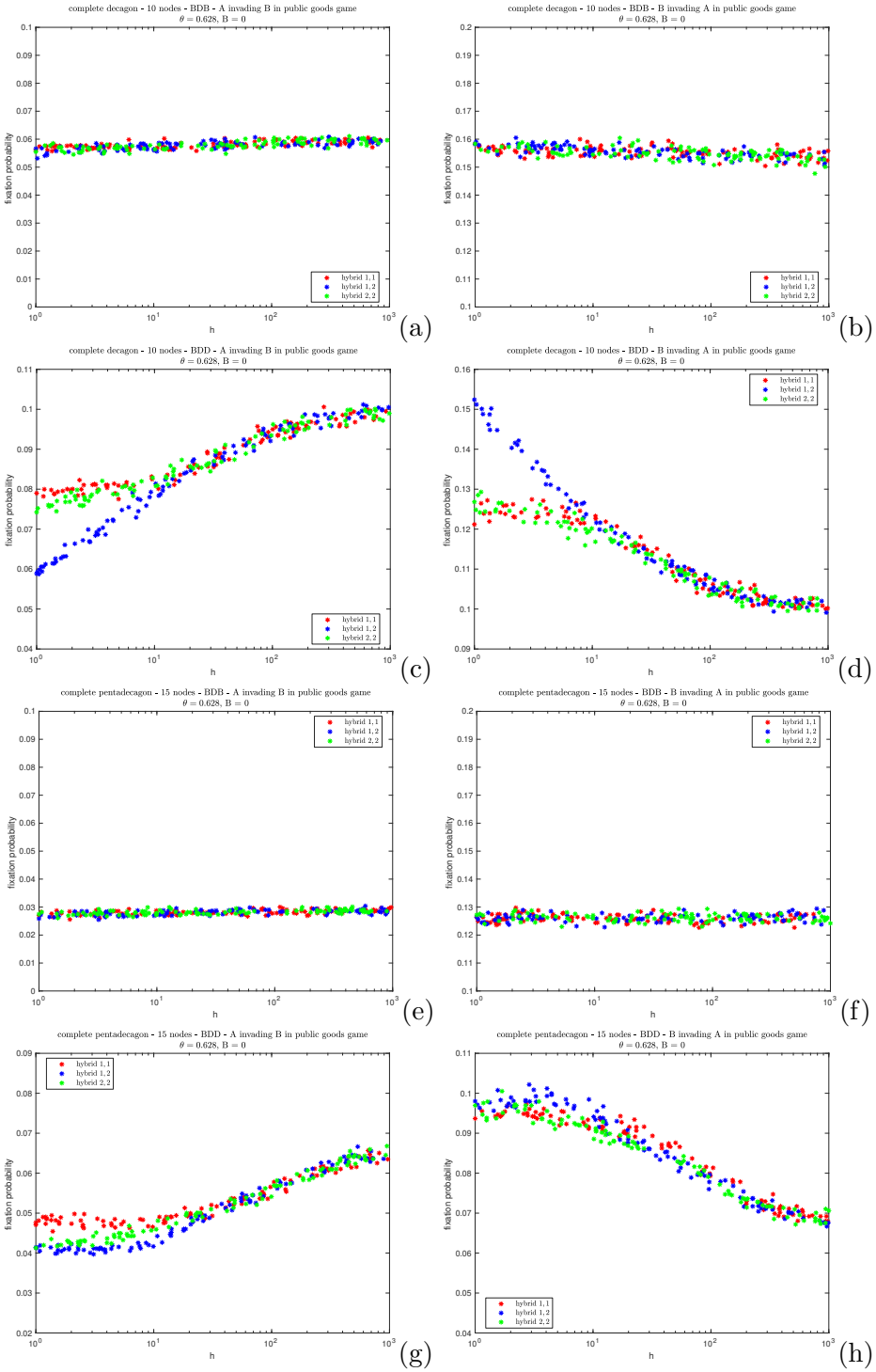

Figure 5.1: The fixation probability of a mutant cooperator and defector plotted against the home fidelity parameter, h in the Public Goods game under the hybrid models on the complete decagon and pentadecagon graphs. (a), (c), (e) and (g) show the cooperator's fixation probability. (b), (d), (f) and (h) show the defector's fixation probability. The hybridised movement processes are the wheel process ($\theta = 2\pi/10$) and the follow the majority process ($B = 0$).

for hawks. If follow the majority is selected, hawks are more likely to interact with each other and incur costs from the violent contests. If dispersal is chosen, hawks

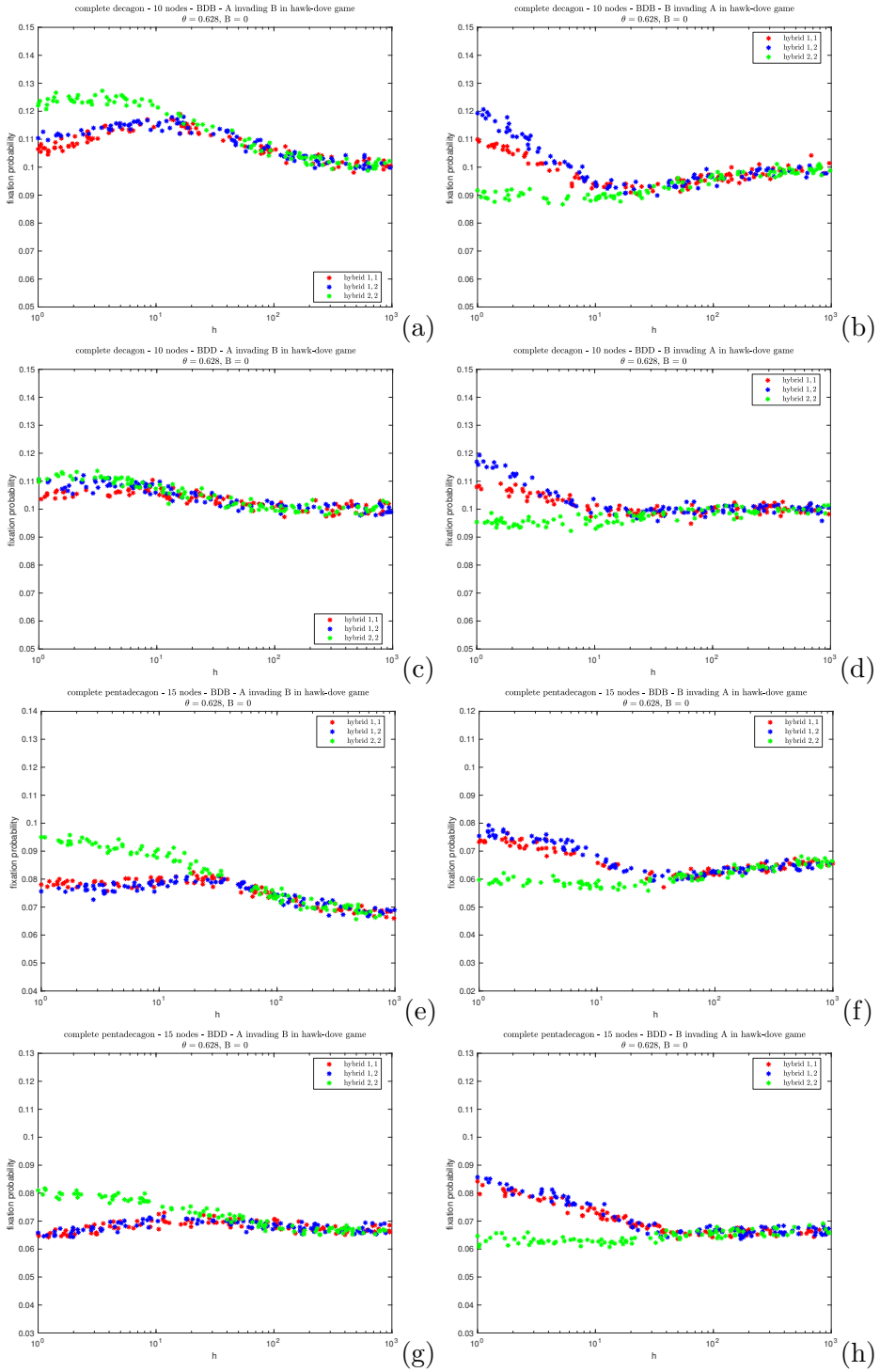

Figure 5.2: The fixation probability of a mutant hawk and dove plotted against the home fidelity parameter, h in the Public Goods game under the hybrid models on the complete decagon graph. (a), (c), (e) and (g) show the hawk's fixation probability. (b), (d), (f) and (h) show the dove's fixation probability. The hybridised movement processes are the wheel process ($\theta = 2\pi/10$) and the follow the majority process ($B = 0$).

cannot meet doves and deny them their rewards. Therefore, the lack of strategic, reliable movement gives the lowest fixation probability for hawks. However, hybrid type $2, 2$ enables each individual to probabilistically select their own movement

process to follow at every time step. This flexibility creates heterogeneous group structures where some hawks herd and deny doves a share of the reward, while others disperse to avoid violent encounters with other hawks. This strategic variation increases the likelihood of hawks both exploiting doves and avoiding mutual conflict, resulting in the highest fixation probability for hawks.

Figures 5.1 (e-h) and Figures 5.2 (e-h) show similar simulations on the pentadecagon. Because $\theta = 2\pi/10$, the wheel process does not correspond to near-dispersal movement as *theta* would need to equal $2\pi/15$ for that. Therefore, the trends in these figures are less pronounced compared to the corresponding figures on the decagon.

5.5 Discussion

In this chapter, we have explored a new direction within the modelling framework introduced by Broom & Rychtar (2012), by integrating the hybrid models developed in Broom et al. (2020) into the evolutionary setting of the territorial raider model introduced by Broom et al. (2015) for the first time. Our work extends previous research by incorporating probabilistic decision-making at both the population and individual levels in the movement phase, providing a more dynamic modelling environment. This chapter directly builds on the modelling foundations established in chapter 2, which introduced and analysed single movement processes on complete graphs, and on chapter 4, which extended these methods to incomplete graphs. While the previous chapters demonstrated how the movement mechanisms and network topology can influence evolutionary outcomes, this chapter demonstrates how diversity in movement mechanisms adds a further layer of complexity, altering outcomes on simple graphs.

We analytically formalised two broad classes of hybrid models, type 1 and type 2, and developed methods to embed them into the evolutionary setting. For hybrid type 1, the movement mechanism is chosen at the population level from a weighted set of movement procedures. In the type $1,1$ model, the population selects one movement mechanism at the beginning and follows it throughout the evolutionary process. This yields a simple weighted average of the fixation probabilities under each considered movement process. The type $1,2$ model allows the entire population to randomly select a new movement procedure at each dynamic time step, therefore

the transition probabilities from each movement process are averaged accordingly. For hybrid type 2, each individual probabilistically selects their own movement procedure. Although type $2,1$, where individuals randomly choose a movement process to follow throughout the evolutionary process, was analytically complex due to complications with individual tracking and movement inheritance, we considered a type $2,2$ model, where each individual selects a new rule at each time step, avoiding the need to track the replacement of certain individuals.

By utilising numerical simulations, we found differing outcomes in how hybridisation influences evolutionary success depending on the game and dynamics used. In the Public Goods game under BDB dynamics, hybridisation has minimal effect when the network is sufficiently large, with fixation probabilities remaining similar across the different hybrid types. However, under BDD dynamics, fixation probabilities vary significantly. Hybrid type $1,1$ yields the highest fixation probability for the mutant cooperator, while type $1,2$ produced the lowest fixation probability. This suggests that consistent dispersal, even if probabilistically chosen, supports the evolutionary success of cooperation better than frequent switching between herding and dispersal, which disrupts the environmental stability for cooperators.

In the Hawk-Dove game, hybrid type $1,1$ led to the lowest fixation probability for hawks, because fixed herding or dispersal either resulted in costly violent contests or prevented hawks from interacting with doves. However, type $2,2$ led to the highest fixation probability for hawks. This flexibility allows some hawks to herd and deny doves rewards while other hawks disperse to avoid violent contests with other hawks.

These preliminary findings highlight that combining movement procedures can play a central role in influencing evolutionary outcomes. Hybrid models capture these complex scenarios with robust flexibility, offering new insights into population behaviours that cannot be represented by traditional models. This preliminary research acts as the foundation for future work to explore hybridisation under varied games, complex networks and updating mechanisms.

Chapter 6

Conclusion

This thesis has extensively explored the mathematical modelling of the evolution of structured populations involving multiplayer interactions under row-dependent movement, with the motivation of incorporating more realistic features that the classical models often lacked. Using the Broom-Rychtář framework (Broom & Rychtar 2012) as the theoretical foundation, we have extended the framework in several directions, primarily providing theoretical and methodological advances while maintaining conceptual links to biology. These extensions are important because they allow the analysis of evolutionary dynamics that previous models, focused on either pairwise contests or independent movement, could not capture. Our models provide a new understanding of how structured populations evolve under coordinated movement. By incorporating row-dependent movement mechanisms, this thesis extends a well-established framework for understanding how theoretical and methodological advances can reveal insights that would be overlooked in simpler models.

Theoretically, we developed a new methodology enabling the row-dependent movement mechanisms from Broom et al. (2020) to be incorporated into the territorial raider model (Broom et al. 2015). This enabled us to analyse new models involving coordinated movement and multiplayer group interactions. This involved deriving expressions for fixation probabilities under BDB and BDD dynamics and investigate evolutionary outcomes under weak selection by establishing neutrality and equilibrium conditions, extending results from pairwise models, revealing how movement and multiplayer interactions influence evolutionary processes. Furthermore, the movement methodology enabled the analysis of key predictors of fixation and novel measures of aggregation, providing a more comprehensive theoretical un-

derstanding of the relationship between row-dependent movement and the evolution of cooperation.

Methodologically, this thesis introduces row-dependent movement mechanisms on graphical structures, including deterministic follow the majority, probabilistic Polya-urn and the wheel process. The introduction of these movement systems improves the realism of the territorial raider model by capturing real-life coordinated movement exhibited in animal species. For example, follow the majority captures herding behaviour observed in fish schools and bird flocks (Couzin et al. 2005, Hinz & de Polavieja 2017, Winklmayr et al. 2020). Polya-Urn models can be used to capture pheromone-guided movement in ant colonies (Deneubourg et al. 1990, Dorigo & Stützle 2004, Shah et al. 2010). The wheel process represents simultaneous movement with a certain degree of separation, analagous to behaviour in surf scoters (Lukeman et al. 2010). Furthermore, this thesis extends the wheel mechanisms to incomplete networks by developing an alignment algorithm to approximate maximum herding. The hybrid models combine movement processes at individual and population levels, enabling complex simulations of the movement processes. These methodological advances are significant because they allow more realistic simulations and analytical analysis, enabling the investigation of evolutionary outcomes in more complex models that could not be captured before.

Although largely theoretical, the models incorporate conceptual biological behaviours. Across the chapters, the simulations of social dilemma games showed that, at least on complete graphs, aggregation among unrelated individuals tends to hinder the evolutionary success of cooperation. This effect may not necessarily hold on heterogeneous structures, as certain individuals are often more related to others compared to other individuals due to the underlying population structure. In such cases, aggregation may not disadvantage cooperation in the same way. Therefore, while the complete graph setting provides clear explanations, different structures could produce more varied outcomes. As an example, our findings are consistent with infanticide by male lions (Pusey & Packer 1994), where unrelated infants are killed so that the male can increase his own reproductive success. However, other biological scenarios will not align our findings.

In chapter 2, we developed a general movement methodology to incorporate row-dependent movement into the evolutionary framework on complete graphs, building on previous analysis (Broom & Rychtar 2012, Broom et al. 2015, 2020). Unlike

previous models where individuals moved independently (Broom et al. 2015, Pattni et al. 2017) or in a history-dependent manner (Pattni et al. 2018, Erovenko et al. 2019, Pires et al. 2023, Erovenko & Broom 2024), our models allow for more realistic movement behaviours within evolutionary settings. Using this methodology, we investigated how the row-dependent movement mechanisms affect the evolution of cooperation in the Public Goods and Hawk-Dove games.

Although previous research, such as Krieger et al. (2017) have demonstrated that an abstract type of motion where individuals swap vertices on the graph (in the context of evolutionary graph theory) has no impact on the evolutionary dynamics on complete networks, our findings in this chapter revealed that the nature of the movement distribution can significantly influence the evolution of cooperation, even in well-mixed populations on complete networks. However, the work presented in this chapter is very different, as individuals move more realistically and can interact in arbitrary group sizes.

In the context of the Public Goods game, we demonstrated that aggregation inhibits the evolution of cooperation as herding provides defectors access to groups containing cooperators. However, dispersal proves beneficial for cooperators by limiting the opportunities defectors have to exploit them despite the significant disadvantage posed by the BDB updating process, which keeps the mutant cooperator's fixation probability below $1/N$, explained in Ohtsuki et al. (2006). In the Hawk-Dove game, aggregation benefits doves by increasing interactions between hawks who endure greater costs from the violent contests. While earlier work by Broom et al. (2015) demonstrated that the dove's fixation probability can exceed $1/N$ from certain reward adjustments, our results illustrate that herding alone can raise the dove's fixation probability above $1/N$, without altering the payoffs. While dispersal also favours doves, herding exerts a more pronounced effect.

We derived analytical expressions for fixation probabilities for both considered games under both BDB and BDD dynamics, and extended previous work by Tarnita et al. (2009) and Taylor et al. (2004), who focused on pairwise interactions. However, our analysis established neutrality and equilibrium conditions under weak selection approximations involving multiplayer interactions. These conditions align with our expectations, showing that hawks tend to perform worse in our models developed in this chapter than in the traditional evolutionary graph theory models. By capturing interactions in arbitrary group sizes, our results show that increasing

group sizes negatively impact the hawk's fixation probability.

A potential future direction may involve adapting the movement mechanisms to respond to strategy distributions such as individuals favouring patches with more cooperators. Also, another possible direction may involve investigating how row-dependent movement can be simultaneously implemented with history-dependent movement from Pattni et al. (2018) to capture more complex, behavioural movement procedures within evolutionary processes on complete networks.

In chapter 3, we extended the modelling framework of Broom & Rychtar (2012) in a different direction by utilising the evolutionary setting of chapter 2 (Haq et al. 2024) to examine how row-dependent movement (Broom et al. 2020) influences strong predictors of fixation probability, namely mean group size and temperature. These predictors were identified in previous work such as (Broom et al. 2015, Pattni et al. 2017, Schimit et al. 2019, 2022) where individuals moved independently. We have observed trends in our models that have not been previously identified in evolutionary graph theory (Pattni et al. 2015, Traulsen et al. 2007). In the Public Goods game, we observed that temperature is a stronger predictor of fixation than the mean group size for all values of h, across all of the movement processes. For a fixed temperature value, the movement processes yield the same fixation value, representing the temperature's importance as the most crucial measure in the evolutionary process. A similar result was given in Broom et al. (2015) but only for high levels of h and under independent movement. Within the Hawk-Dove game, temperature consistently outperforms other variables in predicting fixation probabilities. In the Hawk-Dove game, temperature continues to be a stronger predictor of fixation. However, due to the greater complexity of the game compared to the Public Goods game, there is a breakdown of the linear relationship between temperature and fixation, at higher temperatures. With a detailed analytical explanation, we showed that while temperature is generally a reliable predictor, the game and the underlying movement mechanism significantly influence this relationship.

In previous work, (Broom et al. 2015, Pattni et al. 2017, Schimit et al. 2019, 2022), the predictors of fixation were primarily examined to explore their theoretical significance. While we have adopted a similar perspective, we have also extended this approach by demonstrating that these measures, specifically, T, mean group size and temperature can be practically calculated for a range of movement processes. We showed how the aggregation measure T, introduced by Broom et al. (2020), relates

directly to the mean group size, and provided explicit formulae for calculating all three measures under different movement mechanisms.

Previous research by (Broom et al. 2015, Pattni et al. 2017, Schimit et al. 2019, 2022, Haq et al. 2024) exclusively looked at the Public Goods, Hawk-Dove and Fixed Fitness games therefore we extended the current literature by considering the Stag-Hunt game. Our analysis showed that herding can hinder the evolution of cooperation, to the extent where selection opposes its evolution. However, other movement processes such as the wheel can enhance the cooperator's fixation probability above that of the neutral benchmark and the defector, thus facilitating the evolution of cooperation. Compared to the Public Goods game examined by Haq et al. (2024), row-dependent movement has a stronger influence on evolutionary outcomes in the Stag-Hunt game. Dispersal can also undermine cooperators by preventing cooperators involved in the movement process from interacting with one another, thereby lowering their likelihood of forming groups that satisfy the cooperation threshold.

Additionally, we investigated the differences between two processes used in the territorial raider model (Broom et al. 2015, Pattni et al. 2017, Schimit et al. 2019, 2022). The process explained in Broom et al. (2015) and Pattni et al. (2017) assumes that individuals participate in effectively an infinite number of games prior to each dynamic time step. However, the process described in Schimit et al. (2019, 2022), assumes that individuals play a single game prior to each update. We identified these two processes differ due to three averaging effects from the payoffs, weights and reciprocals of fitness terms, depending on the governing dynamics. While the simulation process in Schimit et al. (2019, 2022) can be viewed as an extension of the process from Broom et al. (2015) and Pattni et al. (2017) under BDB dynamics, this equivalence does not naturally hold for the other dynamics. A potential future direction would be to revisit the evolutionary models of Schimit et al. (2019, 2022) and adapt them to incorporate a large number of games per dynamic time step, but this would require significant computational resources.

Chapter 4 extended the analysis carried out in chapter 2 by investigating row-dependent movement on incomplete networks involving multiplayer interactions, marking the first integration of such movement behaviours within incomplete graph structures. Previous research involving the territorial raider model on incomplete networks assumed independent or history-dependent movement (Broom et al. 2015, Erovenko et al. 2019, Schimit et al. 2019, Pires et al. 2023). The models developed in

this chapter introduce a novel perspective with the introduction of row-dependent movement on incomplete graphs. Extending previous results from Broom et al. (2020), who derived the measure T (1.49), to determine the probability a pair of individuals are together. We examined T_{max}, in section 4.3.1, and derived upper and lower bounds for general network structures (4.1) (4.2). These bounds were tested on regular, line, and more complex graphs. In doing so, we extended the theoretical work of Broom et al. (2020) by embedding these aggregation measures into a well-established evolutionary setting, demonstrating how such measures can be used to provide meaningful analysis.

An important result in this chapter is that we provided a simple counterexample showing that the movement methodology from section 2.3.1 fails to achieve the apriori target distribution under sequential movement processes (follow the majority and the Polya-urn) due to the underlying network structure being incomplete. This was first explored in Broom et al. (2020), who showed that assuming all individuals share the same distribution, the Polya-urn process remains faithful with the apriori target distribution. This property was a significant motivating factor in the development of the movement methodology developed in chapter 2 (Haq et al. 2024) who considered complete networks. In this chapter, however, we showed that on incomplete networks, this methodology does not always guarantee the target distribution is met. This limitation was illustrated with a simple counterexample on a line graph with three nodes in section 4.3.2. However, the wheel process remains robust in this context.

In chapters 2 and 3 (Haq et al. 2024, 2025), the wheel process was used when the underlying population structure was a complete graph. To consider the wheel process in an evolutionary setting involving an incomplete graph, the wheel process had to first be extended (discussed in section 4.3.3). Previous findings from Haq et al. (2024, 2025) demonstrated that the wheel process ($\theta = 0$) was equivalent to the follow the majority process, however, this equivalence no longer holds true on incomplete graph structures. Therefore, to approximate herding for the wheel, we developed an alignment algorithm that approximates the optimal alignment on a general network (discussed in section 4.3.4).

In the multiplayer Public Goods game, the wheel alignment process had negligible impact on the cooperator's fixation probability under BDB dynamics due to the limiting group sizes caused by the underlying network structure. Ohtsuki et al.

(2006) showed that birth-death processes do not favour the evolution of cooperation. Therefore, in the Public Goods game, our results show that the cooperator's fixation probability typically remains below $1/N$. Similarly, this was observed in Haq et al. (2024) for complete networks, and the results in this chapter demonstrate that this trend persists for the considered incomplete networks.

In the multiplayer Hawk-Dove game, our results showed that herding benefits hawks, contrary to the findings from chapter 2 (Haq et al. 2024), where aggregation negatively impacted their fixation probability. This effect is due to the limiting group sizes that can form on the line and circle graphs, which prevent hawks from interacting with each other within large groups, thus reducing their likelihood of incurring significant costs from the violent contests, which increases their fixation probability. In Broom et al. (2015), the dove's fixation probability was higher than $1/N$ if the reward payoff was adjusted and Haq et al. (2024) showed that the follow the majority process can increase the dove's fixation probability above $1/N$ without altering the game payoffs. This, however, differs from our results where a very similar movement process now worsens the likelihood of the mutant dove's evolutionary success, emphasising the importance of the underlying population structure and its impact on the evolutionary process.

There are several directions for future work. One avenue involves further investigation in the upper and lower bounds of T_{max}. The current lower bound (4.2) gives a conservative value, therefore, it may be beneficial to improve this for more complex or irregular graph structures. Another direction is the further optimisation of the alignment algorithm to improve its accuracy on arbitrary graph topologies. This can be tested against the developed bounds of T_{max}. Furthermore, future work may involve simulations on heterogeneous graph structures such as those considered by Schimit et al. (2019), who implemented Erdős-Renyi (random) network, small-world, scale-free, random regular and Barábasi-Albert graphs into their processes.

In the final chapter, we explored a preliminary direction by integrating newly developed hybrid models by Broom et al. (2020) into the evolutionary setting developed in chapter 2 (Haq et al. 2024). This work extends previous research by incorporating probabilistic decision-making at both the population and individual levels during the movement phase, allowing for more realistic biological scenarios where individuals adapt their movement based on external influences. We analytically developed two classes of hybrid models, type 1 and type 2. Our simulations

revealed important effects of hybridisation on evolutionary success, with results varying across different games and dynamics. In the Public Goods game, hybridisation had minimal impact under large networks but led to significant differences under BDD dynamics. In the Hawk-Dove game, flexibility in movement strategies, particularly with hybrid type $2, 2$ led to higher fixation probabilities for hawks. These findings emphasise the importance of combining movement strategies in evolutionary models, providing a foundation for further research into hybridisation in complex evolutionary systems.

Despite the several contributions made in this thesis, there are several limitations that warrant discussion. The row-dependent movement mechanisms explored in this thesis include: follow the majority, Polya-urn (utility positively correlates with patch occupancy) and the wheel. These mechanisms could be potentially adapted to incorporate more realistic, strategy-dependent movement distributions, where individuals prefer to move places containing a large number of cooperators and avoid places with a large defector presence. However, such movement is currently being investigated in an alternative direction of the Broom-Rychtar framework, with the exploration of the Markov movement models (Pattni et al. 2018, Erovenko et al. 2019, Pires et al. 2023, Erovenko & Broom 2024).

Also, there remain various movement mechanisms potentially worthy of exploration. Broom et al. (2020) also developed other sequential movement models such as follow the leader and follow the predecessor, which are very similar to the follow the majority process. We chose to implement the follow the majority process as it not only accurately reflected realistic animal behaviours, observed in bird flocks, fish schools and mammalian hunting groups (Fretwell & Lucas 1969, Ford & Swearer 2013), but also made the mathematics more analytically tractable. In the models developed in this thesis, for the sequential movement processes, it is assumed that all individuals have equal likelihood of moving first. This egalitarian assumption has been observed in red-fronted lemurs (Pyritz et al. 2011). Moreover, dispersal behaviour was explored solely through the wheel process within this thesis. Alternative models developed in Broom et al. (2020) could be utilised, such as a Polya-urn process where utility negatively correlates with patch occupancy. This would allow for an alternative exploration of dispersal behaviour, moving beyond the wheel process.

Finally, a general limitation of this work is its theoretical nature. The models

developed in this thesis have not been tested against empirical data collected from complex, biological systems. However, this is not a significant flaw, as the fundamental aim of this thesis was to mathematically advance the theoretical framework for modelling the evolution of structured populations involving multiplayer games and coordinated movement. Our results have been rigorously compared to, and in some cases extended from, classical results from evolutionary graph theory, ensuring consistency with an established modelling framework, while providing a robust basis for future exploration.

Appendix

Average group distribution on complete triangle graph

Using the methodology defined in section 2.3.1, we showed how to calculate the average group distribution by considering a well-mixed population of three individuals I_1, I_2, and I_3 on a complete triangle graph under the follow the majority, Polya-urn, and wheel processes.

The average group distribution for the follow the majority process is

- P(all individuals are together) $= \frac{9(h-1)}{(h+2)^3} + \frac{27}{(h+2)^3} = \frac{27+9(h-1)}{(h+2)^3}$,
- P(I_1 and I_2 are together while I_3 is alone) $= \frac{2(h-1)^2}{(h+2)^3} + \frac{6(h-1)}{(h+2)^3} = \frac{2(h-1)^2+6(h-1)}{(h+2)^3}$,
- P(I_1 and I_3 are together while I_2 is alone) $= \frac{2(h-1)^2}{(h+2)^3} + \frac{6(h-1)}{(h+2)^3} = \frac{2(h-1)^2+6(h-1)}{(h+2)^3}$,
- P(I_2 and I_3 are together while I_1 is alone) $= \frac{2(h-1)^2}{(h+2)^3} + \frac{6(h-1)}{(h+2)^3} = \frac{2(h-1)^2+6(h-1)}{(h+2)^3}$,
- P(all individuals are alone) $= \frac{3(h-1)^2}{(h+2)^3} + \frac{(h-1)^3}{(h+2)^3} = \frac{3(h-1)^2+(h-1)^3}{(h+2)^3}$.

The average group distribution under a general polya-urn process is given by

- P(all individuals are together) $= \frac{3(h-1)(B+3)(B+2)+3(B+3)(B+6)}{(h+2)^3(B+1)(B+2)}$,
- P(I_1 and I_2 are together while I_3 is alone) $= \frac{2(h-1)^2(B+1)(B+2)+6(h-1)(B+3)(B+6)+3(B+3)(2B)}{(h+2)^3(B+1)(B+2)}$,
- P(I_1 and I_3 are together while I_2 is alone) $= \frac{2(h-1)^2(B+1)(B+2)+6(h-1)(B+3)(B+6)+3(B+3)(2B)}{(h+2)^3(B+1)(B+2)}$,
- P(I_2 and I_3 are together while I_1 is alone) $= \frac{2(h-1)^2(B+1)(B+2)+6(h-1)(B+3)(B+6)+3(B+3)(2B)}{(h+2)^3(B+1)(B+2)}$,
- P(all individuals are alone) $= \frac{3(h-1)^2(B+1)(B+2)+3(h-1)(2B)(B+2)+3B(2B)+(h-1)^3(B+1)(B+2)}{(h+2)^3(B+1)(B+2)}$.

For the wheel process, we considered an example where $0 \leq \theta < \frac{\pi}{3}$,

- P(All individuals are together) $= \frac{9h(1-\frac{2\theta}{\pi})+18-\frac{63\theta}{\pi}}{(h+2)^3}$,

- P(I_1 and I_2 are together but not with I_3) = $\frac{2(h-1)^2+6(h-1)+\frac{27\theta}{\pi}}{(h+2)^3}$
- P(I_1 and I_3 are together but not with I_2) = $\frac{2(h-1)^2+6(h-1)+\frac{27\theta}{\pi}}{(h+2)^3}$,
- P(I_2 and I_3 are together but not with I_1) = $\frac{2(h-1)^2+6(h-1)+\frac{27\theta}{\pi}}{(h+2)^3}$,
- P(All individuals are separate) = $\frac{3(h-1)^2+27(h-1)(\frac{2\theta}{3\pi})+(h-1)^3}{(h+2)^3}$.

The fitness of a dove and hawk

In the Hawk-Dove game, we opted to assume only independent movement to simplify the fitness calculation. This simplification was necessary because the Hawk-Dove game exhibits greater complexity in the payoffs to each strategy, which are contingent on group composition and, therefore, the movement distribution. By focusing on solely independent movement for this game, we were able to evaluate the fitness of hawks and doves within this framework more effectively.

Consider a population of size N, well-mixed, and composed of k doves and $N-k$ hawks. A dove will only receive a proportion of a reward V if it is present in a group that contains no hawks. This can occur in four distinct scenarios. Consider two doves, D_1, D_2 and a hawk H_1:

- D_1 remains in its home, and a group of L doves forms on D_1's home patch.
- D_1 moves to D_2's home patch, where D_2 stays at home, and a group of L doves forms on D_2's home patch.
- D_1 moves to D_2's home patch, where an L-sized group of doves forms, but D_2 leaves their home and moves elsewhere.
- D_1 moves to H_1's home patch, where an L-sized group of doves forms, but H_1 leaves their home and moves elsewhere.

To compute the average fitness of a dove, we weighted the reward that D_1 receives in each of these scenarios by the probability of each group forming. We consider the first scenario as an example. The probability of D_1 staying at home and an L-sized group of doves forming on D_1's home patch is given by

$$\beta_L = \left(\frac{h}{h+N-1}\right)\left(\frac{1}{h+N-1}\right)^{L-1}\binom{k-1}{L-1}\left(\frac{h+N-2}{h+N-1}\right)^{N-k}\left(\frac{h+N-2}{h+N-1}\right)^{k-L}.$$

Note that the term $\left(\frac{h+N-2}{h+N-1}\right)^{N-k}$ ensures the absence of hawks in the group, and $\left(\frac{h+N-2}{h+N-1}\right)^{k-L}$ ensures that all other $k-L$ doves are located elsewhere. We must then weight β_L by the number of doves in the group, as each dove receives an equal share of the reward, resulting in $\beta_L(\frac{1}{L})V$. This is summed over all possible group sizes to cover the entire range, $\sum_{L=1}^{k} \beta_L(\frac{1}{L})V$. This expression can be simplified as follows

$$\sum_{L=1}^{k} \beta_L(\frac{1}{L}) = \frac{h}{k}\left(\left(\frac{h+N-2}{h+N-1}\right)^{N-k} - \left(\frac{h+N-2}{h+N-1}\right)^{N}\right).$$

By employing similar methods for the other scenarios and combining these expressions, we derive the average fitness of a dove as:

$$R + \left(\left(\frac{h+N-2}{h+N-1}\right)^{N-k} - \left(\frac{(h+N-2)^{N-1}}{(h+N-1)^{N}}\right)\left(\frac{k(N-1)+(N-k)(N-1)}{k}\right) + \frac{(N-k)(N-1)(h+N-2)^{N-k-1}}{k(h+N-1)^{N-k}}\right)$$

which we re-express as

$$R + \tau(h, N, k)V, \tag{1}$$

where

$$\tau(h,N,k) = \left(\left(\frac{h+N-2}{h+N-1}\right)^{N-k} - \left(\frac{(h+N-2)^{N-1}}{(h+N-1)^{N}}\right)\left(\frac{k(N-1)+(N-k)(N-1)}{k}\right) + \frac{(N-k)(N-1)(h+N-2)^{N-k-1}}{k(h+N-1)^{N-k}}\right)$$

Similarly, to calculate the fitness of a hawk, we must consider all scenarios in which a hawk can receive a share of the reward and possibly endure a cost. Hawks are indifferent to the presence of doves within the group, as they will always flee from a hawk's presence, leading to them receiving no share of the reward. The portion of V that a hawk receives depends on whether other hawks are present within the group. Consider two hawks, H_1 and H_2, along with a dove, D_1:

- H_1 stays at home, and a group of L hawks forms on H_1's home patch.
- H_1 moves to D_1's home patch, where a group of L hawks forms.
- H_1 moves to H_2's home patch, where H_2 stays home and a group of L hawks is formed.

- H_1 moves to H_2's home patch, where a group of L hawks forms, but H_2 has moved elsewhere.

To calculate the average fitness of a hawk, we must weight the reward that H_1 receives in each of these scenarios by the probability of each group forming. Consider the first scenario as an example. The probability of H_1 staying at home and a group of L hawks forming on H_1's home patch is given by

$$\alpha_L = \left(\frac{h}{h+N-1}\right)\left(\frac{1}{h+N-1}\right)^{L-1}\binom{N-k-1}{L-1}\left(\frac{h+N-2}{h+N-1}\right)^{N-k-L}.$$

Note that the term $\left(\frac{h+N-2}{h+N-1}\right)^{N-k-L}$ ensures that only L hawks are present on H_1's home patch, with the remaining $N-k-L$ hawks elsewhere. α_L must be weighed by the number of hawks in the group, resulting in $\alpha_L(\frac{1}{L})V$. However, the cost that the average hawk endures must be weighed by $\left(\frac{L-1}{L}\right)C$. This is then summed over all possible group sizes to cover the entire range, $\sum_{L=1}^{N-k}\alpha_L(\frac{1}{L})V$ and $\sum_{L=1}^{N-k}\alpha_L(\frac{L-1}{L})C$. These expressions can be simplified as follows:

For the reward component:

$$\sum_{L=1}^{N-k}\alpha_L(\frac{1}{L}) = \frac{h}{N-k}\left(1-\left(\frac{h+N-2}{h+N-1}\right)^{N-k}\right).$$

And for the cost component:

$$\sum_{L=1}^{N-k}\alpha_L(\frac{L-1}{L}) = \frac{h}{h+N-1}\left(1-\left(\frac{h+N-2}{h+N-1}\right)^{N-k-1}\right).$$

By using similar methods for the other scenarios and combining these expressions, we derive the average fitness of a hawk as:

$$\begin{aligned} R &+ \left(1+\frac{k}{N-k}-\frac{(N-1)(h+N-2)^{N-k-1}}{(h+N-1)^{N-k}}-\frac{k(h+N-2)^{N-k}}{(N-k)(h+N-1)^{N-k}}\right)V \\ &- \left(\frac{k-N+1}{h+N-1}-\frac{k}{N-k}+\frac{h(N-k-1)+(N-k-1)(N-1)}{(h+N-1)^2}\right. \\ &\left.+\frac{k(h+N-2)^{N-k}}{(N-k)(h+N-1)^{N-k}}+\frac{(N-1)(h+N-2)^{N-k-1}}{(h+N-1)^{N-k}}\right)C. \end{aligned}$$

which we re-express as

$$R+\omega(h,N,k)V-\nu(h,N,k)C. \tag{2}$$

where

$$\omega(h,N,k)=\left(1+\frac{k}{N-k}-\frac{(N-1)(h+N-2)^{N-k-1}}{(h+N-1)^{N-k}}-\frac{k(h+N-2)^{N-k}}{(N-k)(h+N-1)^{N-k}}\right),$$

$$\begin{aligned}\nu(h,N,k)=\Bigg(&\frac{k-N+1}{h+N-1}-\frac{k}{N-k}+\frac{h(N-k-1)+(N-k-1)(N-1)}{(h+N-1)^2}\\&+\frac{k(h+N-2)^{N-k}}{(N-k)(h+N-1)^{N-k}}+\frac{(N-1)(h+N-2)^{N-k-1}}{(h+N-1)^{N-k}}\Bigg).\end{aligned}$$

Weak selection: dove's fixation probability

The Dove's fixation probability under BDB dynamics is given by

$$\rho_1^B=\frac{1}{1+\sum_{j=1}^{N-1}\prod_{k=1}^{j}\frac{R+\omega V-\nu C}{R+\tau V}}. \tag{3}$$

We carried out weak selection methods on (3). Consider the expression inside the product term of (3).

$$\frac{R+\omega V-\nu C}{R+\tau V}=\frac{1+\frac{A}{R}}{1+\frac{B}{R}},$$

where

$$A=\omega V-\nu C,\ \text{and}\ B=\tau V,$$

$$\frac{1+\frac{A}{R}}{1+\frac{B}{R}}\approxeq 1+\frac{A-B}{R}.$$

The term inside the product of (3) now becomes

$$\begin{aligned}\prod_{k=1}^{j}\left(\frac{1+\frac{A}{R}}{1+\frac{B}{R}}\right)&=\left(1+\frac{A(1)-B(1)}{R}\right)\left(1+\frac{A(2)-B(2)}{R}\right)...\left(1+\frac{A(j)-B(j)}{R}\right)\\&=1+\sum_{k=1}^{j}\left(\frac{A(k)-B(k)}{R}\right).\end{aligned} \tag{4}$$

So from equation (3)

$$\begin{aligned}\sum_{j=1}^{N-1}\prod_{k=1}^{j}\frac{R+\omega V-\nu C}{R+\tau V}&=\sum_{j=1}^{N-1}\left(1+\sum_{k=1}^{j}\left(\frac{A(k)-B(k)}{R}\right)\right)\\&=N-1+\frac{1}{R}\sum_{k=1}^{N-1}\Big(\omega V-\nu C-\tau V\Big)\Big(N-k\Big),\end{aligned}$$

which simplifies to

$$N-1+\frac{1}{R}\Big(\sum_{k=1}^{N-1}(\omega V)(N-k)-\sum_{k=1}^{N-1}(\nu C)(N-k)-\sum_{k=1}^{N-1}(\tau V)(N-k)\Big). \quad (5)$$

By substituting the fitnesses from (1) and (2) and simplifying, we have

$$\sum_{k=1}^{N-1}(\omega V)(N-k)=\Big(N(N-1-\frac{x-x^N}{1-x}) + (\frac{(N-1)x^{N+1}-Nx^N+x}{(x-1)^2})(\frac{h-1}{h+N-2})\Big)V,$$

$$\sum_{k=1}^{N-1}(\nu C)(N-k)=\Big((\frac{1-h}{h+N-2})(\frac{(N-1)x^{N+1}-Nx^N+x}{(x-1)^2}) - \frac{1}{2}N(N-1)+N(\frac{x-x^N}{1-x})\Big)C,$$

$$\sum_{k=1}^{N-1}\Big(\tau V\Big)\Big(N-k\Big)=-\Big(N(N-1)(h+N-2)^{N-1}(h+N-1)^{-N} + \frac{h-1}{h+N-2}\Big(\frac{(N-1)x^{N+1}-Nx^N+x}{(x-1)^2}\Big) + \frac{N(N-1)}{h+N-2}\Big(Nx^N H[N-1,\frac{1}{x^k}]-\frac{x-x^N}{1-x}\Big)\Big), \quad (6)$$

where

$$H[N-1,a]=\sum_{k=1}^{N-1}\frac{a^k}{k} \text{ and } x=\frac{h+N-2}{h+N-1}. \quad (7)$$

By inserting (6), (6) and (6) into (5), we arrive at the following

$$N-1+\frac{N}{R}\Big(\Big((N-1-\frac{x-x^N}{1-x})+(N-1)\Big(\frac{(h+N-2)^{N-1}}{(h+N-1)^N}\Big)(NH[N-1,1]+1-N) - \frac{(N-1)}{h+N-2}(Nx^N H[N-1,\frac{1}{x^k}]-\frac{x-x^N}{1-x})\Big)V - \Big((\frac{1-h}{h+N-2})(\frac{(N-1)x^{N+1}-Nx^N+x}{N(x-1)^2})-\frac{1}{2}(N-1)+(\frac{x-x^N}{1-x})\Big)C\Big). \quad (8)$$

Substituting (8) into (3) and simplifying, we have

$$\frac{1}{N+\frac{N}{R}\Big((\lambda_1+\lambda_2-\lambda_3)V-(\lambda_4)C\Big)}\approx\frac{1}{N}\Big(1-\frac{1}{R}((\lambda_1+\lambda_2-\lambda_3)V-(\lambda_4)C)\Big), \quad (9)$$

which is the approximation of the fixation probability of a mutant dove under BDB dynamics where

$$\lambda_1 = \left(N - 1 - \frac{x - x^N}{1 - x}\right), \tag{10}$$

$$\lambda_2 = (N-1)\left(\frac{(h+N-2)^{N-1}}{(h+N-1)^N}\right)(NH[N-1,1] + 1 - N), \tag{11}$$

$$\lambda_3 = \frac{(N-1)}{h+N-2}\left(Nx^N H[N-1, \frac{1}{x^k}] - \frac{x - x^N}{1-x}\right), \tag{12}$$

$$\lambda_4 = \left(\frac{1-h}{h+N-2}\right)\left(\frac{(N-1)x^{N+1} - Nx^N + x}{N(x-1)^2}\right) - \frac{1}{2}(N-1) + \left(\frac{x - x^N}{1-x}\right). \tag{13}$$

We assumed an infinite well-mixed population i.e. as $N \to \infty$. We consider each λ_i for $i \in \{1, 2, 3, 4\}$ and deduce an approximation for each λ_i as N tends to infinity. For (10), we have,

$$\lambda_1 \approxeq \frac{N}{e}. \tag{14}$$

For (11), we have

$$\lambda_2 \approxeq \left(\frac{N-1}{e}\right)\left(\ln(N-1) + \gamma + \frac{1}{N} - 1\right),$$

where γ is the Euler-Mascheroni constant.

For (12) we have,

$$\lambda_3 \approxeq \frac{N}{e} ln(N-1) + \frac{N}{e} f(h) - N + \frac{N}{e}, \tag{15}$$

where $f(h) = H[N-1, \left(\frac{h+N-1}{h+N-2}\right)^k] - \ln(N-1)$.

From (13) we have,

$$\lambda_4 \approxeq (1-h)(1 - \frac{2}{e}) + N(\frac{1}{2} - \frac{1}{e}) + \frac{1}{2}. \tag{16}$$

By simplifying (14), (15), and (15),

$$(\lambda_1 + \lambda_2 - \lambda_3)V = \frac{N}{\mathrm{e}}\left(\gamma - 1 - f(h,N)\right) + \frac{1}{e}\left(2 - \ln(N-1) - \gamma - \frac{1}{N}\right) + N. \tag{17}$$

Substituting (17) and (16) into (9), we have

$$\frac{1}{N}\Bigg(1-\frac{1}{R}\Bigg(\Bigg(\frac{N}{\mathrm{e}}\Bigg(\gamma-1-f(h,N)\Bigg)+\frac{1}{e}\Bigg(2-\ln(N-1)-\gamma-\frac{1}{N}\Bigg)+N\Bigg)V \\ -\Bigg((1-h)(1-\frac{2}{\mathrm{e}})+N(\frac{1}{2}-\frac{1}{\mathrm{e}})+\frac{1}{2}\Bigg)C\Bigg)\Bigg), \tag{18}$$

which is an approximation of the fixation probability of a mutant dove in an infinite, well-mixed population. The neutrality condition for this case is given by $\rho_1^B = \frac{1}{N}$ i.e.

$$\frac{N}{\mathrm{e}}\Bigg(\gamma-1-f(h,N)\Bigg)+\frac{1}{e}\Bigg(2-\ln(N-1)-\gamma-\frac{1}{N}\Bigg)+N\Bigg)V \\ -\Bigg((1-h)(1-\frac{2}{\mathrm{e}})+N(\frac{1}{2}-\frac{1}{\mathrm{e}})+\frac{1}{2}\Bigg)C=0, \tag{19}$$

which simplifies to

$$V=\frac{(\frac{1}{2}-\frac{1}{\mathrm{e}})}{(\frac{1}{\mathrm{e}}(\gamma-1-f(h))+1)}C. \tag{20}$$

By using similar methods to the dove's fixation probability under BDD dynamics (2.12), we deduce a similar weak selection approximation given by

$$\frac{1}{N}\Bigg(1-\frac{(N+2w^*)}{R(N+w^*)}((\lambda_1+\lambda_2-\lambda_3)V-(\lambda_4)C)\Bigg). \tag{21}$$

where the neutrality condition remains unchanged.

Mean group size calculation

When we calculated the mean group size under independent movement, we considered a process where L individuals partake in the movement process. These individuals can either move to an empty place or to a place already containing an individual that did not move. The mean group size under independent movement is given by

$$|G|=\sum_{L=0}^{N}\Bigg(\frac{L}{N}\sum_{j=0}^{L}\Bigg(\frac{1}{N}\Bigg)^j\Bigg(\frac{N-1}{N}\Bigg)^{L-j}\binom{L}{j}(j)^2 \\ +\Bigg(1-\frac{L}{N}\Bigg)\sum_{j=0}^{L}\Bigg(\frac{1}{N}\Bigg)^j\Bigg(\frac{N-1}{N}\Bigg)^{L-j}\binom{L}{j}(j+1)^2\Bigg)(\lambda)^L(1-\lambda)^{N-L}\binom{N}{L}.$$

By expanding the summations and simplifying, we have

$$|G|=1+\lambda\Bigg(2-\frac{1}{N}(2+\lambda N-\lambda)\Bigg). \tag{22}$$

Therefore, by using (3.3), T, under independent movement is given by

$$T = \frac{1}{N-1}\lambda\bigg(2 - \frac{1}{N}(2 + \lambda N - \lambda)\bigg). \tag{23}$$

For the wheel process, we first calculated T (1.49) and then used (3.3) to then determine the mean group size. In an N-sized, well-mixed population, there are the various ways I_i and I_j can be together. For instance, I_i and I_j may both partake in the movement process and move to the same place. Alternatively, I_i may partake in the movement process and move to I_j's home vertex, while I_j does not partake in the movement process and remains on their home vertex, or vice versa.

$$\begin{aligned}\mathrm{P}(I_i \text{ and } I_j \text{ are together}) = &\sum_{L=2}^{N-1}\sum_{j=1}^{j_m}(L-j)(1-\frac{\theta j N}{2\pi})(\lambda)^L(1-\lambda)^{N-L}\binom{N-2}{L-2} \\ &+ \sum_{L=1}^{N}(2)(\lambda)^L(1-\lambda)^{N-L}\binom{N-2}{L-1}\bigg(\frac{1}{N}\bigg).\end{aligned}$$

The first summation represents the probability of individuals I_i and I_j of distance j spikes, being together at the same place and $j_m = \min(\lfloor\frac{2\pi}{N\theta}\rfloor, r)$ represents the cut-off point where this no longer holds. By expanding the summations and simplifying, T is given by

$$\begin{aligned}T = \frac{1}{N(N-1)}\bigg(\bigg(&\sum_{\lfloor\frac{2\pi}{N\theta}\rfloor}^{N}\bigg(\lfloor\frac{2\pi}{N\theta}\rfloor^2 + \frac{1}{2}(\lfloor\frac{2\pi}{N\theta}\rfloor^2 + \lfloor\frac{2\pi}{N\theta}\rfloor)\bigg)\bigg(\frac{N\theta}{2\pi}(1-\lfloor\frac{2\pi}{N\theta}\rfloor)-1\bigg) \\ &+ \sum_{L=2}^{\lfloor\frac{2\pi}{N\theta}\rfloor-1}\bigg(L^2 + \frac{L^2+L}{2}(\frac{N\theta}{6\pi}(1-L)-1)\bigg)\bigg)(\lambda)^L(1-\lambda)^{N-L}\binom{N-2}{L-2} \\ &+ \frac{2(\lambda-\lambda^2)}{N}\bigg).\end{aligned} \tag{24}$$

Therefore, by using (3.3), the mean group size is

$$\begin{aligned}|G| = 1 + \frac{1}{N}\bigg(\bigg(&\sum_{\lfloor\frac{2\pi}{N\theta}\rfloor}^{N}\bigg(\lfloor\frac{2\pi}{N\theta}\rfloor^2 + \frac{1}{2}(\lfloor\frac{2\pi}{N\theta}\rfloor^2 + \lfloor\frac{2\pi}{N\theta}\rfloor)\bigg)\bigg(\frac{N\theta}{2\pi}(1-\lfloor\frac{2\pi}{N\theta}\rfloor)-1\bigg) \\ &+ \sum_{L=2}^{\lfloor\frac{2\pi}{N\theta}\rfloor-1}\bigg(L^2 + \frac{L^2+L}{2}(\frac{N\theta}{6\pi}(1-L)-1)\bigg)\bigg)(\lambda)^L(1-\lambda)^{N-L}\binom{N-2}{L-2} \\ &+ \frac{2(\lambda-\lambda^2)}{N}\bigg).\end{aligned} \tag{25}$$

Temperature calculations

When calculating the temperature of an individual under independent movement, it was simpler to consider the probability of an individual being alone, as the temperature is also equal to 1− P(alone). In an N-sized, well-mixed population, there are various ways I_i can be alone. For instance, I_i may not partake in the movement process, remain on their home vertex and have no one else move to the same place. Alternatively, I_i may partake in the movement process, move to their home vertex, and find themselves alone, with no other individuals moving to the same vertex. Another possibility is that I_i and I_j both partake in the movement process, I_i moves to I_j's home vertex, and is alone, provided no other individuals move to the same place.

$$\begin{aligned}\mathrm{P}(I_i \text{ is alone}) = &\sum_{L=0}^{N-1}(\lambda)^L(1-\lambda)^{N-L}\binom{N-1}{L}\left(1-\frac{1}{N}\right)^L \\ &+\sum_{L=2}^{N}(\lambda)^L(1-\lambda)^{N-L}\binom{N-2}{L-2}\left(\frac{N-1}{N}\right)\left(1-\frac{1}{N}\right)^{L-1} \\ &+\sum_{L=1}^{N}(\lambda)^L(1-\lambda)^{N-L}\binom{N-1}{L-1}\left(\frac{1}{N}\right)\left(1-\frac{1}{N}\right)^{L-1}.\end{aligned}$$

Expanding the summations and simplifying,

$$\mathrm{P}(I_i \text{ is alone}) = \frac{N(N+N\lambda(\lambda-1)-\lambda^2)(N-\lambda)^{N-2}(1-\lambda)^N}{(N-N\lambda)^N}.$$

Therefore, the temperature under independent movement is given by

$$\tau_N = 1 - \frac{(N+N\lambda(\lambda-1)-\lambda^2)(N-\lambda)^{N-2}}{N^{N-1}}. \tag{26}$$

Using a similar approach to calculate the temperature for the wheel, we considered theta in two possible ranges $0 \leq \theta \leq \frac{\pi}{N}$ and $\frac{\pi}{N} \leq \theta \leq \frac{2\pi}{N}$ as this includes the cases where all spikes can aggregate, to complete separation. Consider individual I_i where $0 \leq \theta \leq \frac{\pi}{N}$:

- I_i partakes in the wheel process and moves to their home vertex and no one else joins them.
- I_i partakes in the wheel process and moves to someone else's vertex, alone.
- I_i does not partake in the wheel process and stays on their home vertex, alone.

- No one in the population partakes in the movement process, therefore I_i remains alone.

$$\begin{aligned}\mathrm{P}(I_i \text{ is alone}) = (\lambda)\sum_{L=1}^{N}(\lambda)^{L-1}(1-\lambda)^{N-L}\binom{N-1}{L-1}\left(\frac{N\theta}{L\pi}\right)\left(\frac{1}{N}\right)\\ + (\lambda)^2\sum_{L=2}^{N}(\lambda)^{L-2}(1-\lambda)^{N-L}\binom{N-2}{L-2}\left(\frac{N\theta}{L\pi}\right)\left(1-\frac{1}{N}\right)\\ + (1-\lambda)\sum_{L=1}^{N}(\lambda)^{L}(1-\lambda)^{N-L-1}\binom{N-1}{L}\left(1-\frac{((L-1)\theta+\frac{2\pi}{N})}{2\pi}\right)\\ + (1-\lambda)^N.\end{aligned}$$

By expanding the summations and simplifying, the probability of being alone is

$$\begin{aligned}\mathrm{P}(I_i \text{ is alone}) = \frac{1}{N}(N-1)(1-\lambda)((1-\lambda)^{N-1}-1)+(1-\lambda)^N\\ + \frac{\theta}{\pi}\left(\lambda+\frac{1}{2}((1-\lambda)(1-(1-\lambda)^{N-1})+(N-1)(\lambda-1)(\lambda))\right).\end{aligned}$$

and, therefore, the temperature for $0 \leq \theta \leq \frac{\pi}{N}$ is given by

$$\begin{aligned}\tau_N = 1-\left(\frac{1}{N}(N-1)(1-\lambda)(1-(1-\lambda)^{N-1})+(1-\lambda)^N\right.\\ \left.+\frac{\theta}{\pi}\left(\lambda+\frac{1}{2}((1-\lambda)(1-(1-\lambda)^{N-1})+(N-1)(\lambda-1)(\lambda))\right)\right).\end{aligned} \tag{27}$$

By using very similar methods, the temperature for $\frac{\pi}{N} \leq \theta \leq \frac{2\pi}{N}$ is given by

$$\begin{aligned}\tau_N = 1-\left(\frac{1}{N}\left(-1+(1-\lambda)^N+\lambda(\lambda+2)-N(\lambda^2+\lambda-1)\right)\right.\\ \left.-\frac{\theta}{2\pi}\left(-1+(1-\lambda)^N+\lambda(N+3\lambda-3N\lambda)\right)\right).\end{aligned} \tag{28}$$

Bibliography

Akdeniz, A. & van Veelen, M. (2020), 'The cancellation effect at the group level', *Evolution* **74**(7), 1246–1254.
URL: *https://doi.org/10.1111/evo.14023*

Aktipis, C. (2004), 'Know when to walk away: contingent movement and the evolution of cooperation', *Journal of Theoretical Biology* **231**(2), 249–260.

Aktipis, C. (2011), 'Is cooperation viable in mobile organisms? simple walk away rule favors the evolution of cooperation in groups', *Evolution and Human Behavior* **32**(4), 263–276.

Antal, T., Redner, S. & Sood, V. (2006), 'Evolutionary dynamics on degree-heterogeneous graphs', *Physical Review Letters* **96**(18), 188104.

Antal, T. & Scheuring, I. (2006), 'Fixation of strategies for an evolutionary game in finite populations', *Bulletin of Mathematical Biology* **68**(8), 1923–1944.

Archetti, M. & Scheuring, I. (2012), 'Game theory of public goods in one-shot social dilemmas without assortment', *Journal of Theoretical Biology* **299**, 9–20.

Bach, L. A., Helvik, T. & Christiansen, F. B. (2006), 'n-player cooperation—threshold games and ess bifurcations', *Journal of Theoretical Biology* **238**(2), 426–434.

Ball, F. & House, T. (2017), 'Heterogeneous network epidemics: real-time growth, variance and extinction of infection', *Journal of Mathematical Biology* **75**(3), 577–619.

Broom, M., Cannings, C. & Vickers, G. (1997), 'Multi-player matrix games', *Bulletin of Mathematical Biology* **59**, 931–952.

Broom, M., Cressman, R. & Křivan, V. (2019), 'Revisiting the "fallacy of averages" in ecology: Expected gain per unit time equals expected gain divided by expected time', *Journal of Theoretical Biology* **483**, 109993.

Broom, M., Erovenko, I., Rowell, J. & Rychtar, J. (2020), 'Models and measures of animal aggregation and dispersal', *Journal of Theoretical Biology* **494**, 110002.

Broom, M., Erovenko, I. & Rychtár, J. (2021), 'Modelling evolution in structured populations involving multiplayer interactions', *Dynamic Games and Applications* **11**, 270–293.

Broom, M., Hadjichrysanthou, C. & Rychtar, J. (2010), 'Evolutionary games on graphs and the speed of the evolutionary process', *Proceedings of the Royal Society A* **466**, 1327–1346.

Broom, M., Lafaye, C., Pattni, K. & Rychtar, J. (2015), 'A study of the dynamics of multi-player games on small networks using territorial interactions', *Journal of Mathematical Biology* **71**, 1551–1574.

Broom, M., Pattni, K. & Rychtar, J. (2018), 'Generalized social dilemmas: The evolution of cooperation in populations with variable group size', *Bulletin of Mathematical Biology* .

Broom, M., Pattni, K. & Rychtar, J. (2019), 'Generalised social dilemmas: The evolution of cooperation in populations with variable group size', *Bulletin of Mathematical Biology* **255**(1), 81–91.

Broom, M. & Rychtar, J. (2008), 'An analysis of the fixation probability of a mutant on special classes of non-directed graphs', *Proceedings of the Royal Society of London A* **464**, 2609–2627.

Broom, M. & Rychtar, J. (2012), 'A general framework for analysing multiplayer games in networks using territorial interactions as a case study', *Journal of Theoretical Biology* **302**, 70–80.

Broom, M. & Rychtar, J. (2013), *Game-Theoretical Models in Biology*, CRC Press, Boca Raton, FL.

Bruni, M., Broom, M. & Rychtář, J. (2014), 'Analysing territorial models on graphs', *Involve, a Journal of Mathematics* **7**(2), 129–149.

Buhl, J., Sumpter, D. J., Couzin, I. D., Hale, J. J., Despland, E., Miller, E. R. & Simpson, S. J. (2006), 'From disorder to order in marching locusts', *Science* **312**(5778), 1402–1406.

Bukowski, M. & Miekisz, J. (2004), 'Evolutionary and asymptotic stability in symmetric multi-player games', *International Journal of Game Theory* **33**(1), 41–54.

Clutton-Brock, T. H. & Albon, S. D. (1979), 'The roaring of red deer and the evolution of honest advertising', *Behaviour* **69**, 145–170.

Couzin, I., Krause, J., Franks, N. R. & Levin, S. A. (2005), 'Effective leadership and decision-making in animal groups on the move', *Nature* **433**, 513–516.
URL: *https://doi.org/10.1038/nature03236*

Csardi, G. & Nepusz, T. (2006), 'The igraph software package for complex network research', *InterJournal, Complex Systems* **1695**.

Cuesta, F. A., Sequeiros, P. G. & Rojo, A. L. (2017), 'Suppressors of selection', *PLOS One* **12**(7), e0180549.

Darwin, C. (1874), *The Descent of Man and Selection in Relation to Sex*, Murray, London.

Deneubourg, J.-L., Aron, S., Goss, S. & Pasteels, J.-M. (1990), 'The self-organizing exploratory pattern of the argentine ant', *Journal of Insect Behaviour* **3**, 159–168.

Dingle, H. (2006), 'Animal migration: is there a common migratory syndrome?', *Journal of Ornithology* **147**(2), 212–220.

Dingle, H. (2014), *Migration: The Biology of Life on the Move*, Oxford University Press, USA.

Dingle, H. & Drake, V. A. (2007), 'What is migration?', *Bioscience* **57**(2), 113–121.

Dorigo, M. & Stützle, T. (2004), *Ant Colony Optimization*, MIT Press, Cambridge, MA.

Edwards, A. W. F. (2000), *Foundations of Mathematical Genetics*, Cambridge University Press, Cambridge, UK.

Erovenko, I. E., Bauer, J., Broom, M., Pattni, K. & Rychtar, J. (2019), 'The effect of network topology on optimal exploration strategies and the evolution of cooperation in a mobile population', *Proceedings of the Royal Society of London A* **475**, 20190399.

Erovenko, I. V. & Broom, M. (2024), 'The evolution of cooperation in a mobile population on random networks: network topology matters only for low-degree networks', *Dynamic Games and Applications* .

Fic, M. & Gokhale, C. S. (2024), 'Catalysing cooperation: the power of collective beliefs in structured populations', *npj Complex Systems* **1**, 6.

Fisher, R. A. (1930), *The Genetical Theory of Natural Selection*, Clarendon Press, Oxford, UK.

Ford, J. R. & Swearer, S. E. (2013), 'Two's company, three's a crowd: Food and shelter limitation outweigh the benefits of group living in a shoaling fish', *Ecology* **94**(5), 1069–1077.

Frean, M., Rainey, P. B. & Traulsen, A. (2013), 'The effect of population structure on the rate of evolution', *Proceedings of the Royal Society B: Biological Sciences* **280**(1762), 20130211.

Fretwell, S. D. & Lucas, H. L. (1969), 'On territorial behavior and other factors influencing habitat distribution of birds', *Acta Biotheoretica* **19**, 16–36.

Ginsberg, J. & Macdonald, D. (1990), *Foxes, Wolves, Jackals, and Dogs: An Action Plan for the Conservation of Canids*, IUCN, Gland, Switzerland.

Gokhale, C. S. & Traulsen, A. (2010), 'Evolutionary games in the multiverse', *Proceedings of the National Academy of Sciences* **107**(12), 5500–5504.

Gokhale, C. S. & Traulsen, A. (2014), 'Evolutionary multiplayer games', *Dynamic Games and Applications* .

Guttal, V. & Couzin, I. D. (2010), 'Social interactions, information use, and the evolution of collective migration', *Proceedings of the National Academy of Sciences* **107**(37), 16172–16177.

Hadjichrysanthou, C., Broom, M. & Rychtar, J. (2011), 'Evolutionary games on star graphs under various updating rules', *Dynamic Games and Applications* **1**(3), 386–407.

Hamilton, W. D. (1967), 'Extraordinary sex ratios', *Science* **156**, 477–488.

Hanski, I. (1998), 'Metapopulation dynamics', *Nature* **396**, 41–49.
URL: *https://www.nature.com/articles/23876*

Haq, H., Schimit, P. H. T. & Broom, M. (2024), 'The effects of herding and dispersal behaviour on the evolution of cooperation on complete networks', *Journal of Mathematical Biology* **89**, 49.

Haq, H., Schimit, P. H. T. & Broom, M. (2025), 'Predictors of fixation probability on complete networks involving multiplayer interactions under coordinated movement systems', *Dynamic Games and Applications* .

Herbinger, I., Boesch, C. & Rothe, H. (2001), 'Territory characteristics among three neighboring chimpanzee communities in the taï national park, côte d'ivoire', *International Journal of Primatology* **22**(2), 143–167.

Hindersin, L. & Traulsen, A. (2014), 'Counterintuitive properties of the fixation time in network-structured populations', *Journal of The Royal Society Interface* **11**(99), 20140606.

Hinz, R. C. & de Polavieja, G. G. (2017), 'Ontogeny of collective behavior reveals a simple attraction rule', *Proceedings of the National Academy of Sciences of the United States of America* **114**(9), 2295–2300.
URL: *https://doi.org/10.1073/pnas.1616926114*

Hofbauer, J., Schuster, P. & Sigmund, K. (1979), 'A note on evolutionarily stable strategies and game dynamics', *Journal of Theoretical Biology* **81**(3), 609–612.

Hofbauer, J. & Sigmund, K. (1998), *Evolutionary games and population dynamics*, Cambridge University Press.

Johnson, N. L. & Kotz, S. (1977), *Urn models and their application; an approach to modern discrete probability theory*, Wiley, New York, NY (USA).

Karlin, S. & Taylor, H. (1975), *A First Course in Stochastic Processes*, Academic Press, London.

Keeling, M. J. & Eames, K. T. D. (2005), 'Networks and epidemic models', *Journal of the Royal Society Interface* **2**(4), 295–307.

Kelley, S., Ransom Jr, D., Butcher, J., Schulz, G., Surber, B., Pinchak, W., Santamaria, C. & Hurtado, L. (2011), 'Home range dynamics, habitat selection, and survival of greater roadrunners', *Journal of Field Ornithology* **82**(2), 165–174.

Kermack, W. O. & McKendrick, A. G. (1927), 'A contribution to the mathematical theory of epidemics', *Proceedings of the Royal Society of London. Series A* **115**(772), 700–721.

Kermack, W. O. & McKendrick, A. G. (1932), 'Contributions to the mathematical theory of epidemics ii. the problem of endemicity', *Proceedings of the Royal Society of London. Series A* **138**(834), 55–83.

Kermack, W. O. & McKendrick, A. G. (1933), 'Contributions to the mathematical theory of epidemics. iii. further studies of the problem of endemicity', *Proceedings of the Royal Society of London. Series A* **141**(843), 94–122.

Kimura, M. (1964), 'Diffusion models in population genetics', *Journal of Applied Probability* **1**(2), 177–232.

Krieger, M. S., McAvoy, A. & Nowak, M. A. (2017), 'Effects of motion in structured populations', *Journal of The Royal Society Interface* **14**, 20170509.

Kurokawa, S. & Ihara, Y. (2009), 'Emergence of cooperation in public goods games', *Proceedings of the Royal Society B: Biological Sciences* **276**(1660), 1379–1384.

Kurokawa, S. & Ihara, Y. (2013), 'Evolution of social behavior in finite populations: a payoff transformation in general n-player games and its implications', *Theoretical Population Biology* **84**, 1–8.

Lessard, S. (2011), 'On the robustness of the extension of the one-third law of evolution to the multi-player game', *Dynamic Games and Applications* **1**(3), 408–418.

Li, A., Broom, M., Du, J. & Wang, L. (2016), 'Evolutionary dynamics of general group interactions in structured populations', *Physical Review E* **93**, 022407.

Li, C., Zhang, B., Cressman, R. & Tao, Y. (2013), 'Evolution of cooperation in a heterogeneous graph: fixation probabilities under weak selection', *PLOS One* **8**(6), e66560.

Lieberman, E., Hauert, C. & Nowak, M. (2005), 'Evolutionary dynamics on graphs', *Nature* **433**(7023), 312–316.

Lukeman, R., Li, Y. & Edelstein-Keshet, L. (2010), 'Inferring individual rules from collective behavior', *Proceedings of the National Academy of Sciences of the United States of America* **107**(28), 12576–12580.
URL: *https://doi.org/10.1073/pnas.1001763107*

Maciejewski, W. (2014), 'Reproductive value in graph-structured populations', *Journal of Theoretical Biology* **340**, 285–293.

Marker, L., Dickman, A., Mills, M., Jeo, R. & Macdonald, D. (2008), 'Spatial ecology of cheetahs on north-central namibian farmlands', *Journal of Zoology* **274**(3), 226–238.

Masuda, N. (2009), 'Directionality of contact networks suppresses selection pressure in evolutionary dynamics', *Journal of Theoretical Biology* **258**(2), 323–334.

Masuda, N. & Ohtsuki, H. (2009), 'Evolutionary dynamics and fixation probabilities in directed networks', *New Journal of Physics* **11**, 033012.

Maynard Smith, J. (1982), *Evolution and the Theory of Games*, Cambridge University Press, Cambridge.

Maynard Smith, J. & Price, G. R. (1973), 'The logic of animal conflict', *Nature* **246**, 15–18.

Miekisz, J. (2008), 'Evolutionary game theory and population dynamics', **1940**, 269–316.

Milinski, M., Semmann, D., Krambeck, H. & Marotzke, J. (2006), 'Stabilizing the earth's climate is not a losing game: supporting evidence from public goods experiments', *Proceedings of the National Academy of Sciences of the United States of America* **103**(11), 3994–3998.

Moran, P. (1958), 'Random processes in genetics', *Mathematical Proceedings of the Cambridge Philosophical Society* **54**, 60–71.

Moran, P. (1962), *The statistical processes of evolutionary theory*, Clarendon Press, Oxford.

Möller, M., Hindersin, L. & Traulsen, A. (2019), 'Exploring and mapping the universe of evolutionary graphs identifies structural properties affecting fixation probability and time', *Communications Biology* **2**(1), 137.

Nash, J. (1951), 'Non-cooperative games', *Annals of Mathematics* **54**(2), 286–295.

Nowak, M. (2006), *Evolutionary dynamics, exploring the equations of life*, Harvard University Press, Cambridge, MA.

Nowak, M. A., Sasaki, A., Taylor, C. & Fudenberg, D. (2004), 'Emergence of cooperation and evolutionary stability in finite populations', *Nature* **428**(6983), 646–650.

Ohtsuki, H., Hauert, C., Lieberman, E. & Nowak, M. (2006), 'A simple rule for the evolution of cooperation on graphs and social networks', *Nature* **441**, 502–5.

Pacheco, J. M., Santos, F. C., Souza, M. O. & Skyrms, B. (2009), 'Evolutionary dynamics of collective action in n-person stag hunt dilemmas', *Proceedings of the Royal Society B: Biological Sciences* **276**(1655), 315–321.

Palm, G. (1984), 'Evolutionary stable strategies and game dynamics for n-person games', *Journal of Mathematical Biology* **19**(3), 329–334.

Paris, C., Servin, B. & Boitard, S. (2019), 'Inference of selection from genetic time series using various parametric approximations to the wright-fisher model', *G3: Genes—Genomes—Genetics* **9**(12), 4073–4086.
URL: *https://doi.org/10.1534/g3.119.400778*

Pattni, K., Broom, M. & Rychtar, J. (2017), 'Evolutionary dynamics and the evolution of multiplayer cooperation in a subdivided population', *Journal of Theoretical Biology* **429**, 105–115.

Pattni, K., Broom, M. & Rychtar, J. (2018), 'Evolving multiplayer networks: modelling the evolution of cooperation in a mobile population', *Discrete and Continuous Dynamical Systems B* **23**, 1975–2004.

Pattni, K., Broom, M., Rychtar, J. & Silvers, A. J. (2015), 'Evolutionary graph theory revisited: when is an evolutionary process equivalent to the moran process?', *Proceedings of the Royal Society A* **471**, 20150334.

Petit, O. & Bon, R. (2010), 'Decision-making processes: The case of collective movements', *Behavioural Processes* **84**(3), 635–647.

Pires, D. L. & Broom, M. (2024), 'The rules of multiplayer cooperation in networks of communities', *PLoS Computational Biology* **20**(8), e1012388.

Pires, D. L., Erovenko, I. V. & Broom, M. (2023), 'Network topology and movement cost, not updating mechanism, determine the evolution of cooperation in mobile structured populations', *PLOS One* **18**(8), 0289366.

Platkowski, T. (2004), 'Evolution of populations playing mixed multiplayer games', *Mathematical and Computer Modelling* **39**(9-10), 981–989.

Platkowski, T. & Bujnowski, P. (2009), 'Cooperation in aspiration-based n-person prisoner's dilemmas', *Physical Review E* **79**(3), 036103.

Pusey, A. E. & Packer, C. (1994), Infanticide in lions: consequences and counterstrategies, *in* S. Parmigiami & F. S. vom Saal, eds, 'Infanticide and Parental Care', Harwood Academic Publishers, London, UK, pp. 277–299.

Pyritz, L. W., Kappeler, P. M. & Fichtel, C. (2011), 'Coordination of group movements in wild red-fronted lemurs (eulemur rufifrons): Processes and influence of ecological and reproductive seasonality', *International Journal of Primatology* **32**(6), 1325–1347.

Santos, F. C. & Pacheco, J. M. (2006), 'A new route to the evolution of cooperation', *Journal of Evolutionary Biology* **19**(3), 726–733.

Santos, F., Santos, M. & Pacheco, J. (2008*a*), 'Social diversity promotes the emergence of cooperation in public goods games', *Nature* **454**(7201), 213–216.

Santos, F., Santos, M. & Pacheco, J. (2008*b*), 'Social diversity promotes the emergence of cooperation in public goods games', *Nature* **454**(7201), 213–216.

Schimit, P. H. T., Pattni, K. & Broom, M. (2019), 'Dynamics of multiplayer games on complex networks using territorial interactions', *Physical Review E* **99**(3).

Schimit, P. H. T., Pereira, F. H. & Broom, M. (2022), 'Good predictors for the fixation probability on complex networks of multi-player games using territorial interactions', *Ecological Complexity* **51**, 101017.

Schmidt, K., Jedrzejewski, W. & Okarma, H. (1997), 'Spatial organization and social relations in the eurasian lynx population in bialowieza primeval forest, poland', *Acta Theriologica* **42**, 289–312.

Shah, S., Kothari, R. & Jayadeva (2010), 'Trail formation in ants: A generalized polya urn process', *Swarm Intelligence* **4**, 145–171.
URL: *https://doi.org/10.1007/s11721-010-0041-9*

Shakarian, P., Roos, P. & Johnson, A. (2012), 'A review of evolutionary graph theory with applications to game theory', *Biosystems* **107**, 66–80.

Shakarian, P., Roos, P. & Moores, G. (2013), 'A novel analytical method for evolutionary graph theory problems', *Biosystems* **111**(2), 136–144. Epub 2013 Jan 23.

Souza, M. O., Pacheco, J. M. & Santos, F. C. (2009), 'Evolution of cooperation under n-person snowdrift games', *Journal of Theoretical Biology* **260**(4), 581–588.

Tarnita, C. E., Ohtsuki, H., Antal, T., Fu, F. & Nowak, M. A. (2009), 'Strategy selection in structured populations', *Journal of Theoretical Biology* **259**(3), 570–581.

Taylor, C., Fudenberg, D., Sasaki, A. & Nowak, M. (2004), 'Evolutionary game dynamics in finite populations', *Bulletin of Mathematical Biology* **66**(6), 1621–1644.

Taylor, P. & Jonker, L. (1978), 'Evolutionarily stable strategies and game dynamics', *Mathematical Biosciences* **40**, 145–156.

Tkadlec, J., Pavlogiannis, A., Chatterjee, K. & Nowak, M. A. (2020), 'Limits on amplifiers of natural selection under death-birth updating', *PLOS Computational Biology* **16**(1), e1007494.

Traulsen, A., Nowak, M. A. & Pacheco, J. M. (2007), 'Stochastic payoff evaluation increases the temperature of selection', *Journal of Theoretical Biology* **244**(2), 349–356.

Traulsen, A., Shoresh, N. & Nowak, M. A. (2008), 'Analytical results for individual and group selection of any intensity', *Bulletin of Mathematical Biology* **70**, 1410–

1424.
URL: *https://doi.org/10.1007/s11538-008-9305-6*

van Veelen, M. & Nowak, M. A. (2012), 'Multi-player games on the cycle', *Journal of Theoretical Biology* **292**, 116–128.

von Neumann, J. & Morgenstern, O. (1944), *Theory of Games and Economic Behavior*, Princeton University Press, Princeton, NJ.

Voorhees, B. (2013), 'Birth-death fixation probabilities for structured populations', *Proceedings of the Royal Society A: Mathematical, Physical and Engineering Sciences* **469**(2153), 20120248.

Voorhees, B. & Murray, A. (2013), 'Fixation probabilities for simple digraphs', *Proceedings of the Royal Society A: Mathematical, Physical and Engineering Sciences* .

Ward, A. J., Sumpter, D. J. T., Couzin, I. D., Hart, P. J. & Krause, J. (2008), 'Quorum decision-making facilitates information transfer in fish shoals', *Proceedings of the National Academy of Sciences of the United States of America* **105**(19), 6948–6953.
URL: *https://doi.org/10.1073/pnas.0710344105*

Waxman, D. (2011), 'Comparison and content of the wright-fisher model of random genetic drift, the diffusion approximation and an intermediate model', *Journal of Theoretical Biology* **269**(1), 79–87.

Winklmayr, C., Kao, A. B., Bak-Coleman, J. B. & Romanczuk, P. (2020), 'The wisdom of stalemates: consensus and clustering as filtering mechanisms for improving collective accuracy', *Proceedings of the Royal Society B* **287**(20201802).
URL: *http://doi.org/10.1098/rspb.2020.1802*

Wright, S. (1930), 'Evolution in mendelian populations', *Genetics* **16**, 97–159.

Yagoobi, S., Sharma, N. & Traulsen, A. (2023), 'Categorizing update mechanisms for graph-structured metapopulations', *Journal of the Royal Society Interface* **20**(20220769), 20220769.
URL: *https://doi.org/10.1098/rsif.2022.0769*

Zheng, X., Cressman, R. & Tao, Y. (2011), 'The diffusion approximation of stochastic evolutionary game dynamics: Mean effective fixation time and the significance of the one-third law', *Dynamic Games and Applications* **1**(3), 462–477.